

University of Nebraska - Lincoln

DigitalCommons@University of Nebraska - Lincoln

Nebraska Department of Transportation Research
Reports

Nebraska LTAP

10-2010

Rapid Construction of Pacific Street Bridge

Kromel E. Hanna

University of Nebraska - Lincoln, kromelhanna@mail.unomaha.edu

George Morcouc

University of Nebraska-Lincoln, gmorcouc2@unl.edu

Mahe K. Tadros

University of Nebraska - Lincoln, mtadros1@unl.edu

Follow this and additional works at: <http://digitalcommons.unl.edu/ndor>



Part of the [Transportation Engineering Commons](#)

Hanna, Kromel E.; Morcouc, George; and Tadros, Mahe K., "Rapid Construction of Pacific Street Bridge" (2010). *Nebraska Department of Transportation Research Reports*. 94.

<http://digitalcommons.unl.edu/ndor/94>

This Article is brought to you for free and open access by the Nebraska LTAP at DigitalCommons@University of Nebraska - Lincoln. It has been accepted for inclusion in Nebraska Department of Transportation Research Reports by an authorized administrator of DigitalCommons@University of Nebraska - Lincoln.

Rapid Construction of Pacific Street Bridge

PROJECT: SPR-PL-1 (037) P587



October 2010



Rapid Construction of Pacific Street Bridge

PROJECT: SPR-PL-1 (037) P587

FINAL REPORT

BY:

Kromel E Hanna, George Morcous, and Maher K Tadros

UNDER THE SPONSORSHIP OF:

NEBRASKA DEPARTMENT OF ROADS

SUBMITTED:

October 2010

Technical Report Documentation Page

1. Report No.	2. Government Accession No.	3. Recipient's Catalog No.	
1. Title and Subtitle Rapid Construction of Pacific Street Bridge with 0.7 inch Strands		2. Report Date October, 2010	3. Performing Organization Code
4. Author(s) Kromel E. Hanna, George Morcoux, and Maher K. Tadros		5. Performing Organization Report No.	
6. Performing Organization Name and Address Department of Civil Engineering University of Nebraska-Lincoln Omaha, Nebraska 68182-0178		7. Work Unit No.	8. Contract or Grant No. SPR-PL-1 (037) P587
9. Sponsoring Agency Name and Address Nebraska Department of Roads,		10. Type of Report and Period Covered Final Report	
		11. Sponsoring Agency Code	
12. Supplementary Notes			
13. Abstract <p>The Pacific Street Bridge over I-680 in Omaha, NE is the first bridge in the United States to use 0.7-in.-diameter prestressing strands in pretensioned concrete girders. This project was funded by FHWA through NDOR under the Innovative Bridge Research and Deployment (IBRD) program. The bridge construction was completed in August 2008 as a replacement to an existing bridge. The old bridge was 74-ft-wide and had four spans that were 44-ft 6-in. 73-ft, 73-ft 6-in., and 30-ft long. Each span consisted of 11 steel I-girders at 7-ft spacing. The new bridge consists of two identical spans, 98-ft-long each with 17 deg. skew angle.</p> <p>The bridge has six traffic lanes with a total width of 105 ft 8 in. (32.2 m). The bridge superstructure consists of twenty NU900 I-girders (ten for each span) that are 35.4 in.-deep and spaced at 10-ft, 8 in. Each girder was pretensioned using thirty 0.7-in.-diameter strands that are spaced at 2 in. horizontal spacing and 2.5 in. vertical spacing. Since the design and production of the bridge girders were completed before the successful testing of a girder with 2 in. by 2 in. spacing, that optimal spacing was not allowed on this bridge.</p> <p>This report presents the testing of second and third generations of threaded rod continuity systems. The negative moment area (over the pier) using progressively simplified reinforcement details was tested twice, as labeled "second generation" and "third generation" threaded rod connection details. The details show excellent performance with little extra details compared to conventional continuous-for-live-load details. Under this threaded rod system, superior long term performance at an optimum cost is achieved.</p>			
14. Keywords: Threaded Rod, 0.7 inch Strands , Transfer length, development length		15. Distribution Statement	
16. Security Classification (of this report) Unclassified	17. Security Classification (of this page) Unclassified	18. No. of Pages 158	22. Price

DISCLAIMER

The contents of this report reflect the views of the authors who are responsible for the facts and the accuracy of the data presented herein. The contents do not necessarily reflect the official views or policies of the Nebraska Department of Roads, nor of the University of Nebraska-Lincoln. This report does not constitute a standard, specification, or regulation. Trade or manufacturers' names, which may appear in this report, are cited only because they are considered essential to the objectives of the report. The United States (U.S.) government and the State of Nebraska do not endorse products or manufacturers.

ACKNOWLEDGEMENTS

This project was sponsored by the Federal Highway Administration (FHWA), the Nebraska Department of Roads (NDOR), and the University of Nebraska-Lincoln. The support of the technical advisory committee (TAC) members is gratefully acknowledged. The design team at NDOR Bridge Division is also acknowledged; they spent considerable time and effort in coordinating this project and discussing its technical direction. Concrete industries and Coreslab donated the testing specimens. Special thanks go to Mr. Lyman Freemon, former state bridge engineer, for inspiring the research team to be innovative and visionary. Special thanks also go to Nick Reisers, Alec Stubbe, Nathan Toenies and Dr. Ning Wang, the graduate students participating in this project, as well as Kelvin Lein, the technician at the PKI structural laboratory.

ABSTRACT

The Pacific Street Bridge over I-680 in Omaha, Nebraska is the first bridge in the United States to use 0.7-in. diameter prestressing strands in pretensioned concrete girders. This project was funded by FHWA through NDOR under the Innovative Bridge Research and Deployment (IBRD) program. The bridge construction was completed in August 2008 as a replacement to an existing substandard bridge. The old bridge was 74-ft wide and had four spans that are 44-ft 6-in., 73-ft, 73-ft 6-in., and 30-ft-long. Each span consisted of 11 steel I-girders at 7 ft spacing. The new bridge consists of two identical spans, 98-ft-long each with 17 deg. skew angle.

The bridge has six traffic lanes with a total width of 105-ft 8-in. Each span has 10 girders at a spacing of 10-ft 8-in. Each girder is 35.4 in. deep and pretensioned with thirty 0.7-in. diameter strands that are spaced at 2 in. horizontal spacing and 2.5 in. vertical spacing. Since the design and production of the bridge girders were completed before testing a girder with optimal 2 in. by 2 in. spacing, the use of smaller strand spacing was not allowed.

Large 0.7 in. diameter strands are used in stays of cable-stayed bridges in the US, and for post-tensioned tendons in Europe and Japan. The Pacific Street Bridge over I-680 in Omaha, NE, is the first bridge in the United States to use 0.7 in. diameter strands in precast-pretensioned concrete girders. The cross section area of each strand is 0.294 in^2 , which allows for 35.5% more prestressing than 0.6 in. strands and 92% more prestressing than 0.5 in. strands. This allows for longer spans and/or larger girder spacing. Also, 0.7 inch strands under the same prestressing force as 0.6 in. or 0.5 in. strands result in fewer strands to jack and detension, fewer chucks, and a higher flexural capacity due to the ability to place the strands close to the tension face of the member.

This project combined the use of 0.7 in (17.8 mm) diameter strands with high strength concrete to optimize the use of the large size strands. The average concrete compressive strength was 11,000 psi at 28 days, exceeding the specified minimum strength of 10,000 psi. Overnight release strengths averaged approximately 7000 psi. Special measures were employed to ensure that the developed mix with a water/cementitious materials ratio (w/B) of 0.28 had the necessary workability, consistency, and strength.

The Threaded Rod (TR) continuity system is another innovative feature of this project. TR continuity allows I-girders to be continuous for deck weight, railing, wearing surface, and live loads – or in other words roughly two-thirds of total bridge loads. This is contrasted with the conventional continuity systems, where the bridge is made continuous with reinforcing bars in the deck to resist only the superimposed dead load and live loads, approximately one-third of the total load. The TR continuity system is an economical and practical way to improve the load-carrying capacity of I-girders, reduce girder deflection, and minimize deck cracking over pier supports caused by deck placement and creep effects. TR continuity results in optimal use of materials, an increased span-to-depth ratio, and improved bridge durability. In the Pacific Street Bridge project, the precast-prestressed concrete I-girders (NU900) were connected over the intermediate support using ten Grade 150 high strength threaded 1 3/8” in. diameter rods above the top flange of each girder. The connection between girders was poured along with the intermediate diaphragm to make the girders continuous before deck concrete was placed.

To improve deck durability, longitudinal post-tensioning was applied to the cast-in-place concrete deck. A total of thirty-six 0.6 in. diameter encapsulated mono-strands were used at 3 ft spacing to control deck cracking. This simple and economical method of post-tensioning was done by the general contractor without a need for a specialty contractor.

TABLE OF CONTENTS

DISCLAIMER	IV
ACKNOWLEDGEMENTS	V
ABSTRACT	VI
LIST OF TABLES	X
LIST FIGURES	XI
1. INTRODUCTION	15
1.1 REPORT ORGANIZATION	15
1.2 RESEARCH OBJECTIVES	15
2. TESTING OF 0.7 INCH STRAND	16
2.1 BACKGROUND.....	16
2.2 EXPERIMENTAL INVESTIGATION	18
2.3 DESIGN SUMMARY.....	19
2.4 CONSTRUCTABILITY CHALLENGES	22
2.4.1 Jacking History	22
2.4.2 Strand Anchorage and Chucks.....	25
2.5 FABRICATION OF THE TEST GIRDER.....	29
2.6 STRAND RELEASE AND INITIAL CAMBER	31
2.7 END ZONE CRACKING.....	33
2.8 DECK PLACEMENT	35
2.9 TRANSFER LENGTH MEASUREMENTS	36
2.10 STRAND BENDING AND DIAPHRAGM	41
2.11 TESTING.....	43
2.11.1 Test Set-up.....	44
2.11.2 Compressive Strength.....	45
2.11.3 Predicted Ultimate Load Capacity.....	47
2.11.4 Load Test results	50
2.11.5 Strand Bond.....	58
2.12 CONCLUSIONS.....	61
3. SECOND GENERATION THREADED ROD TESTING	62
3.1 DESIGN OF A TARGET BRIDGE	62
3.2 TESTING PROGRAM.....	71
3.3 CONSTRUCTION AND TESTING	94
3.4 CONCLUSIONS AND RECOMMENDATIONS	114
4. THREADED ROD THIRD GENERATION	115
4.1 INTRODUCTION	115
4.2 LESSONS LEARNED FROM SECOND GENERATION	116
4.2.1 Side Confinement Plate.....	117
4.2.2 Bearing Plate	117
4.2.3 Trough Reinforcement.....	118
4.3 DESIGN AND FABRICATION OF NU 900 GIRDERS	119
4.4 THREADED ROD PLACEMENT AND DIAPHRAGM/INTERFACE BLOCK POUR.....	125
4.5 DECK REINFORCEMENT AND POUR	133
4.6 TESTING OF SPECIMEN	136

	ix
5. CONCLUSIONS.....	145
5.1 USE OF 0.7-INCH-DIAMETER STRANDS	145
5.2 THREADED ROD CONTINUITY SYSTEM	145
APPENDIX A: PACIFIC STREET BRIDGE CONSTRUCTION PHOTOS	147
REFERENCES	156

LIST OF TABLES

TABLE 2.1.1: STRAND DIAMETER AND CORRESPONDING AREA, FORCE, AND CAPACITY	17
TABLE 2.11.3.1: FLEXURAL CAPACITY PREDICTION AND CORRESPONDING REQUIRED APPLIED POINT LOAD	49
.....	
TABLE 2.11.4.1 ULTIMATE AND FAILURE LOAD AND DEFLECTION.....	50
TABLE 2.11.4.2: STAIN AT ULTIMATE LOAD AND AT FAILURE (“+” = COMPRESSION)	51
TABLE 2.11.5.1 STRAND DISPLACEMENT MEASUREMENTS	61
TABLE 3.1.1: DESIGN RESULTS OF THE TARGET BRIDGE	63
TABLE 3.1.2: RESULTS OF USING 0.5-INCH THICK SHOE PLATE	64
TABLE 3.1.3: RESULT AT THE END OF SHOE PLATE AWAY FROM PIER CENTERLINE	65
TABLE 3.1.4: GIRDER SECTION PROPERTIES	66
TABLE 3.1.5: RESULTS OF ADDING 3-INCH CONCRETE TO THE TOP FLANGE.....	67
TABLE 3.1.6: RESULTS OF USING 7.5 FT GIRDER SPACING	68
TABLE 3.1.7: RESULTS OF USING 6-INCH HAUNCH.....	69
TABLE 3.1.8: DESIGN RESULTS OF INCREASING THE WEB WIDTH.....	70
TABLE 3.1.9: COMPARISON OF DESIGN METHODS	71
TABLE 3.2.1: DATA FOR CUTOFF DESIGN	72
TABLE 3.2.2: LOAD.....	80
TABLE 3.2.3: CONCRETE MIX OF INTERFACE BLOCK.....	82
TABLE 3.2.4: INTERFACE BLOCK CONCRETE STRENGTH (FIRST CASTING, DESIGNED STRENGTH IS 6 KSI)	83
TABLE 3.2.5: CONCRETE MIX OF DECK	83
TABLE 3.2.6: DECK CONCRETE STRENGTH (SECOND CASTING, DESIGNED STRENGTH IS 4 KSI).....	84
TABLE 3.2.7: MATERIAL DATA.....	86
TABLE 3.2.8: SPECIMEN EXTERNAL LOAD REQUIRED TO MATCH STRENGTH I	86
TABLE 3.2.9: ANTICIPATE FLEXURAL MOMENT CAPACITY OF THE SPECIMEN	86
TABLE 3.2.10 ANTICIPATE FAILURE LOAD	87
TABLE 3.2.11: RESULT OF ANTICIPATED FAILURE LOAD (KIPS).....	88
TABLE 3.2.12: CAMBER	91
TABLE 3.2.13: LENGTH OF VERTICAL TR ABOVE GIRDER TOP FLANGE	92
TABLE 3.2.14: CONFINEMENT ANALYSIS.....	93
TABLE 3.3.1: COMPOSITE SECTION PROPERTIES	107
TABLE 4.3.1 NU 900.....	120
TABLE 4.6.2.1: PREDICTED LOAD VERSUS ACTUAL LOAD	139

LIST FIGURES

FIGURE 2.1.1: SPOOLED STRANDS	17
FIGURE 2.1.2: STRAND DIAMETER	18
FIGURE 2.3.1: NU900 CROSS SECTION WITH 0.7 INCH STRAND PATTERN	20
FIGURE 2.3.2: NU900 CROSS SECTION WITH DECK ADDED	21
FIGURE 2.3.3: SHEAR AND END ZONE REINFORCEMENT	21
FIGURE 2.4.1.1: JACK PUMP/CONTROLS	24
FIGURE 2.4.1.2: JACK PUMP/CONTROLS	24
FIGURE 2.4.1.3: MONO-STRAND JACKING	25
FIGURE 2.4.1.4: STRAND EXTENSION FROM JACKING	25
FIGURE 2.4.2.1: JACKING END PRETENSIONED STRANDS	26
FIGURE 2.4.2.2: DEAD END PATTERN	27
FIGURE 2.4.2.3: STRAND PROFILE ADJUSTMENT TO SPECIFIED PATTERN	27
FIGURE 2.4.2.4: STRAND PATTERN	28
FIGURE 2.4.2.5: REUSABLE AND ONE-TIME USE CHUCK	29
FIGURE 2.4.2.6: RE-USABLE CHUCKS	29
FIGURE 2.5.1: SHEAR AND CONFINEMENT REINFORCEMENT	30
FIGURE 2.5.2: TYPICAL SHEAR REINFORCEMENT, #4 AT 3 IN SPACING	30
FIGURE 2.5.3: END ZONE REINFORCEMENT, 4 PAIRS OF #6 AT 2 IN SPACING	30
FIGURE 2.5.4: TOP REINFORCEMENT	31
FIGURE 2.5.5: POURING THE GIRDER USING SCC	31
FIGURE 2.6.1: STRAND RELEASE	32
FIGURE 2.6.2: 5/8" TO 3/4" INITIAL CAMBER	32
FIGURE 2.6.3: ROUGHENED SURFACE AND HORIZONTAL SHEAR REINFORCEMENT	32
FIGURE 2.7.1: A1 END ZONE CRACKING	33
FIGURE 2.7.2: A2 END ZONE CRACKING	34
FIGURE 2.7.3: B1 END ZONE CRACKING	34
FIGURE 2.7.4: B2 END ZONE CRACKING	35
FIGURE 2.8.1: LONGITUDINAL #5 DECK REINFORCEMENT	35
FIGURE 2.8.2: POURING THE DECK	36
FIGURE 2.9.1: DEMEC POINT PLACEMENT	37
FIGURE 2.9.2: DEMEC POINT PLACEMENT AND CAMBER	37
FIGURE 2.9.3: DEMEC POINT MEASUREMENT	38
FIGURE 2.9.4: SIDE A1 STRAIN VERSUS DISTANCE	39
FIGURE 2.9.5: SIDE A2 STRAIN VERSUS DISTANCE	39
FIGURE 2.9.6: SIDE B1 STRAIN VERSUS DISTANCE	40
FIGURE 2.9.7: SIDE B2 STRAIN VERSUS DISTANCE	40
FIGURE 2.10.1: FIRST 45 DEGREE STRAND BEND	41
FIGURE 2.10.2: SECOND 45 DEGREE STRAND BEND	42
FIGURE 2.10.3: EIGHT TOP STRANDS BENT 90 DEGREES	42
FIGURE 2.10.4: DIAPHRAGM REINFORCEMENT	43
FIGURE 2.11.1.1 LOAD TEST SETUP POINT LOAD END VIEW	44
FIGURE 2.11.1.2: GIRDER TEST SETUP, DOUBLE JACKS AND FRAMES	45
FIGURE 2.11.2.1 GIRDER COMPRESSIVE STRENGTH VERSUS TIME	46
FIGURE 2.11.2.2 DECK COMPRESSIVE STRENGTH VERSUS TIME	46
FIGURE 2.11.2.3 DIAPHRAGM COMPRESSIVE STRENGTH VERSUS TIME	47
FIGURE 2.11.3.1 STRAIN COMPATIBILITY FOR MAXIMUM PREDICTED FLEXURAL CAPACITY, 5,552 K-FT	48
FIGURE 2.11.3.2 THE REQUIRED APPLIED MOMENT RANGE OF 575 KIPS TO 620 KIPS	49
FIGURE 2.11.3.3 STRAIN COMPATIBILITY FOR MINIMUM PREDICTED FLEXURAL CAPACITY, 5,157 K-FT	50
FIGURE 2.11.4.1: STRAIN EAST SIDE OF GIRDER AT ULTIMATE LOAD AND AT FAILURE LOAD	52

FIGURE 2.11.4.2: STRAIN WEST SIDE OF GIRDER AT ULTIMATE LOAD AND AT FAILURE LOAD	52
FIGURE 2.11.4.3: SHEAR CRACKING IN THE WEB	53
FIGURE 2.11.4.4: SHEAR CRACKS PROPAGATING THROUGH FLANGE.....	54
FIGURE 2.11.4.5: IMMEDIATELY AFTER SHEAR FAILURE.....	54
FIGURE 2.11.4.6: SHEAR CRACKING IN WEB AND SPLIT FLANGE	55
FIGURE 2.11.4.7: FLEXURE CRACKING AT LOAD POINT.....	55
FIGURE 2.11.4.8: BUCKLING OF TOP DECK #5 BAR	56
FIGURE 2.11.4.9: TENSILE DECK CRACKING	56
FIGURE 2.11.4.10: SHEAR REINFORCEMENT NON-BENT IN BOTTOM FLANGE	57
FIGURE 2.11.4.11: CONFINED FLANGE NON-FAILED	57
FIGURE 2.11.4.12: LONGITUDINAL FLANGE CRACKING	58
FIGURE 2.11.4.13: LOOSE STRANDS AFTER FAILURE	58
FIGURE 2.11.5.1: STRAND SLIP MEASUREMENT	59
FIGURE 2.11.5.2: CALIPER DISPLACEMENT GAUGES ATTACHED TO THE LOWER STRANDS- SIDE VIEW.....	60
FIGURE 2.11.5.3: CALIPER DISPLACEMENT GAUGES ATTACHED TO THE LOWER STRANDS- END VIEW	60
FIGURE 2.11.5.4: STRAND BOND PATTERN.....	61
FIGURE 3.2.1: LOAD DIAGRAM AND CUTOFF DESIGN FOR PRECAST SECTION.....	72
FIGURE 3.2.2: LOAD DIAGRAM AND CUTOFF DESIGN FOR COMPOSITE SECTION	73
FIGURE 3.2.3: STEEL LAYOUT	74
FIGURE 3.2.4: PRECAST GIRDER REINFORCEMENT AT SHOE PLATE LOCATION.....	74
FIGURE 3.2.5: SHOE PLATE WITH SHEAR STUDS.....	75
FIGURE 3.2.6: SHEAR STUDS LAYOUT	75
FIGURE 3.2.7: STRENGTHENED PRECAST GIRDER BOTTOM FLANGE WITH SHOE PLATE	76
FIGURE 3.2.8: HORIZONTAL AND VERTICAL REINFORCEMENT OF DIAPHRAGM	76
FIGURE 3.2.9: REINFORCEMENT OF DIAPHRAGM AT ELEVATION VIEW	77
FIGURE 3.2.10: REINFORCEMENT OF DIAPHRAGM AT TOP VIEW	78
FIGURE 3.2.12: GIRDER AND DIAPHRAGM.....	79
FIGURE 3.2.13: CROSS SECTION OF THE SPECIMEN	80
FIGURE 3.2.14: DEFLECTION IN RISA 3D ANALYSIS.....	81
FIGURE 3.2.15: STRESS-STRAIN DIAPHRAGM OF TR.....	84
FIGURE 3.2.16: VERTICAL TR CONSTRUCTION PROCEDURE	90
FIGURE 3.2.17: STEEL LAYOUT IN THE DECK AROUND VERTICAL TR.....	90
FIGURE 3.2.18: GIRDER CAMBER AT EACH 10TH LOCATION	91
FIGURE 3.2.19: VERTICAL TR LENGTH CALCULATION DIAGRAM.....	92
FIGURE 3.3.1: CONFINEMENT AT THE END OF THE GIRDER AND C SHAPE BAR AROUND TR	95
FIGURE 3.3.2: VERTICAL TR, C SHAPE BAR, AND HORIZONTAL SHEAR REINFORCEMENT	95
FIGURE 3.3.3: COMMON END PLATE	96
FIGURE 3.3.4: TEN PIECES 1 3/8" TR PLACED ON TOP WITH 0.75" GAP.....	96
FIGURE 3.3.5: WELDING THE SOLE PLATE AND THE SHOE PLATE TOGETHER	97
FIGURE 3.3.6: FORMING FOR THE DECK AND DIAPHRAGM	97
FIGURE 3.3.7: STRAIN GAGES ON TR	99
FIGURE 3.3.8: STRAIN GAGES ON THE END OF GIRDER	100
FIGURE 3.3.9: GAGES IN THE SOLE PLATE AND GIRDER BOTTOM FLANGE.....	101
FIGURE 3.3.10: STRAIN GAGES ON THE GIRDER BOTTOM FLANGE.....	101
FIGURE 3.3.11: DIAPHRAGM REINFORCEMENT.....	102
FIGURE 3.3.12: HORIZONTAL AND VERTICAL TR.....	102
FIGURE 3.3.13: REINFORCEMENT AT THE END WHERE LOAD WORKS ON.....	103
FIGURE 3.3.14: POURING 6.0 KSI CONCRETE FOR THE DIAPHRAGM AND THE 3.5" HIGH INTERFACE BLOCK	103
FIGURE 3.3.15: PLACE DECK REINFORCEMENT	104
FIGURE 3.3.16: POUR DECK CONCRETE	104
FIGURE 3.3.17: DECK, GIRDER AND DIAPHRAGM AFTER TAKING THE FORMS	105
FIGURE 3.3.18: ACTIVE END OF LOADING.....	105
FIGURE 3.3.19: PASSIVE END OF LOADING.....	106

FIGURE 3.3.20: FINAL FLEXURAL- SHEAR CRACK NEAR THE PIER, P = 324 KIPS	106
FIGURE 3.3.21: DEFLECTION AT 324 K	107
FIGURE 3.3.22: TR STRESS.....	108
FIGURE 3.3.23: STEEL PLATE STRESS.....	108
FIGURE 3.3.24: STRESS OF CONCRETE AT BOTTOM FLANGE	109
FIGURE 3.3.25: ADD A ROLLER TO ACHIEVE LARGER ROTATION	110
FIGURE 3.3.26: LARGE DEFLECTION	110
FIGURE 3.3.27: SPECIMEN FAILURE AT 382 KIPS	111
FIGURE 3.3.28: SHOE PLATE BUCKLED AT THE FACE OF DIAPHRAGM	111
FIGURE 3.3.29: CRACK ON THE TOP AT FAILURE.....	112
FIGURE 3.3.30: NO SLIPPAGE BETWEEN TR AND THE CONCRETE AROUND THEM.....	113
FIGURE 3.3.31: TR STRESS.....	113
FIGURE 3.3.32: STEEL PLATE STRESS.....	114
FIGURE 3.3.33: CONCRETE STRESS AT BOTTOM FLANGE	114
FIGURE 4.2.1: SIDE CONFINEMENT PLATES	117
FIGURE 4.2.2: BOTTOM BEARING PLATE	118
FIGURE 4.2.3: TROUGH REINFORCEMENT.....	119
FIGURE 4.3.1: STRAND PATTERN FOR NU 900 TEST GIRDER.....	120
FIGURE 4.3.2: TEST GIRDER CROSS SECTION	121
FIGURE 4.3.3: BOTTOM FLANGE REINFORCEMENT PLAN VIEW.....	121
FIGURE 4.3.4: 18 INCH END PLATE	122
FIGURE 4.3.5: PLACEMENT OF STRANDS	122
FIGURE 4.3.6: PLACEMENT OF CONFINEMENT REINFORCEMENT	123
FIGURE 4.3.7: PLACEMENT OF WEB AND TOP FLANGE REINFORCEMENT	123
FIGURE 4.3.8: POURING OF CONCRETE	124
FIGURE 4.3.9: GIRDERS AFTER RELEASE.....	124
FIGURE 4.3.10: GIRDER AFTER RELEASE	125
FIGURE 4.4.1: PLACEMENT OF GIRDER	126
FIGURE 4.4.2: 2 INCH BEARING PLATES.....	126
FIGURE 4.4.3: PLACED GIRDERS WITH 4 INCH GAP.....	127
FIGURE 4.4.4: CROSS SECTION WITH INTERFACE BLOCK.....	127
FIGURE 4.4.5: PLACEMENT OF THREADED RODS	128
FIGURE 4.4.6: PLACEMENT OF THREADED RODS	128
FIGURE 4.4.7: PLAN VIEW OF DIAPHRAGM.....	129
FIGURE 4.4.8: SIDE VIEW OF DIAPHRAGM.....	129
FIGURE 4.4.9: 2 INCH FOAM SHEET BELOW DIAPHRAGM	130
FIGURE 4.4.10: DIAPHRAGM REINFORCEMENT	130
FIGURE 4.4.11: FORMWORK AROUND DIAPHRAGM.....	131
FIGURE 4.4.12: FORMWORK FOR INTERFACE BLOCK AND DECK	131
FIGURE 4.4.13: POURING OF DIAPHRAGM	132
FIGURE 4.4.14: POURING OF 3.5 INCH INTERFACE BLOCK.....	132
FIGURE 4.4.15: CONCRETE STRENGTH OF INTERFACE BLOCK	133
FIGURE 4.5.1: FINAL CROSS SECTION WITH DECK.....	133
FIGURE 4.5.2: PLACEMENT OF DECK REINFORCEMENT	134
FIGURE 4.5.3: COMPRESSIVE STRENGTH OF DECK CONCRETE.....	135
FIGURE 4.5.4: DECK POUR	135
FIGURE 4.5.5: DECK POUR	136
FIGURE 4.6.1.1: NORTH END.....	137
FIGURE 4.6.1.2: SOUTH END	137
FIGURE 4.6.1.3: STEEL STRAIN GAUGES.....	138
FIGURE 4.6.1.4: CONCRETE STRAIN GAUGES	138
FIGURE 4.6.1.5: JACK AND LOAD CELL	139
FIGURE 4.6.2.1: FAILURE NEAR DIAPHRAGM	140

	xiv
FIGURE 4.6.2.2: FAILURE NEAR DIAPHRAGM	140
FIGURE 4.6.2.3: LOAD DEFLECTION CURVE	141
FIGURE 4.6.2.4: THREAD ROD STRESS-STRAIN DIAGRAM.....	141
FIGURE 4.6.2.5: ARRANGEMENT OF CONCRETE STRAIN GAUGES	142
FIGURE 4.6.2.6: STRESS-STRAIN DIAGRAM OF DECK, INTERFACE, AND TOP FLANGE.....	143
FIGURE 4.6.2.7: STRESS-STRAIN DIAGRAM OF BOTTOM FLANGE.....	144
FIGURE 4.6.2.8: STRESS-STRAIN DIAGRAM OF BOTTOM.....	144
FIGURE A.1: AERIAL VIEW OF PREVIOUS BRIDGE.....	147
FIGURE A.2: NU 900 GIRDERS	148
FIGURE A.3: PLACEMENT OF DECK	148
FIGURE A.4: GIRDERS AT DIAPHRAGM SECTION	149
FIGURE A.5: BRIDGE CONSTRUCTION.....	149
FIGURE A.6: POST TENSIONING JACK.....	150
FIGURE A.7: EXCAVATION	150
FIGURE A.8: BRIDGE CONSTRUCTION	151
FIGURE A.9: BRIDGE CONSTRUCTION	151
FIGURE A.10: BRIDGE CONSTRUCTION	152
FIGURE A.11: POURING OF CONCRETE	152
FIGURE A.12: POURING OF CONCRETE	153
FIGURE A.13: BARRIERS	153
FIGURE A.14: COMPLETED BRIDGE	154
FIGURE A.15: SHRINKAGE CRACKING.....	154
FIGURE A.16: SHRINKAGE CRACKING.....	155
FIGURE A.17: SHRINKAGE CRACKING.....	155

1. INTRODUCTION

1.1 Report Organization

The report is organized as follows:

- ❖ Section 2 summarizes the testing of the first pretensioned girder with 0.7” strands. The design, fabrication challenges, testing and analysis of the results are presented.
- ❖ Section 3 presents the development of the second generation Threaded Rod continuity system. The design, fabrication, and testing of the developed connection are presented.
- ❖ Section 4 summarizes the lessons learned from constructing Pacific Street Bridge over I 680 related to second generation Threaded Rod Continuity System. The developing of the third generation is presented. The testing of the new connection detail is introduced.
- ❖ Section 5 summarizes the project outcome.
- ❖ Appendix A shows photos of the construction of Pacific Street Bridge over I 680, Omaha, NE.

1.2 Research Objectives

Proposed for this project is a simplification to the current threaded rod continuity system. This simplification entails placing the threaded rods within a few inches of concrete on the top flange of the I-beams over the piers. The first objective of this project is to verify that there is adequate anchorage between the threaded rods and the concrete topping during construction, which would develop the required flexural and shear strengths.

Moreover, the threaded rod method is associated with higher compression stresses in the diaphragm at the bottom flange location than conventional bridge systems for the same bridge

span and girder spacing. Thus, the second objective of this project is to simplify the detailing of this high stress area.

Another objective of this project is to develop the quality control and design criteria required to introduce 0.7 in. diameter strand for precast girders.

2. Testing of 0.7 inch Strand

The Pacific Street Bridge utilizes 0.7 inch strand. Research was done at the University of Nebraska on 0.7 inch strand specifically for the Pacific Street Bridge project. The following chapter discusses this research.

2.1 Background

Larger diameter prestress strands can apply significantly greater prestress force to concrete members. The total prestress force can be increased, and/or the number of prestress strands to install per member can be reduced. In addition, less prestress strands in a member create space for other reinforcement or member details. The amount of required labor should decrease with reduced strand placement. In precast girder design, the level of prestressing is the most important element for increasing the span length, and the 0.7 inch strand has potential to increase the span length for all girder sections.

The cross-sectional area of the 0.7 inch strand is 0.294 in² compared to 0.217 in², and 0.153 in² for 0.6 in. and 0.5 in. diameter strands, respectively. This larger area corresponds to approximately 135 and 192 percent increases in prestress capacity over the 0.6 in. and 0.5 in. diameter strands, respectively. Table 2.1.1 shows a comparison of the 0.5, 0.6, and 0.7 inch strands' cross-sectional area, force applied per strand at initial jacking, force per inch squared based on common AASHTO grid sizes, and the increased capacity of the 0.7 inch strand.

The 0.7 inch strand has never been used before in girder prestressing. The increased efficiency, reduced labor, and potential span length increase from a larger diameter prestress strand has led to the testing of 0.7 inch diameter low relaxation grade 270 ksi strand. Figure 2.1.1 and Figure 2.1.2 show the 0.7 inch strand in spooled conditions and a close up view of the strand diameter.

Table 2.1.1: Strand diameter and corresponding area, force, and capacity

270 ksi LL, Strand Diam. (in)	F_{pi}/in^2 Based on Grid Size					0.7" Capacity Increase (%)		
	A_{ps} (in ²)	$F_{pi}/strand = 0.75 * f_{pu} * A_{ps}$ (kips)	1.75"x 1.75" (kip/in)	2.0"x 2.0" (kip/in)	2.25"x 2.25" (kip/in)	1.75" x 1.75"	2.0" x 2.0"	2.25" x 2.25"
0.5	0.153	30.98	10.12	7.75	6.12	192.2	192.2	192.2
0.6	0.217	43.94	14.35	10.99	8.68	135.5	135.5	135.5
0.7	0.294	59.54	19.44	14.88	11.76	-	-	-



Figure 2.1.1: Spooled strands



Figure 2.1.2: Strand diameter

2.2 Experimental Investigation

When using a larger diameter prestress strand, design and production challenges arise. The transfer length, development length, end zone cracking, strand bond, and constructability issues are investigated in this test. The 0.7 inch diameter strand is noticeably heavier and stiffer than the 0.6 inch diameter strand, so constructability is a concern. Machine retooling, jacking capabilities, strand handling, and strand bending are issues which must be addressed when increasing the strand diameter. A successful production test would include addressing all constructability issues and fabricating the test girder within plant tolerances.

Transfer length can be approximately measured through the use of multiple DEMEC measuring discs and a special caliper. In bridge design, the transfer length for 0.5 and 0.6 inch strands is assumed to be 60 times the strand diameter. Using the same assumption for 0.7 inch strand, the estimated transfer length should be less than or equal to 42 inches.

The development length is based on ultimate flexural stress and effective prestress. Using the AASHTO LRFD formulas developed for 0.5 and 0.6 inch strands, the predicted development

length is approximately 15 feet. The beam will be point loaded at this distance from the end of the girder. If ultimate flexural capacity is reached without strand slip, the development length is less than or equal to the assumed value.

End zone cracking is a concern because higher prestress force in smaller areas can lead to greater end zone cracking. Increased span length or wider girder spacing leads to higher shear forces applied to the girder sections and can be the limiting factor for the NU section. Therefore, the $0.25f_c b_v d_v$ shear strength limit is also tested. A successful test would include no end zone cracking and achieving ultimate flexural capacity prior to shear failure.

The amount of 0.7 inch prestress strands placed in this first test girder is a modest attempt and has a slightly wider spacing than the standard 2" by 2" spacing for 0.6 inch strands. A successful load test would include reaching the predicted ultimate flexural capacity without strand slip.

2.3 Design Summary

A summary of the design is shown below, and cross sections are shown in Figure 2.3.1 and Figure 2.3.2. A NU900 girder with a span of 39 ft. has been designed for the test. A total of 24 strands were tensioned to a force of approximately 60 kips/strand, not including additional loss force applied.

The end zone reinforcement was based on the paper "End Zone Reinforcement for Pretensioned Concrete Girders" by Tuan et. al. The shear reinforcement is based on applying a point load at a distance of 15 feet from the end of the girder (14 feet from the bearing centerline) on a simple span. The bearing point is centered at 1 ft. from the end of the girder. The $0.25f_c b_v d_v$ shear strength limit is exceeded in this section design. When using two #4 bars at a

spacing of 3 inches, the ratio is approximately 0.254 at the point of loading and 0.35 at the bearing location. The shear and end zone reinforcement details are shown in Figure 2.3.3.

- 0.7 inch strand
- NU900
- Length = 39'-0"
- 24 -0.7" Gr. 270 strand @ $f_{pi} = 0.75 \cdot 270 = 202.5$ ksi
- $F_i = 59.5$ kips/strand
- Girder strength at release, 28 day: 6 ksi, 8 ksi; Self Consolidating Concrete
- Deck placement second stage: 6" thick deck, width of girder top, 8 ksi at 28 day

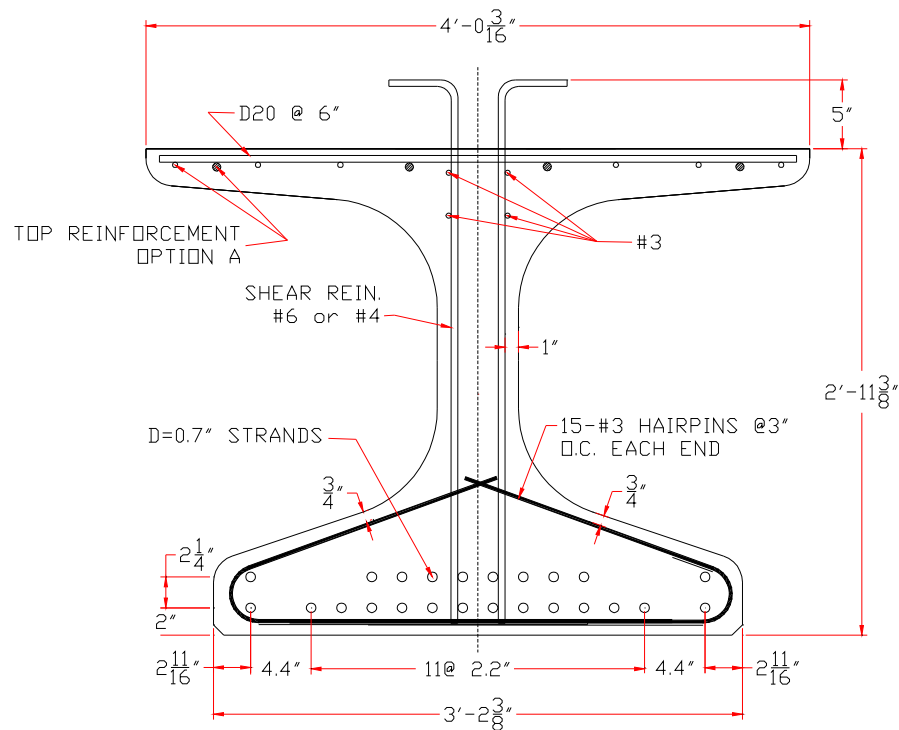


Figure 2.3.1: NU900 cross section with 0.7 inch strand pattern

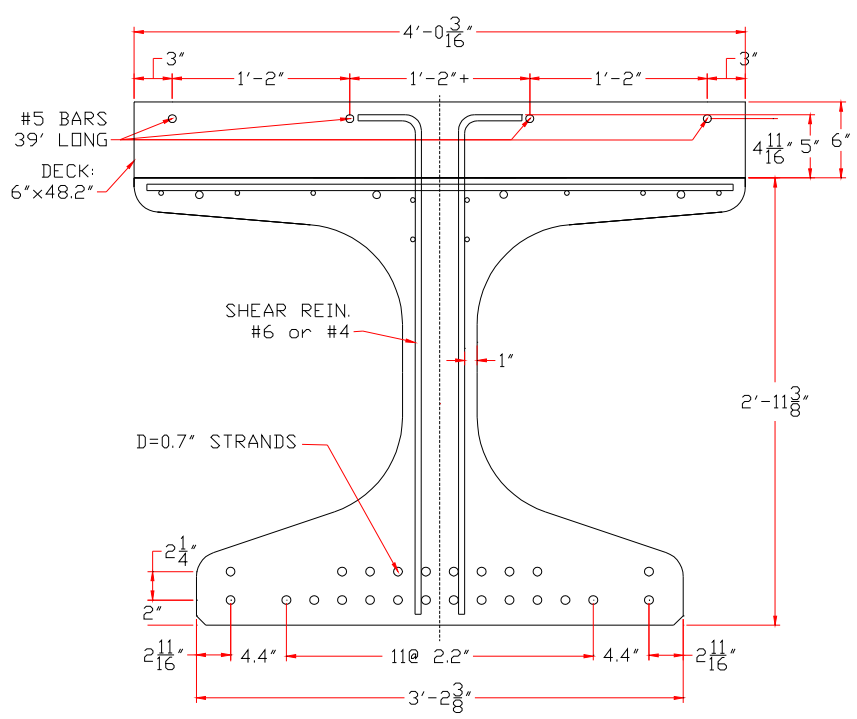
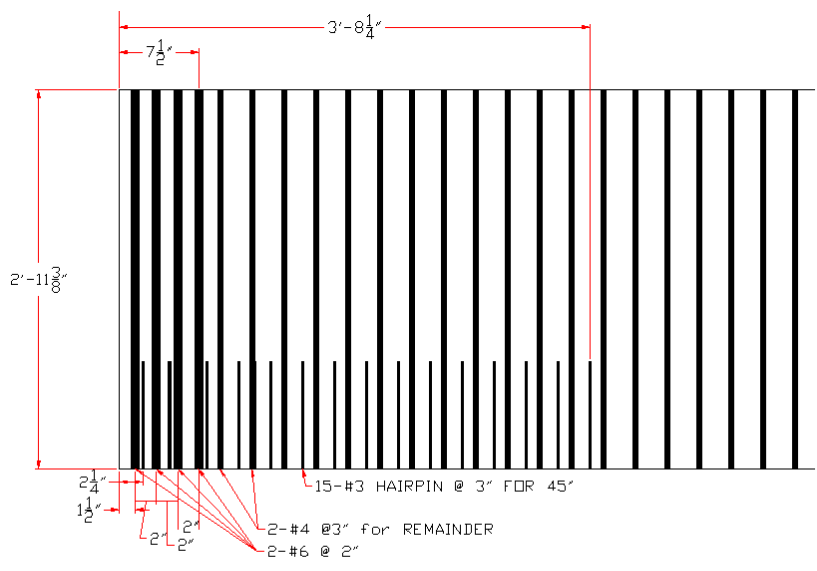


Figure 2.3.2: NU900 cross section with deck added



END SECTION A

Figure 2.3.3: Shear and end zone reinforcement

2.4 Constructability Challenges

When switching to a larger size prestressing strand, constructability becomes an issue as challenges arise to meet the larger prestress force required. Strand jacking is a problem for monostrand jacks as the prestressing force required for 0.7” strand exceeds most 0.6” capable jacks.

2.4.1 Jacking History

Coreslab Structures has both a long and short prestressing bed. The long bed has a dead anchor end and a prestressing end. Rather than monostrand jacking, the prestressing end uses large jacks connected to a single head to tension and release all strands at one time. Releasing the strands gradually prior to cutting is a superior method over torch cutting tensiled strands and having large instantaneous forces applied to the member. This bed and prestressing method is the typical production for girders. The short bed utilizes two dead ends, monostrand jacking, and releasing the strands by torch cutting.

Even though the long bed has a superior prestressing system, the short bed was utilized for the test girder fabrication. The length of each strand must be the same as the bed length, and when the bed is partially unoccupied, the unoccupied length of strand is wasted. The test girder is 39 feet long, so the short bed wasted much less strand. The short bed is also off of the normal production line, and time requirements were favorable to place and take measurements for the DEMEC points prior to strand release at a specific concrete compressive strength.

Along with the benefits of using the short bed, monostrand jacking became a challenge. As shown in Table 2.1.1, the required force applied for 75 percent ultimate strength is 59.5 kips for the 0.7” strand. In addition, anchorage seating losses of about 3.5 kips per strand must be added to the required initial force. The total force required is therefore about 63 kips per strand and

exceeded the monostrand jack capacity. The jack capacity of about 50 kips was designed to tension a maximum strand size of 0.6” to 75 percent ultimate strength plus the additional anchorage losses.

Three solutions to this problem were available using the tools owned by Coreslab and UNL. The preferred method was to increase the monostrand jack capacity enough by installing upgraded valves in the pump. As long as this method worked, it was best because the standard equipment owned by Coreslab could be utilized for this project and potential future work. The jack owned by Coreslab was produced by G.T. Bynum Company of Tulsa Oklahoma.

The second solution was to use the DSI monostrand jack owned/permanently lent by UNL for research purposes. The jack is rated for 65 kips, but the jaw size only had capacity for 0.6” strand. At this time, these jaws are available through special order but time restraints did not allow for this option to be used. The third solution was to use a center-hole jack available from UNL. These jacks have a hollow cylindrical ram which allows a strand to pass through. The capacity of the jack was not an issue but the gripping strand during tensioning was not convenient as there is no guide or jaws.

After the valves were updated, the G.T. Bynum monostrand jack capacity exceeded the required amount needed for 0.7” strand. Therefore, the standard equipment owned by Coreslab was upgraded to have 0.7” strand prestressing capability. Photos of the jack, controls, and pump are shown in Figure 2.4.1.1 and Figure 2.4.1.2.



Figure 2.4.1.1: Jack pump/controls

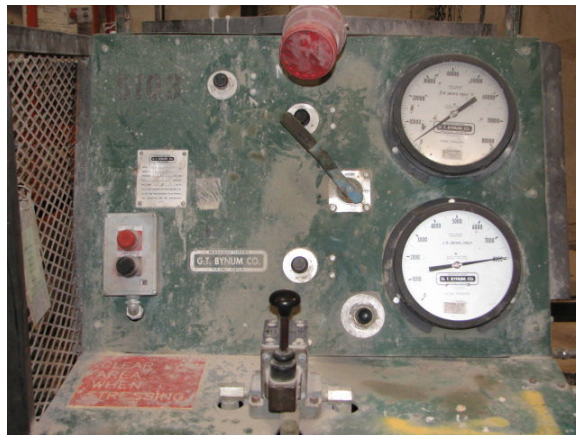


Figure 2.4.1.2: Jack pump/controls

The monostrand jack (see Figure 2.4.1.3 through Figure 2.4.1.4) consists of an open channel beam with a ram attached to a coupling head. The open channel beam transmits the force applied by the ram to the seated anchorage and serves as a guide for the ram and coupling head. Two chucks are used per strand with this monostrand jack because it does not have jaws to grip the strand. One chuck is seated against the anchorage block and the other is movable with the extension of the strand. The coupling head pulls against the movable chuck and applies the force

to the strand. The seated anchorage grips the strand upon jack release, and the strand is tensioned.

The chucks are initially seated and the slack is taken out of the strand using a low tension force. Then, the strands are tensioned to their full capacity in a pattern dictated by the engineer.



Figure 2.4.1.3: Mono-strand jacking



Figure 2.4.1.4: Strand extension from jacking

2.4.2 Strand Anchorage and Chucks

The 0.7” strand anchorages must be strong enough to withstand the greater force applied to them. The strand patterns at the anchorages shown in Figure 2.4.2.1 - 2.4.2.2 are not

representative of the strand pattern achieved in the precast piece. The patterns at the anchorage ends are governed by the jack head placement and the ability to fit the chucks next to one another as the strands pass through the vertical steel plates and then through the holes of the horizontal plate.

Since the chucks for 0.6" and 0.7" have the same outer diameter, this arrangement problem occurs with the 0.6" strand, too. Thus, this is not a new challenge to overcome. The strand pattern is adjusted to the section pattern required as the strands travel from the anchorage to the end section (see Figures 2.4.2.3 - 2.4.2.4). The end section has the desired pattern applied by passing the strands through a pre-fabricated guide. As long as the anchorage pattern is not significantly different, the desired pattern adjusts to the sectional pattern.



Figure 2.4.2.1: Jacking end pretensioned strands

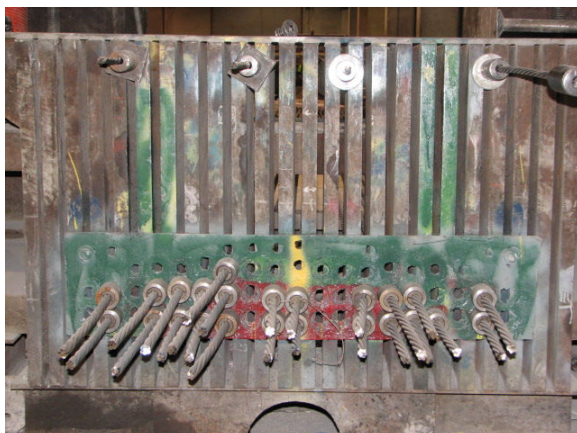


Figure 2.4.2.2: Dead end pattern



Figure 2.4.2.3: Strand profile adjustment to specified pattern

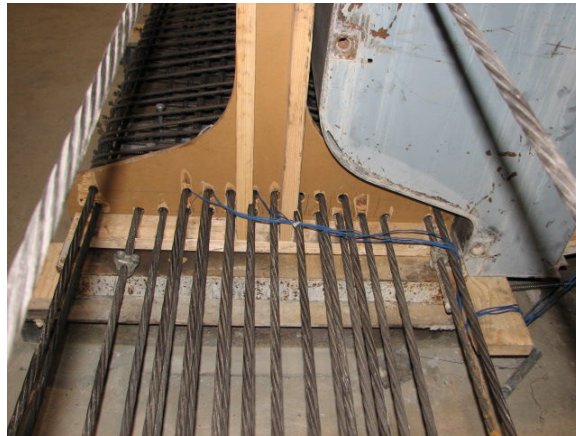


Figure 2.4.2.4: Strand pattern

Two types of chucks were used for this test girder: one time use and re-useable. The one time use and re-useable chucks are shown in Figures 2.4.2.5 – 2.4.2.5.6. Both have an outer diameter of 2 inches. The total length of the re-useable chucks is 4 ½ inches and 2 1/8 inches for the one time use chucks.

The one-time chucks are cheaper and worked well for the non-jacking end but not for the jacking end. The jaws of the onetime chucks seat onto the strand during jacking and cannot be released for successive jacking. The one time use chucks have only two conical tapered jaws versus three in the re-useable chucks. Re-useable chucks very similar to 0.6 inch re-useable chucks were purchased for the 0.7 inch strand. The larger size strand requires a larger inner diameter chuck but not a larger outer diameter. The reusable chucks worked well during the prestressing of the test beam, but some did become non-releasable.



Figure 2.4.2.5: Reusable and one-time use chuck



Figure 2.4.2.6: Re-usable chucks

2.5 Fabrication of the Test Girder

After the strands were tensioned into the desired pattern, the remaining fabrication could begin. Fabrication did not provide any unusual difficulties with the use of the 0.7" strand. The shear, confinement, and end zone reinforcement are shown in Figures 2.5.1-2.5.3. The top reinforcement and pouring the girder using self consolidating concrete are shown in Figures 2.5.4 - 2.5.5.



Figure 2.5.1: Shear and confinement reinforcement



Figure 2.5.2: Typical shear reinforcement, #4 at 3 in spacing



Figure 2.5.3: End zone reinforcement, 4 pairs of #6 at 2 in spacing



Figure 2.5.4: Top reinforcement



Figure 2.5.5: Pouring the girder using SCC

2.6 Strand Release and Initial Camber

Figure 2.6.1 shows the strands being cut. As discussed, this short prestressing bed did not have the ability to release the strands gradually, so torch cutting had to be used. The strands were cut with two torches simultaneously on each end. The strands were cut from outside inwards, and the top four strands were released prior to the bottom strands.

The initial camber was approximately $\frac{5}{8}$ to $\frac{3}{4}$ inch and is shown in Figure 2.6.2. The horizontal shear reinforcement and roughened surface are shown in Figure 2.6.3. The vertical shear reinforcement is bent 90 degrees at about 5 inches above the top of the concrete girder.



Figure 2.6.1: Strand release



Figure 2.6.2: 5/8'' to 3/4'' initial camber



Figure 2.6.3: Roughened surface and horizontal shear reinforcement

2.7 End Zone Cracking

The girder experienced a slight amount of end zone cracking. The majority of the cracks were very small and difficult to see without very close inspection. The cracks were highlighted with marker and are shown in Figures 2.7.1 - 2.7.4.



Figure 2.7.1: A1 end zone cracking



Figure 2.7.2: A2 end zone cracking



Figure 2.7.3: B1 end zone cracking



Figure 2.7.4: B2 end zone cracking

2.8 Deck Placement

The deck was placed 6 inches thick over the width of the girder top in a second casting. A minimal amount of reinforcement was placed in the longitudinal direction. The deck reinforcement and deck pouring are shown in Figure 2.8.1 and Figure 2.8.2. Four number 5 bars are continuous throughout the length of the girder with 1 inch of clear cover.



Figure 2.8.1: Longitudinal #5 deck reinforcement



Figure 2.8.2: Pouring the deck

2.9 Transfer Length Measurements

To measure the transfer length, a series of 19 DEMEC points were placed on each end and each side of the girder bottom flange at the centroid of the prestressing strands (see Figures 2.9.1-2.9.3). DEMEC point readings were taken before and 20 minutes after releasing the prestressing force and at 4, 7, 14, 21, and 29 days after releasing the prestressing strands. The initial measurement is considered to be the baseline. A W.H. Mayes & Son caliper gauge was used to measure the distance between DEMEC points, and the strain in the concrete was calculated from the change in distance between readings. The concrete strain at the centroid of the strands is then plotted along the length of the girder.

After prestress release, the prestressed concrete strain is zero at the girder ends, then increases, and eventually becomes relatively constant as the distance from the girder end increases. The point where the strain becomes constant distinguishes where all of the prestressing forces are transferred to the concrete. The transfer length can be determined by measuring the distance from the end of the girder to the point where 95 percent of the maximum concrete strain is measured (Girgis, Tuan).

Starting 1 inch from the girder end, the 19 DEMEC points were placed every 4 inches for a distance of about 77 inches. The caliper is gauged at approximately 8 inches, so the DEMEC points are used in successive pairs such as points 1-3, 2-4, 3-5, 4-6...etc. The predicted transfer length for the 0.7 inch diameter strand is 42 inches and 35 inches based on the AASHTO LRFD and ACI Codes, respectively. The number of DEMEC points placed was to ensure accurate readings and extend beyond the predicted transfer length. The centroid of the strands is at 2.94 inches above the bottom of the girder. The DEMEC point placement and using the caliper gauge are shown in Figures 3.9.1-3.9.3.



Figure 2.9.1: DEMEC point placement



Figure 2.9.2: DEMEC point placement and camber



Figure 2.9.3: DEMEC point measurement

After taking readings over time, the strain versus distance from the girder ends is plotted for each side of the girder. These plots are shown in Figures 2.9.4 - 2.9.7. The strain stabilizes after about 35 inches from the end of the girder. Thus, the transfer length occurs at approximately 35 inches from the girder end and is closely predicted by the ACI code formula of 50 strand diameters.

After converting the change in distance results from the DEMEC point measurements, strain was obtained at various time stages.

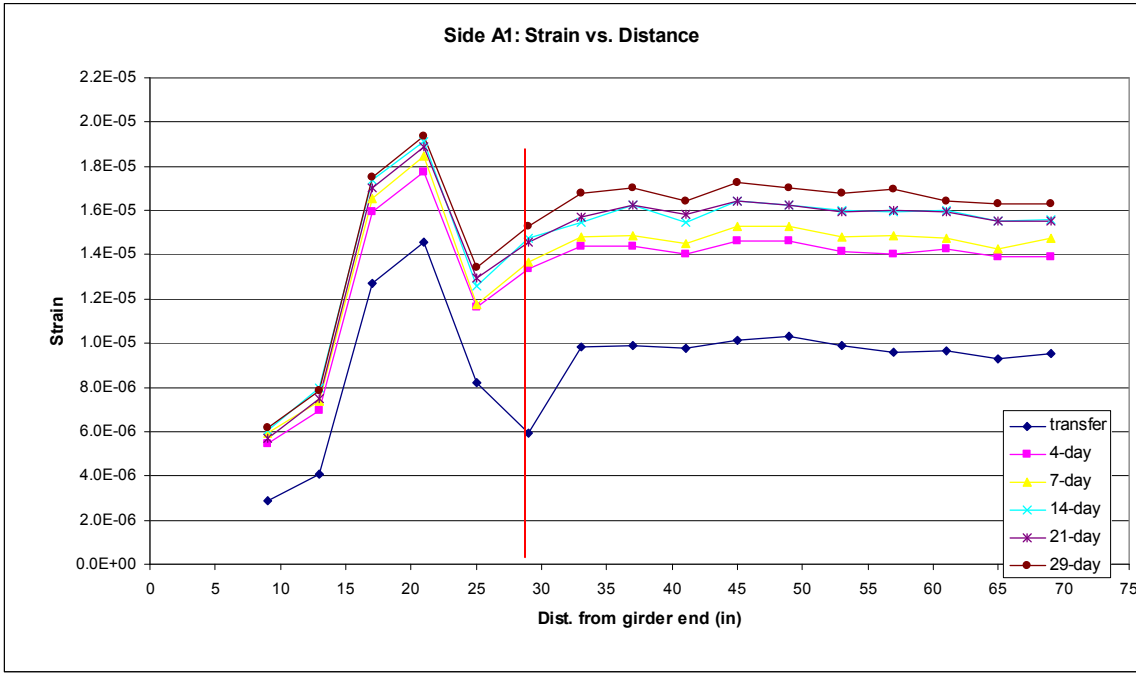


Figure 2.9.4: Side A1 strain versus distance

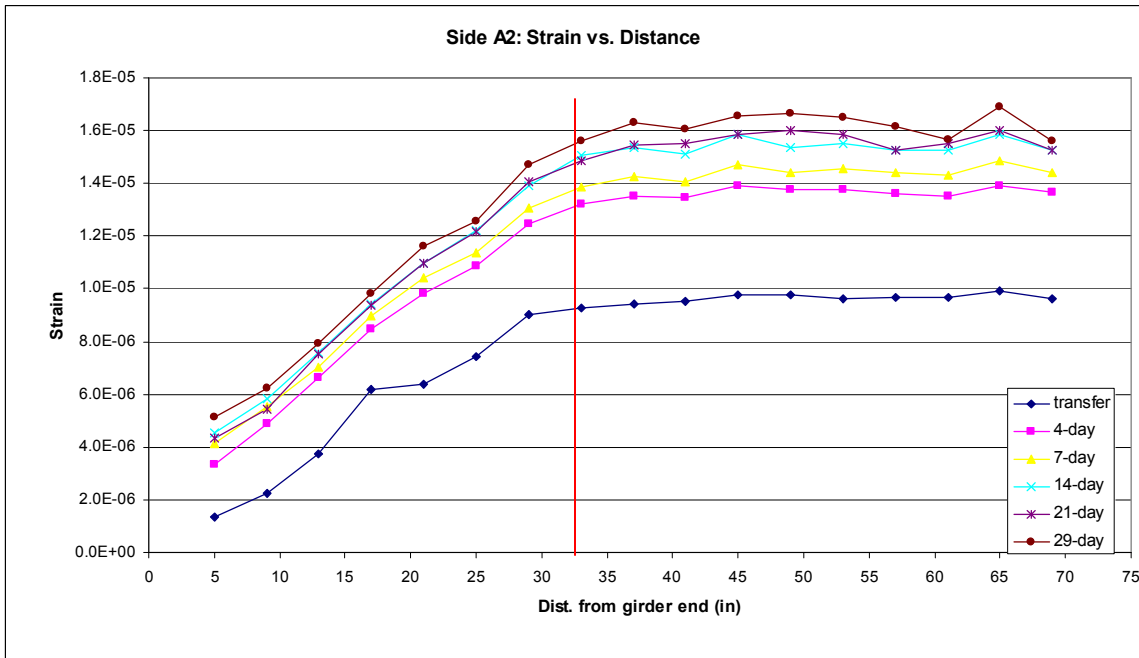


Figure 2.9.5: Side A2 strain versus distance

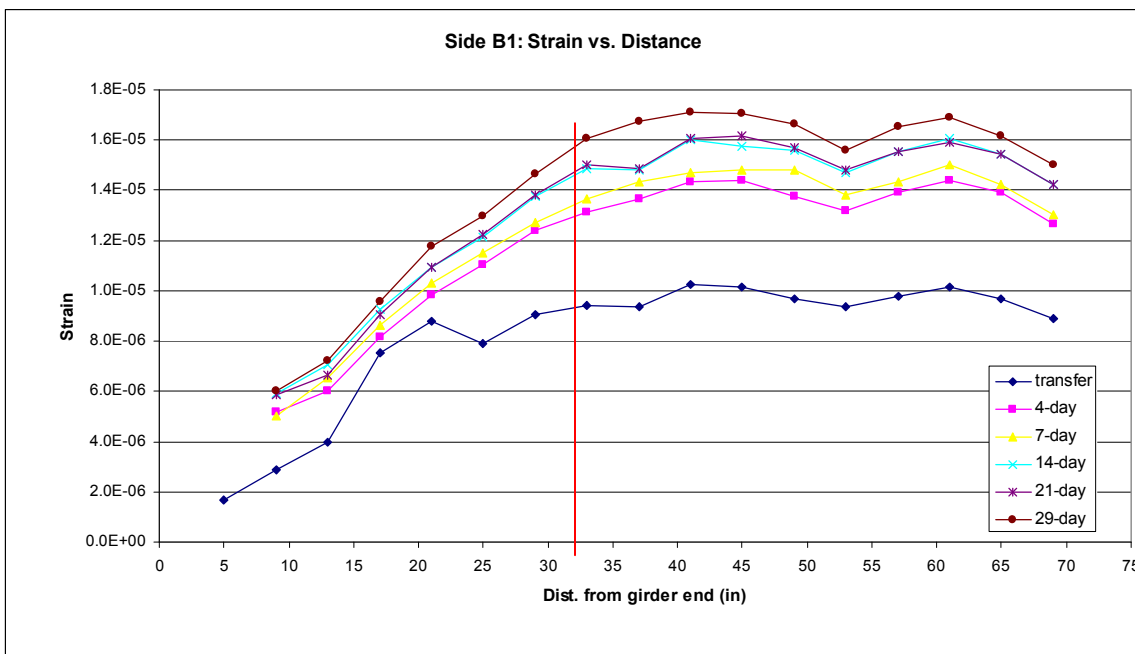


Figure 2.9.6: Side B1 strain versus distance



Figure 2.9.7: Side B2 strain versus distance

2.10 Strand Bending and Diaphragm

A very good practice to develop longitudinal force required for shear is to leave the strands extended about 18 inches past the girder end, bend the strands into a 90 degree curve, and pour a diaphragm around reinforced strands. The center 8 strands of the top row were bent, and a reinforced diaphragm was constructed on each end of the girder to assure the longitudinal force required for shear was developed. The 90 degree bend is achieved in two successive 45 degree bends with a homemade reverse scissor tool.

The upper strands were selected for bending because the lower strands will experience the highest ultimate strain out of the strand layers. Therefore, they are more critical in measuring strand slip for development length determination. Bending the 0.7" strands was not noticeably different than bending 0.6" strands and certainly can be done. Figures 2.10.1 - 2.10.3 illustrate the strand bending tool used and the 90 degree bend strands in the final state. Figure 2.10.4 shows the reinforcement placed in the diaphragm to anchor the bent strands and distribute the longitudinal force.



Figure 2.10.1: First 45 degree strand bend



Figure 2.10.2: Second 45 degree strand bend



Figure 2.10.3: Eight top strands bent 90 degrees



Figure 2.10.4: Diaphragm reinforcement

2.11 Testing

The flexural test is used to determine if the predicted development length for 0.7” strand is correct. The applied point load is asymmetrical for the beam and is placed at the predicted development length. If the beam develops ultimate flexural capacity without strand slip, then the development length is equal to or less than the predicted value. The development length was calculated based off of the formulas used for 0.6” and 0.5” strand. However, no test data exists to support the assumption that the 0.7” strand will follow the same formula.

The test is also used to test the shear force capacity for the section design because the $0.25f_c b_v d_v$ shear strength limit is exceeded in this section design. In a regular continuous for live load bridge with negative moment sections, the moment is high at the critical section for shear. However, in this simple span flexural test setup, the shear force is nearly constant from the point load to the support. In addition, the moment in a simple span near the supports is not significant. Since the Modified Compression Field Theory of AASHTO Sec 5-8 shear reinforcement equations utilize both applied moment and shear force, the greatest shear demand occurs at the point loading and spreads for a distance d_v from the point loading. The limit is exceeded as the section is analyzed going toward the bearing.

2.11.1 Test Set-up

The test set-up consists of seating the 39' beam on simple span supports. The beam has a roller placed underneath each end with 12" steel plates on top of the roller to distribute the force to the bottom of the girder. The rollers are placed 12" on center from the end of the beam, and the centerline to centerline distance between rollers is 37'. Below the rollers are 3' by 3' concrete blocks. Figures 2.11.1.1 is a diagram of the test set-up.

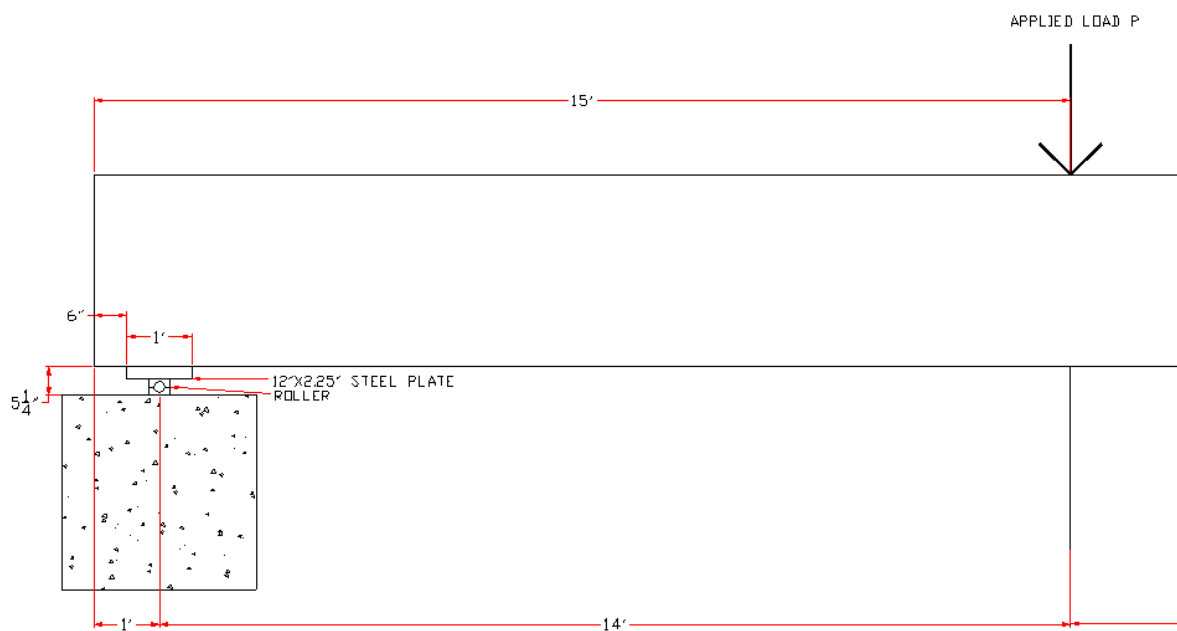


Figure 2.11.1.1 Load test setup point load end view

The actual girder is shown in Figure 2.11.1.2 and is the 15' end of the asymmetrical load. The diaphragm is visible on the end as well as the strain gauges placed in a vertical line 3 feet from the centerline of loading. The strain gauges were placed away from the point load to avoid premature failure of the gauge by cracking or spalling concrete. A deflection gauge was attached exactly below the center of the load point, 15 feet from the girder end.

Two 400 kip jacks were used in a series to achieve the predicted capacity required to reach ultimate flexural strength. The two jack loading was balanced on a spread beam which had a 24” by 30” base plate loading to neoprene pads and then to the girder. The load was applied in 50 kip increments up to failure.



Figure 2.11.1.2: Girder test setup, double jacks and frames

2.11.2 Compressive Strength

The compressive strengths for the various components of the girder are determined to more accurately predict the capacity of the girder. Plots of the compressive strength versus time are shown in Figures 2.11.2.1 - 2.11.2.3.

The final compressive strength of the girder is somewhere between 7.5 ksi and 8.0 ksi. In order to imitate usual f_{ci} required at release between 6.0 and 6.5 ksi, the strength was somewhat compromised. If the final strength was too high, then the release strength would have been more easily passed. The final compressive strength was more closely restricted to 8.0 ksi, so strain measurements at the typical release strength could be taken. The compressive strengths used to predict ultimate load capacity the day of testing are 7.5-8.0 ksi for the girder and 8.5-9.0 ksi for

the deck. The diaphragm just had to be a minimum compressive strength of 6 ksi, which was exceeded.

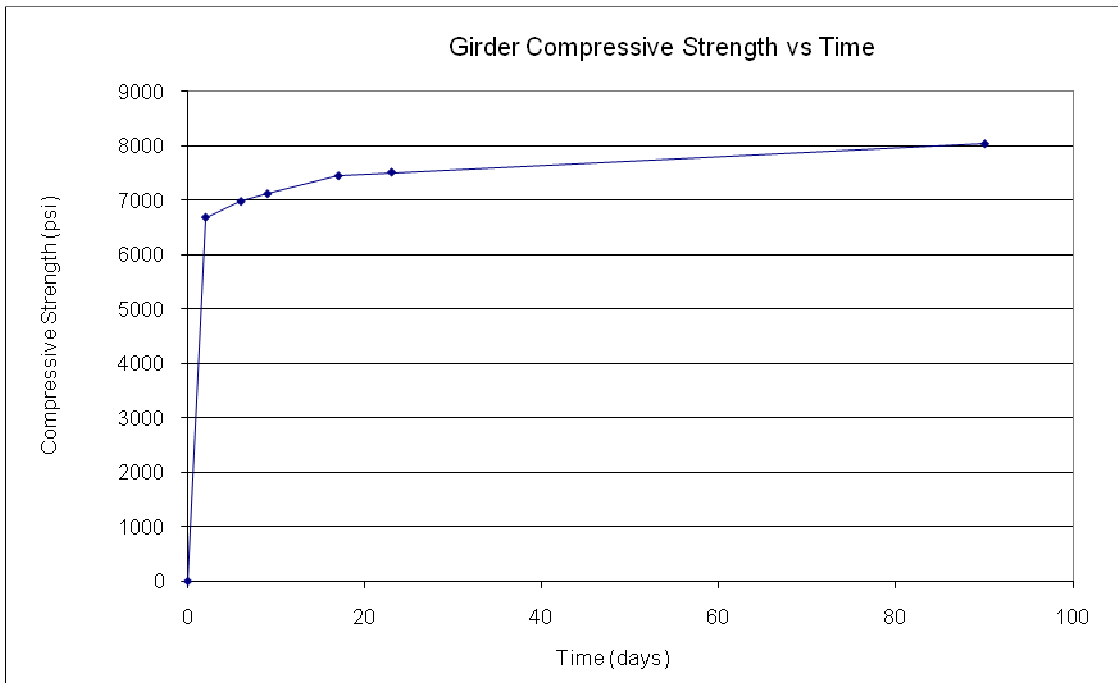


Figure 2.11.2.1 Girder compressive strength versus time

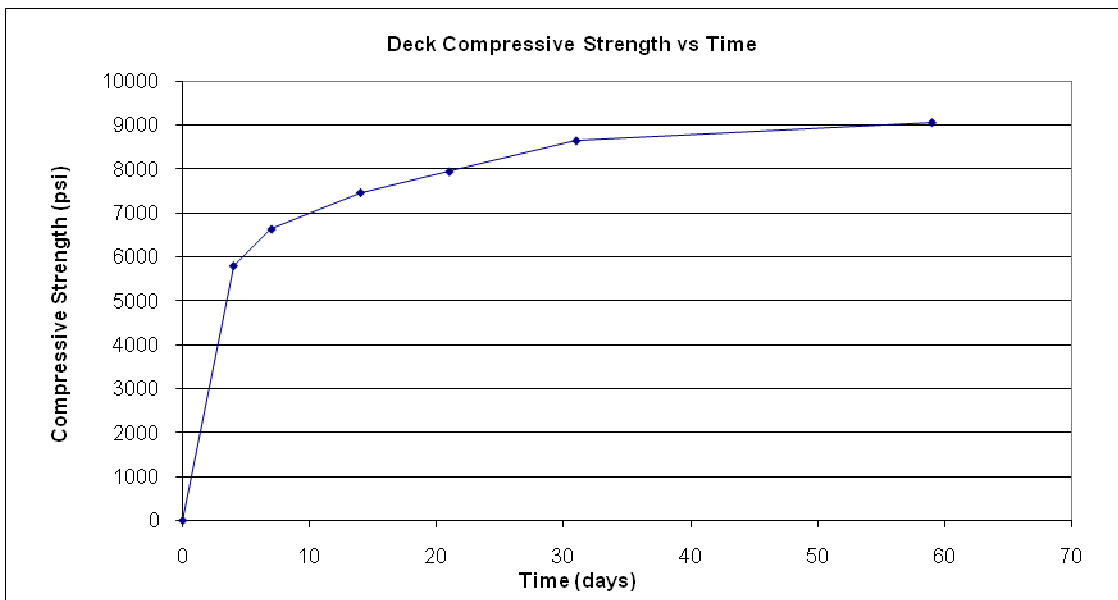


Figure 2.11.2.2 Deck compressive strength versus time

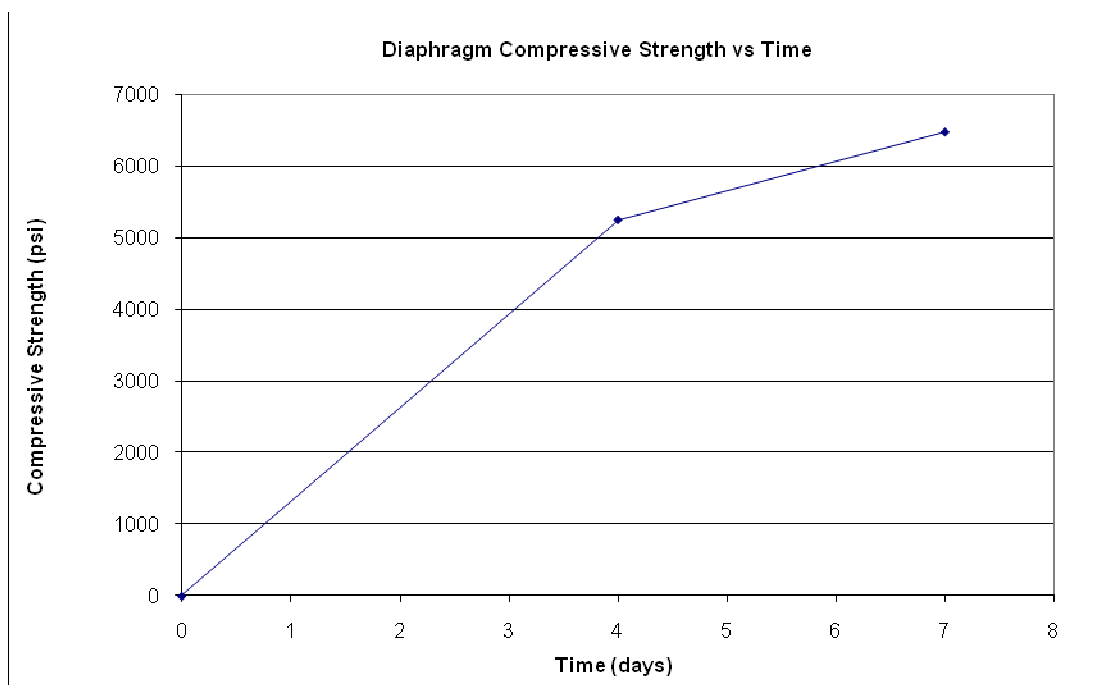


Figure 2.11.2.3 Diaphragm compressive strength versus time

2.11.3 Predicted Ultimate Load Capacity

A parametric study of the effects of concrete strength, ultimate concrete strain, thickness of deck, and depth of tensile steel was performed to predict the ultimate load applied to the test beam. First, maximum values were assumed for concrete strength, usable ultimate concrete strain, deck thickness, and depth of tensile steel.

A maximum theoretical value for ultimate capacity was then calculated from these assumptions: $f'_{cdeck} = 9.0$ ksi, $f'_{cgirder} = 8.0$ ksi, $E_{cu} = 0.003$, and depth of prestressing steel is at the specified 2 and 4.25 inch points. A spreadsheet was used to calculate the flexural capacity using strain compatibility, and the summary is shown in Figure 2.11.3.1. The highest predicted capacity is 5,552 k-ft. The moment due to self weight is subtracted from the section capacity, and then $P_{required}$ was determined from a point load on a simple span.



Figure 2.11.3.1 Strain compatibility for maximum predicted flexural capacity, 5,552 k-ft

After determining the theoretical maximum flexural capacity, the concrete strength was reduced by 0.5 ksi, the depth of tensile steel was reduced by 0.5 in., the thickness of the deck was reduced by 0.5 in., and the ultimate concrete strain was reduced. A summary of the changes and the results of the moment and load required are shown in Table 2.11.3.1. The lowest moment capacity predicted was 5,157 k-ft and the strain compatibility results are shown below.

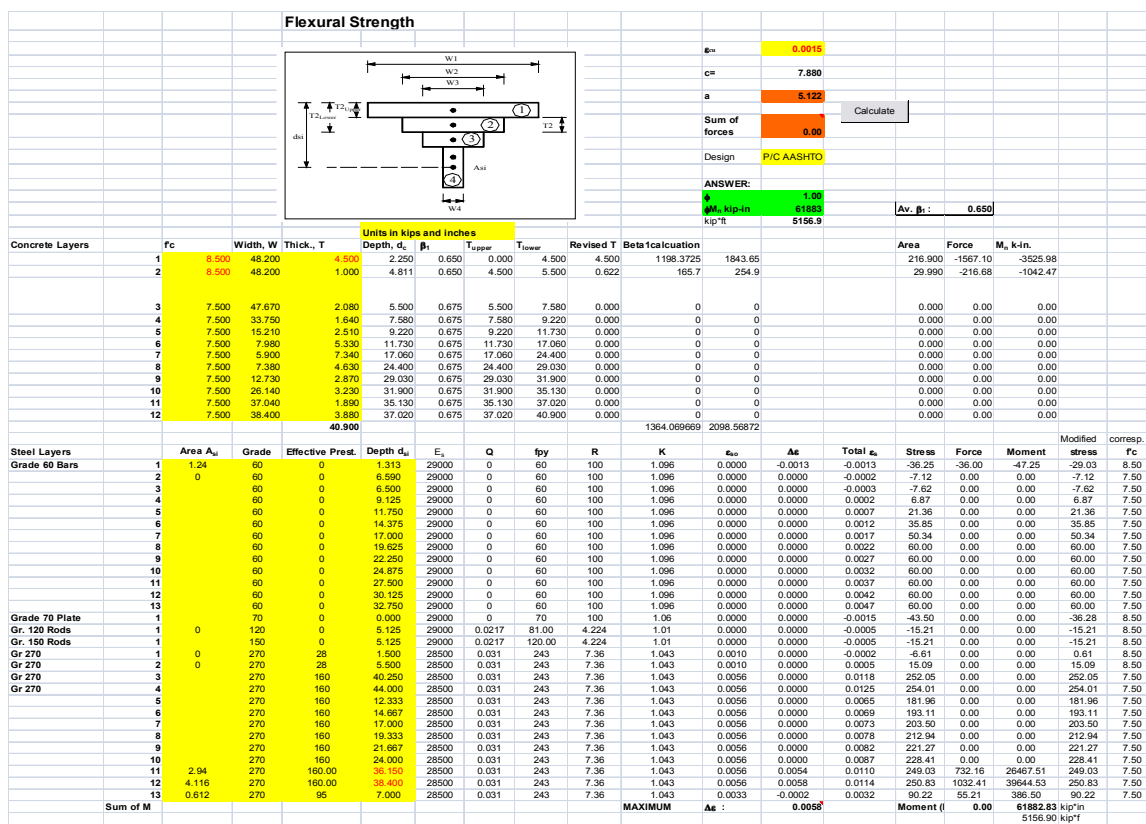


Figure 2.11.3.2 The required applied moment range of 575 kips to 620 kips.

Table 2.11.3.1: Flexural capacity prediction and corresponding required applied point load

	Capacity (k-ft)	Self weight Moment	M _{remain}	P _{Apply} (kips)
1 Max Predicted	5551.8	157.9	5393.9	619.8
2 Reduce Girder f'c; reduce Steel Depth 0.5"	5471.6	157.9	5313.6	610.6
3 2 + reduce Ecu = 0.0025	5433.4	157.9	5275.4	606.2
4 2 + reduce Ecu = 0.0020	5377.7	157.9	5219.8	599.8
5 2 + reduce Ecu = 0.0015	5286.8	157.9	5128.9	589.3
6 5 + reduce deck thickness to 5.5"	5204.6	157.9	5046.7	579.9
7 6 + reduce deck f'c 0.5 ksi	5156.9	157.9	4999.0	574.4
8 2 + reduce Ecu = 0.00129	5222.8	157.9	5064.9	582.0

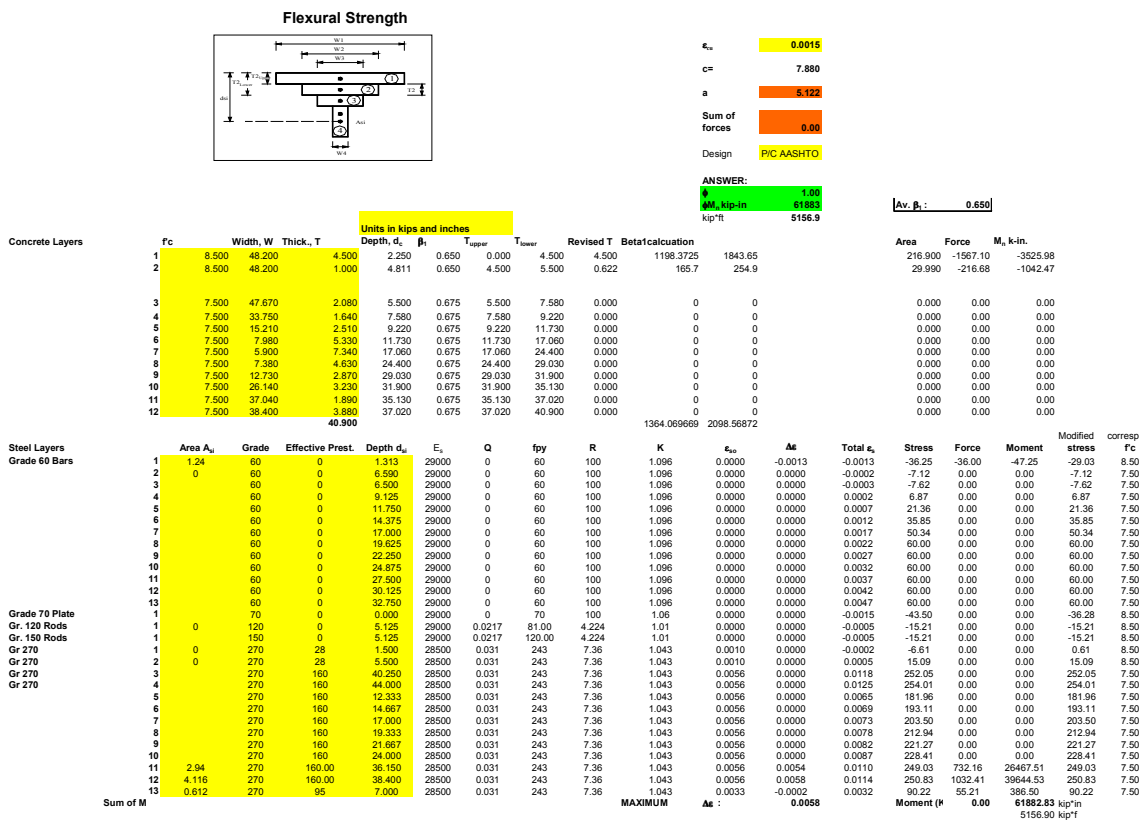


Figure 2.11.3.3 Strain compatibility for minimum predicted flexural capacity, 5,157 k-ft

2.11.4 Load Test results

The beam exceeded the lower predicted ultimate flexural capacity of 5157 k-ft and failed at the middle predicted capacity of 5378 k-ft. The ultimate applied load was 600.4 kips and failed in shear at 572.1 kips. Shown in Table 2.11.4.1 is the ultimate load and failure loads achieved along with the corresponding deflections. The beam reached a maximum deflection of 2.93 inches 15' from the end of the girder.

Table 2.11.4.1 Ultimate and failure load and deflection

	Load (kips)	Deflection (in)
Ultimate	600.4	-2.79
Failure	572.1	-2.93

A total of 10 strain gauges were attached 3' from the centerline of the load point and 12' from the girder end. On each side, 5 strain gauges were placed in a vertical column. The gauges were placed near the surface of the deck, near the surface of the top girder flange, low and high web positions, and at the centroid of the prestressing tensile steel. The following Table 2.11.4.2 is a summary of the strain values at various heights of the girder 12' from the girder end. Both ultimate load and at failure load strains are summarized.

Table 2.11.4.2: Stain at ultimate load and at failure (“+” = compression)

		Dist from	Dist from	μE at			
		top	bottom	μE at P_u	E at P_u	$P_{failure}$	E at $P_{failure}$
1	1 Top East	1.125	34.25	1288.4	0.00129	1231.061	0.001231
2	2 East	6.875	28.5	390.002	0.00039	442.3345	0.000442
3	3 East	17	18.375	687.799	0.00069	671.6009	0.000672
4	4 East	26	9.375	-5563.45	-0.00556	-3627.14	-0.00363
5	5 East	32.435	2.94	-336.423	-0.00034	-343.9	-0.00034
6	1 Top West	1.5	33.875	1067.833	0.00107	884.6691	0.000885
7	2 West	6.75	28.625	335.1774	0.00034	365.0817	0.000365
8	3 West	17	18.375	-743.87	-0.00074	-216.806	-0.00022
9	4 West	26	9.375	-4842.01	-0.00484	-7945.82	-0.00795
10	5 West	32.435	2.94	-419.906	-0.00042	-431.12	-0.00043

The strain at ultimate load is a maximum value of 0.00129 recorded from the top east strain gauge 1.125 inches from the top of the deck. In Table 2.11.4.2, compression is positive. The strains are plotted in Figure 2.11.4.1 - 2.11.4.2.

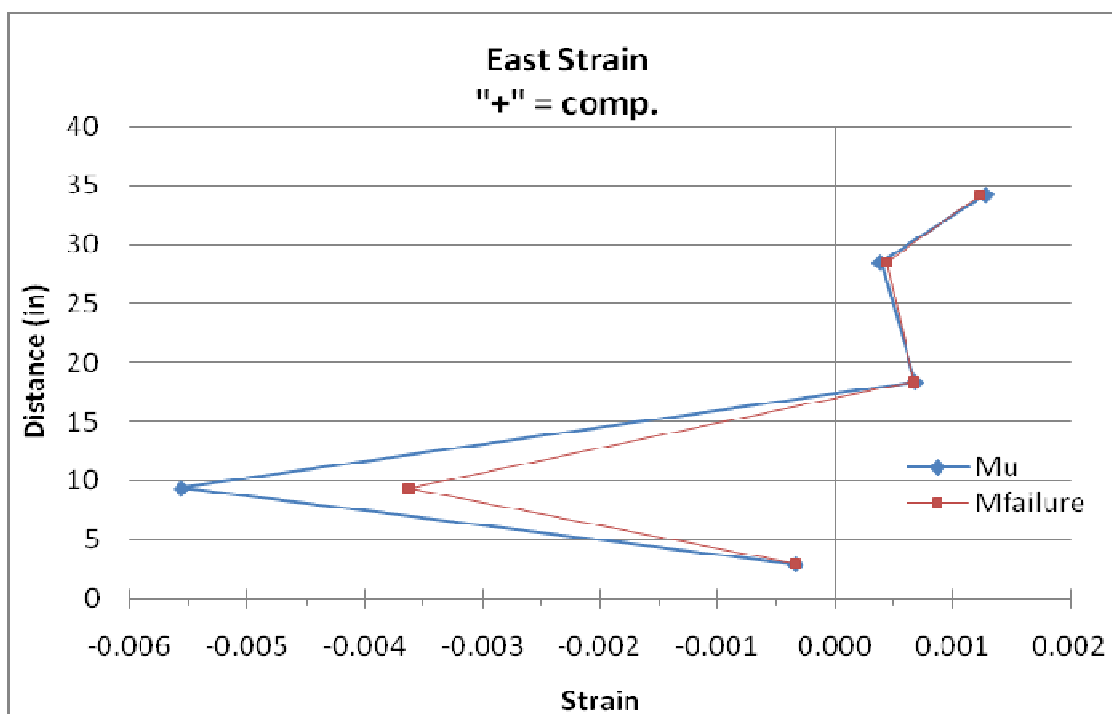


Figure 2.11.4.1: Strain East side of girder at ultimate load and at failure load

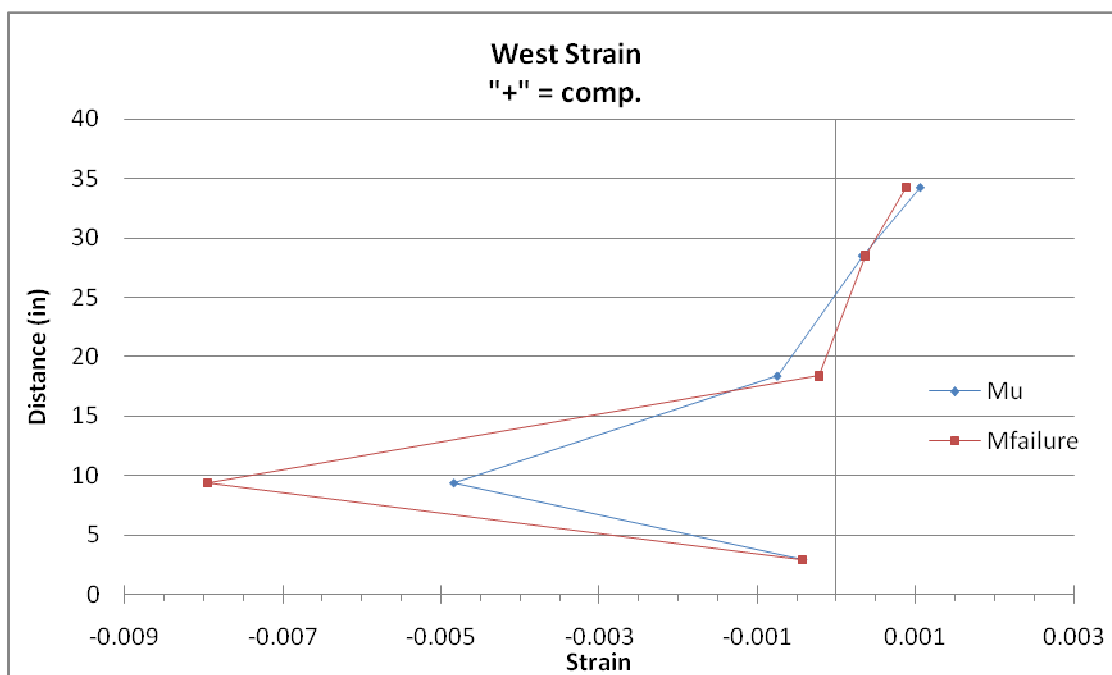


Figure 2.11.4.2: Strain West side of girder at ultimate load and at failure load

The progression of the test and results are shown in the following figures. Figure 2.11.4.3 shows shear cracking occurring in the web during the loading increments of 50 kips. The shear cracks are propagating through the flange as shown in Figure 2.11.4.4. The immediate shear failure is shown in Figure 2.11.4.5. Upon failure, the beam cambered upward and had a brittle explosion of the web and bottom flange. The shear distribution is shown in Figure 2.11.4.6. Flexure cracking was present at the load point and is shown in Figures 2.11.4.7. Another sign of flexural failure is the deck compression cracking at the load point and the buckling of the #5 bar in the deck shown in Figure 2.11.4.8. The deck cracked where the camber occurred and is shown in Figure 2.11.4.9.



Figure 2.11.4.3: Shear cracking in the web

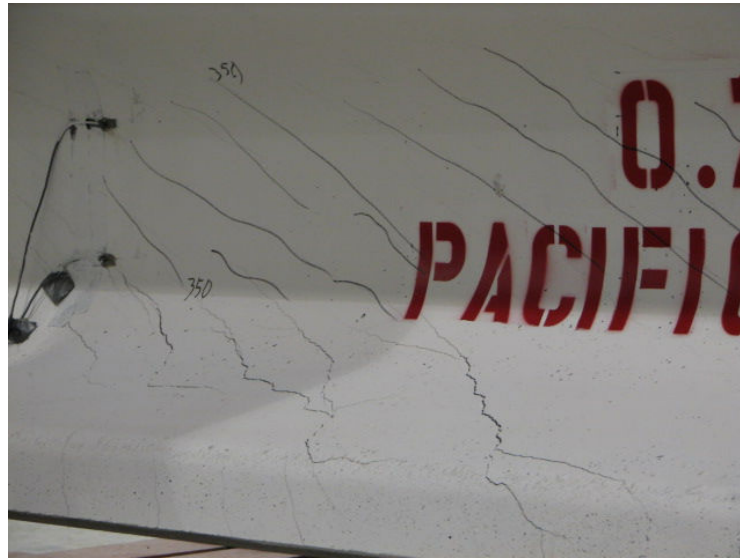


Figure 2.11.4.4: Shear cracks propagating through flange



Figure 2.11.4.5: Immediately after shear failure



Figure 2.11.4.6: Shear cracking in web and split flange



Figure 2.11.4.7: Flexure cracking at load point



Figure 2.11.4.8: Buckling of top deck #5 bar



Figure 2.11.4.9: Tensile deck cracking

The shear reinforcement was not detailed with a 90 degree bend in the bottom flange. The reinforcement was underdeveloped and allowed the web to separate from the bottom flange which resulted in a shear failure. Figure 2.11.4.10 display the straight shear reinforcement bars.



Figure 2.11.4.10: Shear reinforcement non-bent in bottom flange

The hairpin confinement detail was effective throughout the transfer length. The hairpins were placed at 3" centers for 45 inches at each girder end. The confinement kept the bottom flange from splitting from the web. The unfailed portion of the web and hairpin are shown in Figure 2.11.4.11. Longitudinal bottom flange cracking and loose strands are shown in Figure 2.11.4.12 - 2.11.4.13.



Figure 2.11.4.11: Confined flange non-failed



Figure 2.11.4.12: Longitudinal flange cracking



Figure 2.11.4.13: Loose strands after failure

2.11.5 Strand Bond

Two methods were used to determine if the strands had full bond at ultimate capacity for the assumed development length. On the girder end closer to the point loading, it was assumed that the strands would slip before the far end. Therefore, this end was monitored during the test. The first method was marking the lower 14 strands at 2 inches beyond the end of the diaphragm and monitoring the relative displacement at 50 kip incremental loading. This method was not refined

well enough to determine any actual displacement measurements. However, that does mean the strands did not move very significantly over the course of the loading.



Figure 2.11.5.1: Strand slip measurement

For the second method, two caliper displacement gauges were fixed to the two center strands in the bottom row. A flat metal base was clamped onto each individual strand but did not restrain the strand movement. The displacement calipers were fitted onto a magnetic base which was locked to the flat metal base. If the strand slipped toward the girder, the deflection gauge increased in value. Figures 2.11.5.2 and 2.11.5.3 show the caliper displacement set up on the strands.

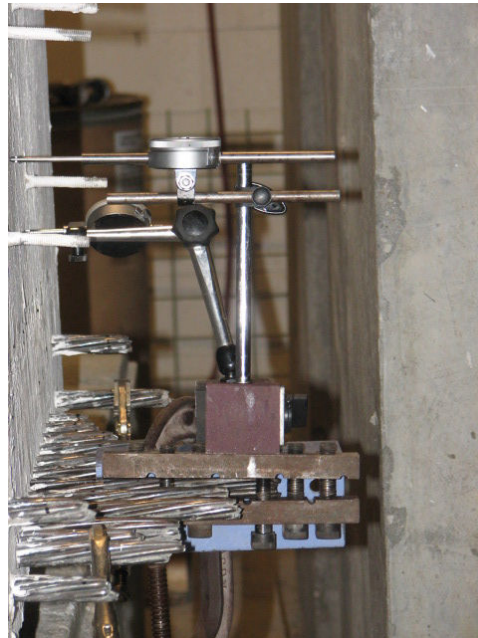


Figure 2.11.5.2: Caliper displacement gauges attached to the lower strands- side view



Figure 2.11.5.3: Caliper displacement gauges attached to the lower strands- end view

Initial measurements were taken as a reference point. Thereafter, readings were taken every 50 kips of loading. The maximum displacement occurred at the ultimate load of 600 kips and was 0.008 inch and 0.012 inch for gauges 1 and 2, respectively. These values are relatively insignificant and show that the strand did not slip under ultimate load.

Table 2.11.5.1 Strand displacement measurements

Load (k)	Gauge 1, Strand 7 (in)	$\Delta 1$ (in)	Change = (Initial - final) /initial	Gauge 2, Strand 8 (in)	$\Delta 2$ (in)	Change= (Initial- final) /initial
0	0.114	-	-	0.017	-	-
50	0.114	0	0	0.017	0	0
100	0.114	0	0	0.017	0	0
150	0.114	0	0	0.017	0	0
200	0.114	0	0	0.017	0	0
250	0.114	0	0	0.017	0	0
300	0.114	0	0	0.017	0	0
350	0.114	0	0	0.021	0.004	0.235
400	0.114	0	0	0.023	0.006	0.353
450	0.114	0	0	0.025	0.008	0.471
500	0.116	0.002	0.018	0.027	0.010	0.588
550	0.119	0.005	0.044	0.028	0.011	0.647
600	0.122	0.008	0.070	0.029	0.012	0.706

The strand bond does not appear to be a problem with the 0.7” strand. The flexural capacity predicted was achieved in the test without significant strand slip. Therefore, the development length predicted by the equations for 0.6” and 0.5” strands worked for 0.7” strand in this test. Fxx shows the strand bond pattern embedded in a piece of the fragmented concrete.



Figure 2.11.5.4: Strand bond pattern

2.12 Conclusions

The transfer length of the 0.7 in. diameter strand is approximately 35 inches and is predicted closely by the ACI formula of 50 strand diameters. The 0.7 inch strand is more difficult to work

with than the 0.6 inch strand due to the stiffness and weight but does work with extra care and some practice. The strand saves space and can provide greater prestress force to the member with fewer strands. Prestress force per unit area is increased.

The 0.7 inch test beam achieved the predicted ultimate flexural capacity without any strand slip. The bond between the strand and concrete is effectively developed and proves the development length is less than or equal to 15 feet.

The shear reinforcement must be detailed with a 90 degree bend on the bottom to keep the flange connected to the web. Welded wire reinforcement does not have this problem because longitudinal bars are welded near the bottom of the vertical shear reinforcement.

Bending 0.7" strands is possible and not overly difficult. Monostrand jacks are capable of prestressing the 0.7" strand but may need to be upgraded. The reusable and one-time use chucks are available and effectively anchor the strands.

3. Second Generation Threaded Rod Testing

Testing was done at the University of Nebraska on a second generation threaded rod continuity system. Two 25 ft NU 900 were tested. This chapter discusses the design of the target bridge, details of the test, construction and testing of the test specimen, and conclusions and recommendations from the test.

3.1 Design of a Target Bridge

DATA GIVEN

- 125'-118' two span, 8'-8" spacing, NU900, 120'-8" bridge width.
- Use SCC 8.5 ksi concrete.
- Diaphragm concrete is 6 ksi and deck concrete is 4 ksi.

The author ran Conspan to get Service I live load and Risa to get the fatigue load and deck weight (unequal spans). All the criteria should be met including maximum shear capacity check, Service III, girder top fatigue at positive section, Strength I at positive section including precast section and composite section, strength at release at 0.4L location, Strength I precast negative section, Strength I negative composite section, fatigue at negative section, crack control at negative section. The results are as shown in the table below. (Note: the negative moment is larger in the 118 ft span and the positive moment is larger in the 125 ft span in fatigue load calculations. There is not a big difference after being multiplied by the distribution factor. Hence, 125 ft - 125 ft span is used in the calculation. The results are shown in Table 3.1.1.

Table 3.1.1: Design Results of the Target Bridge

Girder	NU 900
Span	125 ft
Spacing	8.67 ft
Number Strands	50 (0.6" Dia.)
Deck bar area, G60	31.81 in ²
TR (1 3/8") N	7
TR location	above top flange
Final f'_c	8.940 ksi
f'_{ci}	6.338 ksi
Live load deflection	2.30 in.
$V_n = 0.9(0.25f'_c b_v d_v + V_p)$	353 kips
V_u	404 kips

The required concrete strength is 8.940 ksi larger than the design concrete strength of 8.5 ksi girder. Five methods are used and compared to increase the negative section capacity, as shown in the following.

Method 1: Add Steel Plate at the Girder Bottom

Table 3.1.2: Results of using 0.5-inch Thick Shoe Plate

Girder	NU 900
Span	125 ft
Spacing	8.67 ft
Number Strands	50 (0.6" Dia.)
Deck bar area, G60	31.81 in ²
TR (1 3/8" N)	7
TR location	above top flange
Final f_c	8.500 ksi
f_{ci}	6.338 ksi
Live load deflection	2.34 in.
$V_n = 0.9(0.25f'_c b_v d_v + V_p)$	353 kips
V_u	404 kips

The length of steel plate should be analyzed. Results for the ends sections are show in the table below. A concrete strength of 8.5 ksi should work because the prestressing strands are fully developed at 8 ft away from the girder end and the strands would also be draped.

Table 3.1.3: Result at the End of Shoe Plate away from Pier centerline

Girder	NU 900
Span	125 ft
Spacing	8.67 ft
Number Strands	50 (0.6” Dia.)
Deck bar area, G60	31.8 in ²
TR (1 3/8”) N	4
TR location	above top flange
Final f'_c	10.19 ksi
f'_{ci}	6.338 ksi
Live load deflection	2.2 in.
$V_n = 0.9(0.25 f'_c b_v d_v + V_p)$	352.6 kips
V_u	374.8 kips

The total bridge surface area is $A = 120.67 \times (125 + 118) = 29,322.8 \text{ ft}^2$

There are 14 girder lines. Each girder line needs two shoe plates. The cost of adding steel plates is \$1.0/lb including material and labor fees. A 1 3/8” diameter TR is \$5.00/ft. The total cost of TR and adding shoe plates is:

$$\left(\left(\frac{(38.4)(0.5)}{144} (8)(2) \right) (490 \text{ lb/ft}^3) (\$1) + 7(50)(\$5) \right) (14) \left(\frac{1}{29322.8} \right) = \$1.33/\text{ft}^2$$

Method 2: Increase Diaphragm Width

Increase the diaphragm width from 2 ft to 6 ft. The cost of making a diaphragm is \$350/yd³ which includes the cost of material and forming.

The critical location is at the face of diaphragm which is 3 ft away from the pier centerline. Analysis shows that 11 ksi girder concrete and 10- 1 3/8" diameter TR cannot meet the requirement of Strength I at the negative section.

Method 3: Change the Girder Cross Section

In this method, the author tries to add 3 in. extra thickness to girder top flange. The new girder cross section is shown below.

Table 3.1.4: Girder Section Properties

	NU 900	NU 900 Modified
H (in)	35.4	38.4
A (in ²)	648.1	792.7
I (in ⁴)	110262	163491.6
Y _b (in)	16.1	19.9
W _g (lb/ft)	0.68	0.83

Changing the top flange makes the girder weight increase. Service I live load from Conspan does not change at all. The live load distribution factor changes slightly.

Table 3.1.5: Results of adding 3-inch Concrete to the Top Flange

Girder	NU 900
Span	125 ft
Spacing	8.67 ft
Number Strands	46 (0.6" Dia.)
Deck bar area, G60	31.81 in ²
TR (1 3/8") N	6
TR location	above top flange
Final f'_c	8.500 ksi
f'_{ci}	5.353 ksi
Live load deflection	1.91 in.
$V_n = 0.9(0.25f'_c b_v d_v + V_p)$	377 kips
V_u	415 kips

The cost of material for thickening the girder top flange is \$150/yd³. The cost of TR and increasing the girder top flange is

$$\left((\$150) \times \frac{\left(\frac{3(48.2)}{144} \right) (125 + 118)}{27} + 6 * 50 * \$5.0 \right) (14) \left(\frac{1}{29322.8} \right) = \$1.36/\text{ft}^2$$

Method 4: Use Smaller Girder Spacing

Try decreasing the girder spacing from 8.67 ft to 7.5 ft. Then, there are 17 girder lines instead of 14 in the earlier design. The deck weight, fatigue load, and Service I live load are smaller than before.

Table 3.1.6: Results of Using 7.5 ft Girder Spacing

Girder	NU 900
Span	125 ft
Spacing	7.50 ft
Number of Strands	52 (0.6" Dia.)
Deck bar area, G60	27.53 in ²
TR (1 3/8") Number	7
TR location	above top flange
Final f'_c	8.825 ksi
f'_{ci}	6.636 ksi
Live load deflection	2.21 in.
$V_n = 0.9(0.25f'_c b_v d_v + V_p)$	353 kips
V_u	381 kips

The cost of adding extra girders is \$800/yd³ including the cost of material, forming, girder prestressing, concrete curing and girder shipping. The cost of adding 3 extra girder lines and all TR for 17 girder lines is:

$$\left((\$800) \times \frac{\left(\frac{648.1}{144} \right) (125 + 118)(3)}{27} + \$5.0 * 50 * (17 * 7) \right) \left(\frac{1}{29322.8} \right) = \$4.33/\text{ft}^2$$

Method 5: Increase Haunch Thickness

Increase haunch to 6 inches at both positive section and negative section.

Table 3.1.7: Results of using 6-inch Haunch

Girder	NU 900
Span	125 ft
Spacing	8.67 ft
Number Strands	46 (0.6" Dia.)
Deck bar area, G60	31.81 in ²
TR (1 3/8" N	7
TR location	above top flange
Final f'_c	8.740 ksi
f'_{ci}	5.721 ksi
Live load deflection	1.72 in.
$V_n = 0.9(0.25f'_c b_v d_v + V_p)$	393 kips
V_u	397 kips

The cost for doing this is \$150/yd³ for material. The cost for doing this plus TR cost is:

$$\left((\$150) \times \frac{\left(\frac{5(48.2)}{144} \right) (125 + 118)}{27} + \$5.0(50)(7) \right) (14) \left(\frac{1}{29322.8} \right) = \$1.91/ft^2$$

Method 6: Increase the Web Width to 10 Inches

Table 3.1.8: Design Results of Increasing the Web Width

Girder	NU 900
Span	125 ft
Spacing	8.67 ft
Number Strands	54 (0.6" Dia.)
Deck bar area, G60	31.81 in ²
TR (1 3/8") N	7
TR location	above top flange
Final f'_c	8.590 ksi
f'_{ci}	5.982 ksi
Live load deflection	2.23 in.
$V_n = 0.9(0.25f'_c b_v d_v + V_p)$	598 kips
V_u	410 kips

The cost for doing this is \$150/yd³ for material. The extra cost for doing this plus TR cost is:

$$\left((\$150) \times \frac{\left(\frac{(10 - 5.9)(20.29)}{144} \right) (125 + 118)}{27} + \$5.0(7)(50) \right) (14) \left(\frac{1}{29322.8} \right) = \$1.21/ft^2$$

Table 3.1.9: Comparison of Design Methods

Method	f'_c (ksi)	Cost (\$/ft ²)
1 Add Steel Plate at the Girder Bottom	8.5	1.33
2 Increase Diaphragm Width	Does not work	
3 Change Girder Cross Section	8.5	1.36
4 Use Smaller Girder Spacing	8.825	4.33
5 Increase Haunch Thickness	8.74	1.91
6 Increase the Web Width to 10"	8.59	1.21

From Table 3.1.9, Method 1 uses the specified concrete strength and has a relatively low cost. Method 6 needs higher concrete strength although it has the lowest cost. Therefore Method 1 is adopted in the design.

3.2 Testing Program

For the 125'-125' two-span target bridge, the diagram of the factored load envelope shows that the negative moment due to the deck weight exists within 0.25L of the pier ($0.25 \times 125 = 31.2$ ft). Concentration and crack will happen if the section changes suddenly. Therefore the threaded rod and #8 bars need to be staggered. The extending length after the cutoff point is the greater value between L_d and $12d_b$.

The development length of TR is $48d_b = 48(1.375)/12 = 5.5$ ft

The development length of #8 bars is $48d_b = 48(1.0)/12 = 4$ ft

Using 10 ksi concrete, the cutoff length is shown below. The threaded rod and #8 bars extended from end to end above the two 25' long precast NU900 girders. In case fatigue may control, each capacity needs to be checked.

Table 3.2.1: Data for Cutoff Design

Point #	Note	Distance from pier centerline ft	D / L	TR Area in. ²	Bar Area in. ²	Precast M _n k.ft	Composite M _n k.ft
1	Pier centerline	0	0	15.8	1.58	5702	9047
2	Face of diaphragm	1.5	0.012	15.8	1.58	5702	9047
3	With shoe plate	7	0.056	15.8	1.58	4539	6654
4	No shoe plate	7	0.056	15.8	1.58	3535	4245
5	TR 1st cutoff	10	0.08	15.8	1.58	3535	4245
6	TR 1st cutoff+ Ld	15.5	0.124	9.48	1.58	3501	4244
7	TR 2nd cutoff	15.5	0.124	9.48	1.58	3501	4244
8	TR 2nd cutoff+ Ld	21	0.168	0	1.58	543	4253
9	Bar 1st cutoff	25	0.2	0	1.58	543	4253
10	Bar 1st cutoff+Ld	29	0.232	0	0.79	543	2734
11	Bar 2nd cutoff	30	0.24	0	0.79	543	2734
12	Bar 2nd cutoff+Ld	34	0.272	0	0	543	1081
13	end	125	1	0	0	543	1081

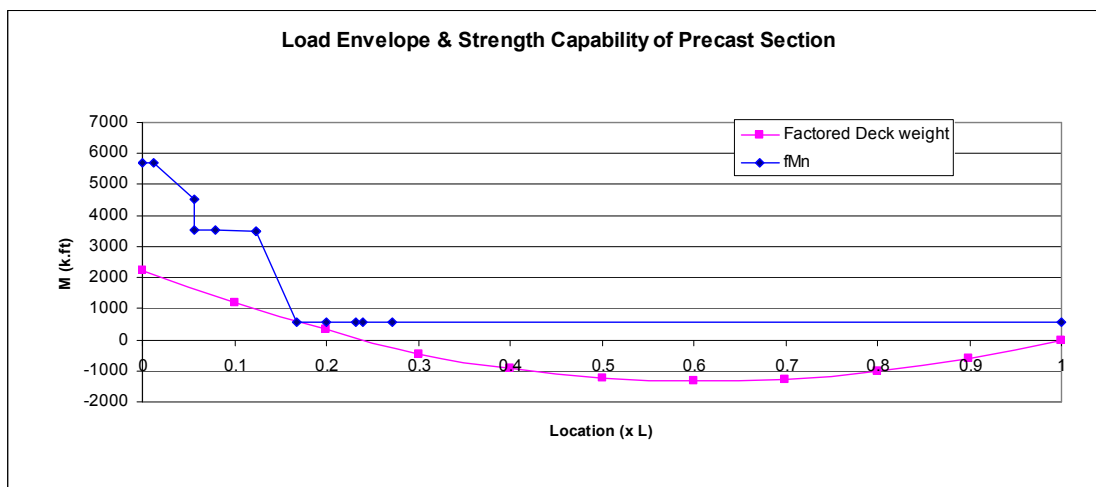


Figure 3.2.1: Load Diagram and Cutoff Design for Precast Section

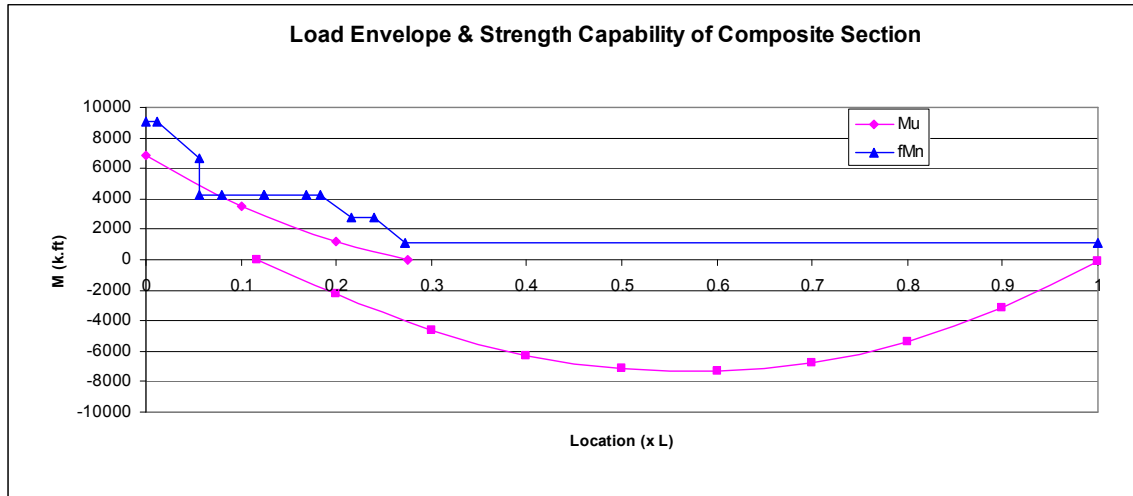
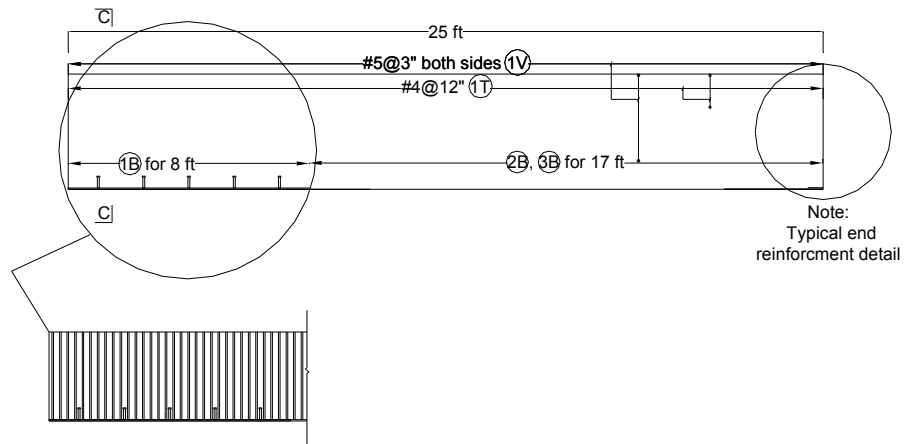


Figure 3.2.2: Load Diagram and Cutoff Design for Composite Section

According to the target bridge design plan, the diaphragm is 8 ft -8 in. long and 3 ft wide. Due to the spacing limit in the laboratory, a narrower deck is made. A smaller amount of deck reinforcement is used in order to make the specimen fail within the loading capacity of the load cell. Preloading is due to the deflection when deck weight is poured. The standard vertical shear reinforcement is 5 inches. In some cases a higher length is needed because of construction error. In this specimen, the horizontal shear reinforcement is TR embedded in the girder web. 150 ksi TR @24" will be embedded in the top flange of precast girder as horizontal shear reinforcement. An 8 ft long steel plate will be placed on the bottom flange of the precast girder near the pier to help resist compression force.

FABRICATION DRAWING

The precast girder and the diaphragm are shown below.



2 NU900 beams 25 ft long each reinforcement layout

Note: Minimum 14 days concrete strength is 9,000 psi

Figure 3.2.3: Steel Layout

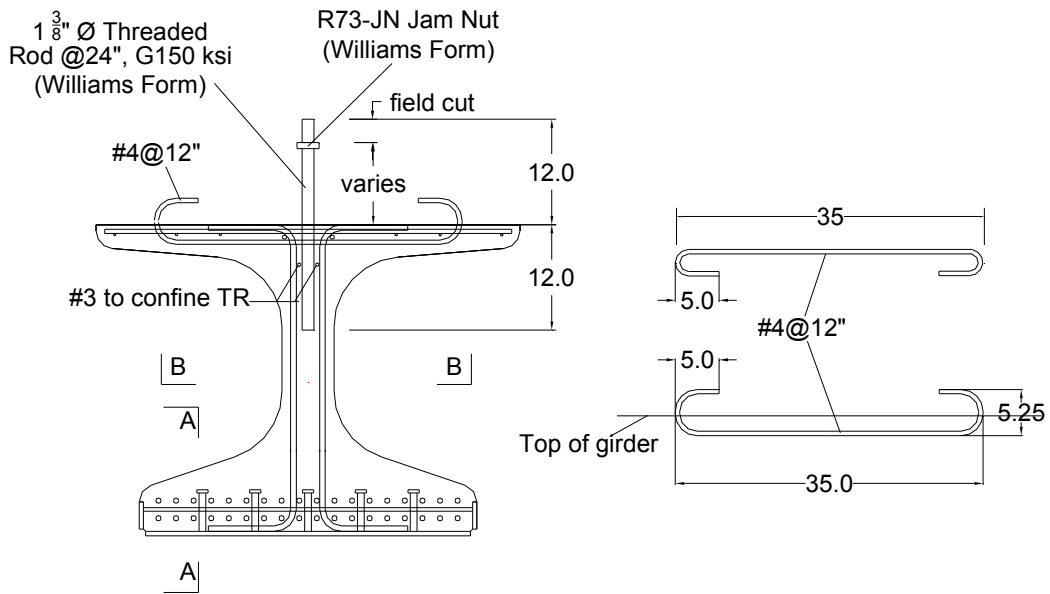
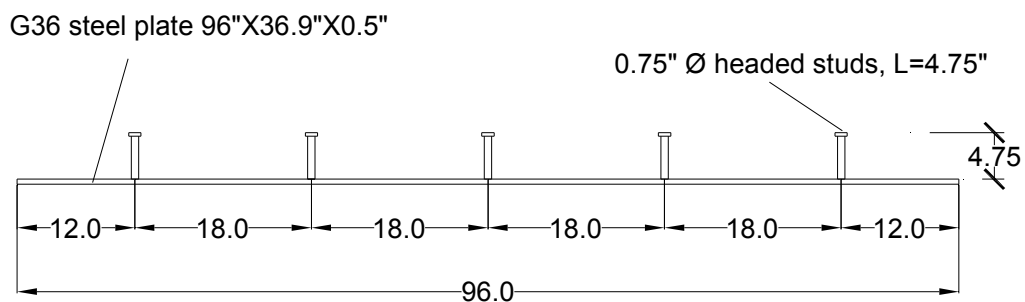
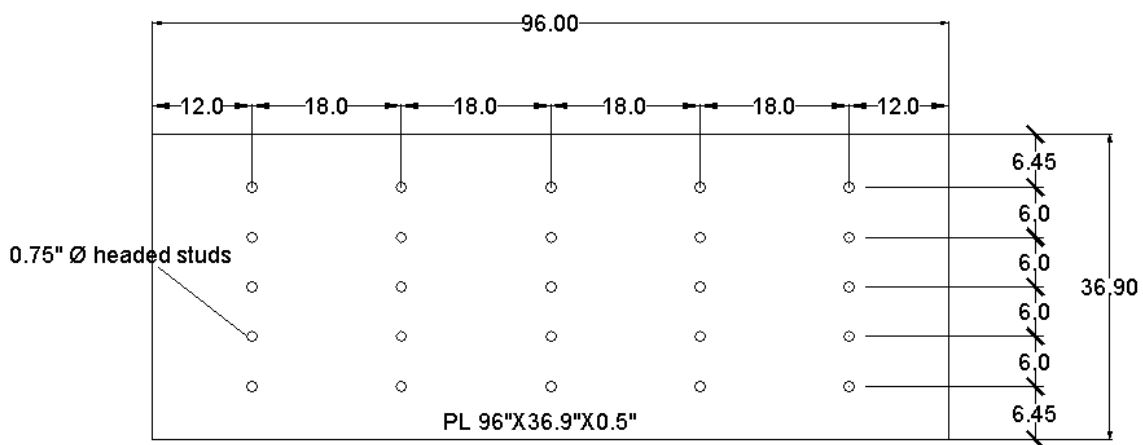


Figure 3.2.4: Precast Girder Reinforcement at Shoe Plate Location



A-A Side view of steel plate and studs

Figure 3.2.5: Shoe Plate with Shear Studs



B-B Plane view (shoe plate & studs)

Note: all the dimensions are in inches

Figure 3.2.6: Shear Studs Layout

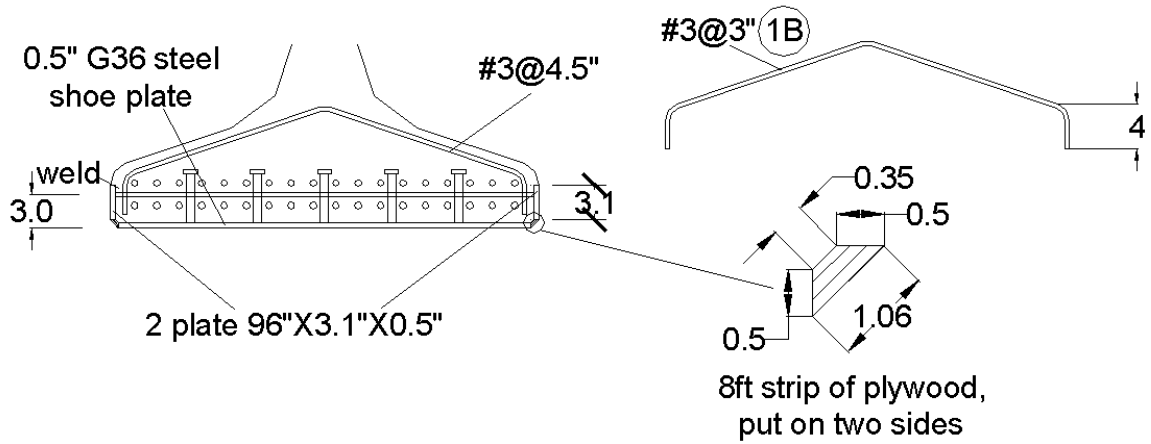


Figure 3.2.7: Strengthened Precast Girder Bottom Flange with Shoe Plate

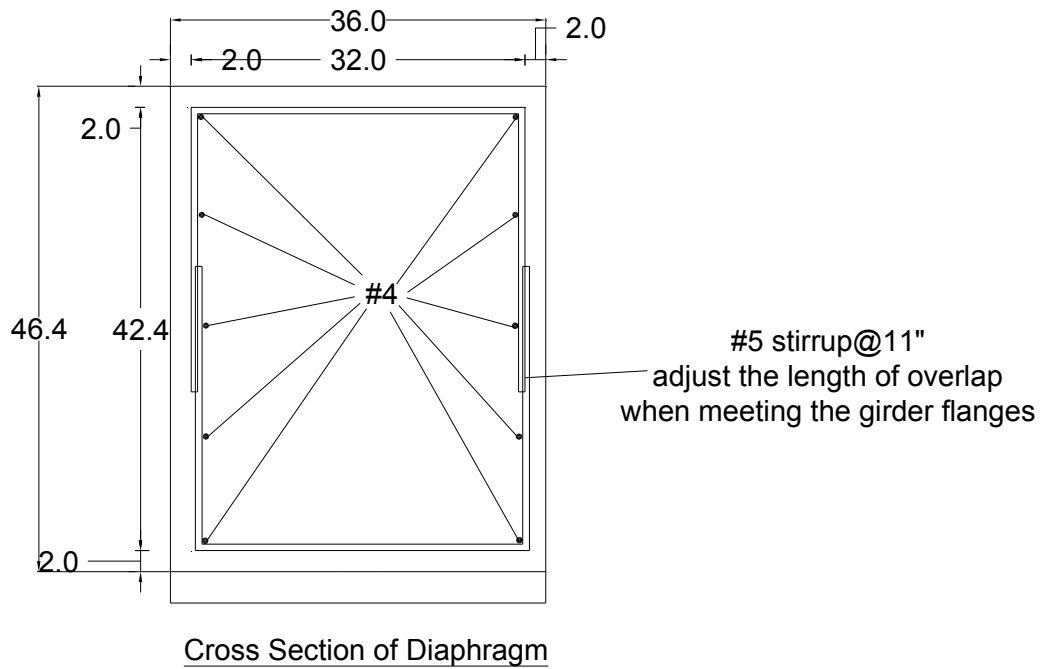
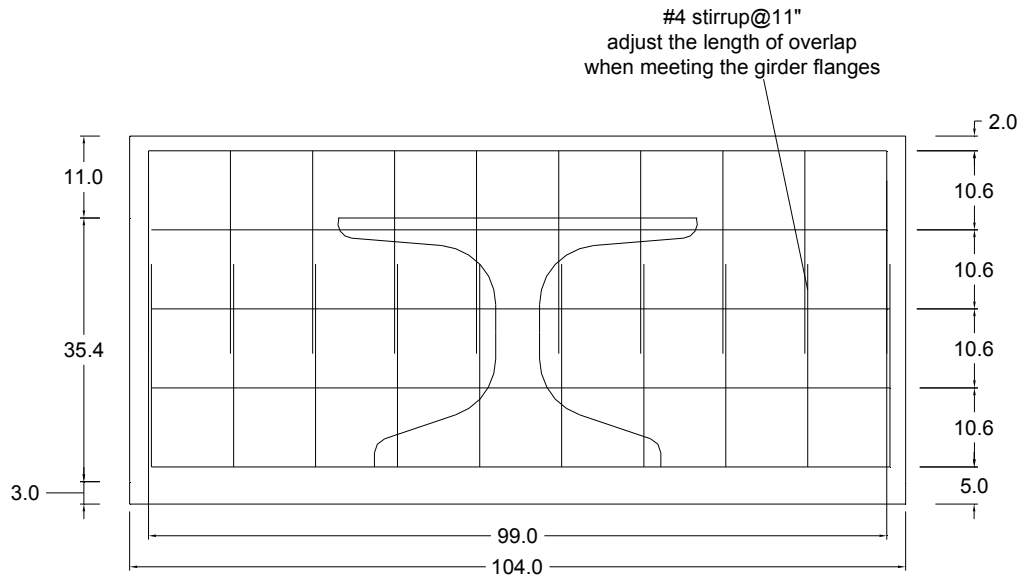


Figure 3.2.8: Horizontal and Vertical Reinforcement of Diaphragm



Side View of Diaphragm

Figure 3.2.9: Reinforcement of Diaphragm at Elevation View

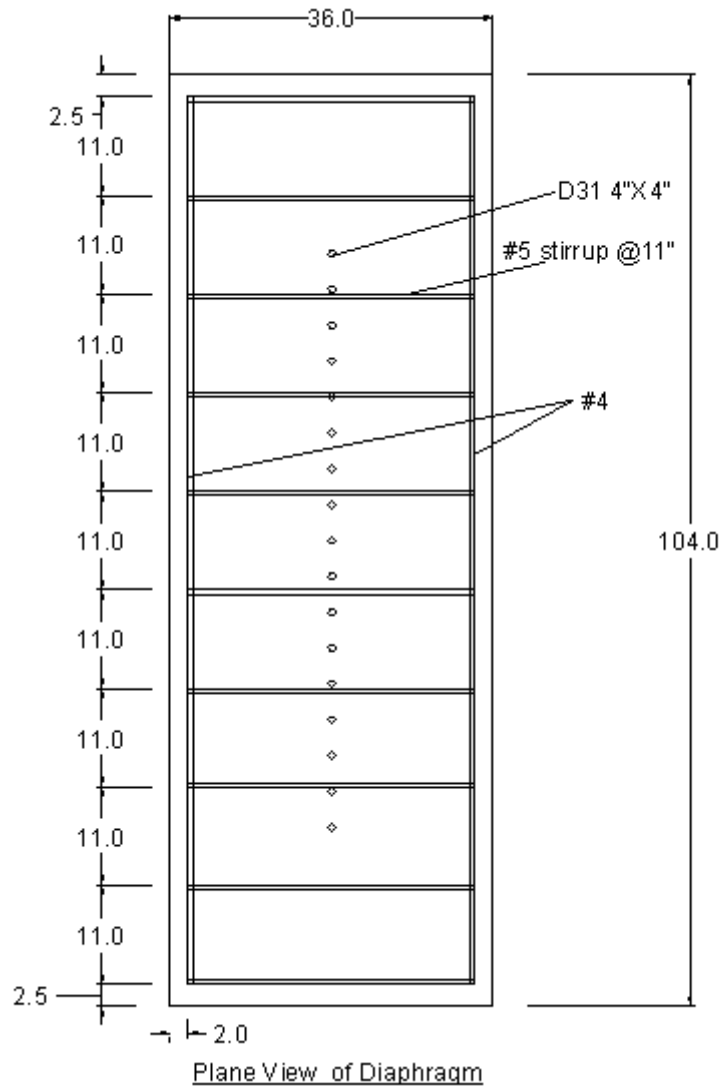


Figure 3.2.10: Reinforcement of Diaphragm at Top View

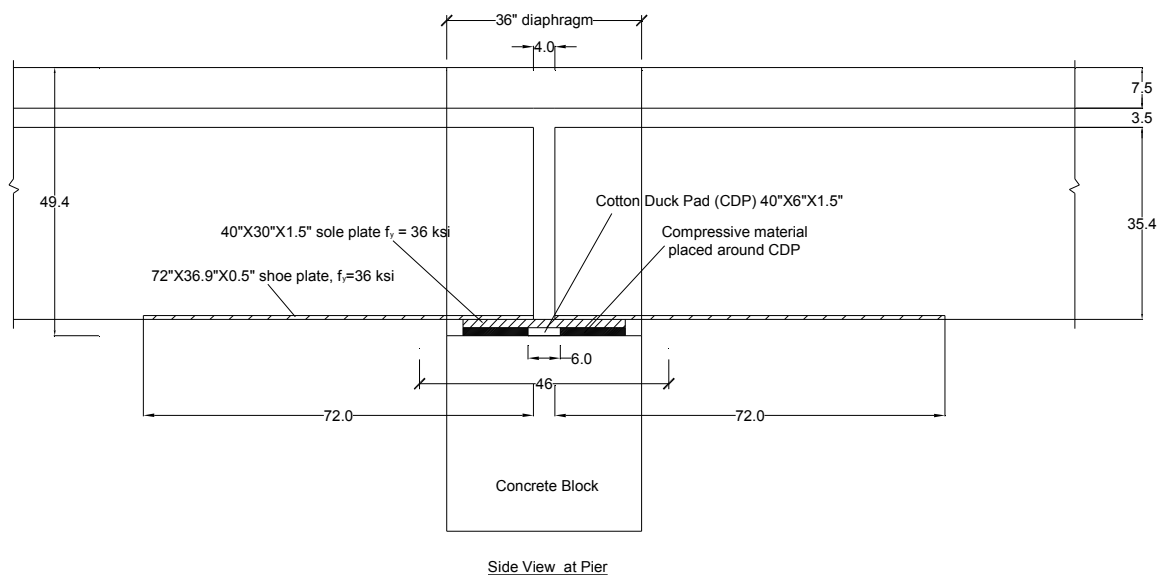


Figure 3.2.11: Girder Bottom Connection

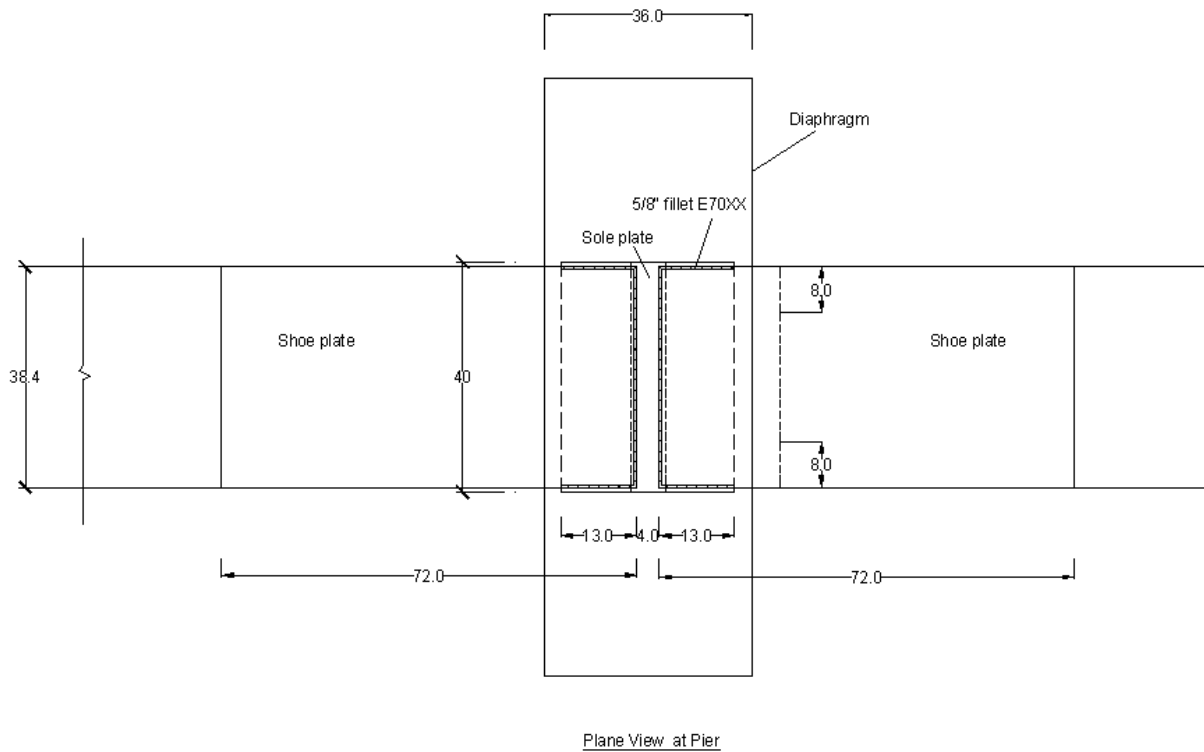


Figure 3.2.12: Girder and Diaphragm

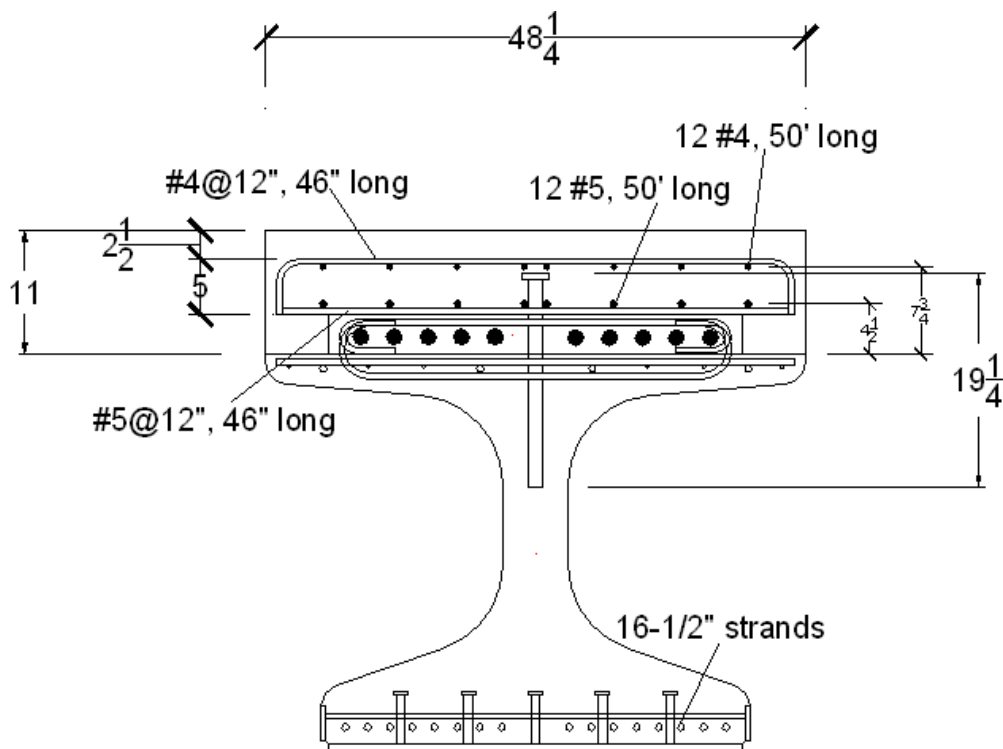


Figure 3.2.13: Cross Section of the Specimen

ANTICIPATE LOAD CAPACITY

1. Get M- of the Target Bridge (Use 125'-125' two spans)

Table 3.2.2: Load

NU 900	Noncomposite section						Composite section									
	Girder Weight		Slab, Including Haunch and Forms				Rail		Future Wearing Surface		Service Live Load			Fatigue load		
	Simple Span (SS)	Continuous Span (CS)	CS+Change due to 10% reduction of max M-	Envelope	CS	CS	for deflection calculation	for Service and Strength Design	V...	M+	M-	V	M	M		
Second span	V	M	V	M	M	M	V	M	V	M	M+	M+	M-	V	M	M
1	43	0	71	-1770	-1593	-1770	4	-107	17	-423	12	17	-1985	120		-616
0.9	34	478	59	-956	-796	-956	4	-58	14	-229	209	292	-1242	106.8		-555
0.8	26	850	48	-283	-142	-283	3	-17	12	-68	591	828				
0.7	17	1116	37	248	372	372	2	15	9	59	979	1370				
0.6	9	1275	25	637	743	743	2	38	6	152	1258	1760				
0.5	0	1328	14	885	973	973	1	53	3	212	1406	1967				
0.4	-8	1275	3	991	1062	1062	0	60	1	237	1422	1990			1070	
0.3	-17	1116	-8	956	1009	1009	-1	58	-2	229	1301	1820				
0.2	-26	850	-20	779	814	814	-1	47	-5	186	1031	1443				
0.1	-34	478	-31	460	478	478	-2	28	-7	110	592	829				
0	-43	0	-42	0	0	0	-3	0	-10	0	0	0				
Value at face of diaphragm	41	57	69			-1672	4	-101	17	-400			-1896	118		-609

2. Calculate the Deflection at 25' from Pier in the Target Bridge When Deck is Poured

To simplify the design, a conservative approach for deflection estimation is to use the positive moment live load envelope per lane developed for Service I. Distribution Factor for live load of one lane loaded is (N of lanes) / (N of girders) x (Multiple Presence Factor).

For the deflection of members with one end pinned and the other end fixed, PCI Design Handbook, Page 11-14, states:

$$\Delta_x = \frac{wx}{48EI} (l^3 - 3lx^2 + 2x^3), \text{ x is the distance away from the pinned support.}$$

In this target bridge, $x = 125 - 25 = 100'$. To simplify the calculation, use uncracked section properties. Therefore at 25 ft from pier, the deflection is

$$\Delta_x = \frac{0.91(100)}{48(5506)(110262)} (125^3 - 3(125)(100)^2 + 2(100)^3)(12)^3 = 1.1''$$

Double check with Risa 3D:

The positive section is a prestressed non-cracked section. The moment of inertia of a non-cracked section is $110,262 \text{ in}^4$. The negative section near the pier is a reinforced cracked section. Assume that the moment of inertia of a cracked section is $110,262 / 3 = 36,754 \text{ in}^4$. Using non-cracked section properties, the deflection at Point N13 which is 25' away from the pier centerline is $1.103''$. Assume that within 25' distance from the pier centerline, the section is cracked. Using cracked section properties within 25' and non-cracked section properties outside of that area, Risa gives $1.918''$.

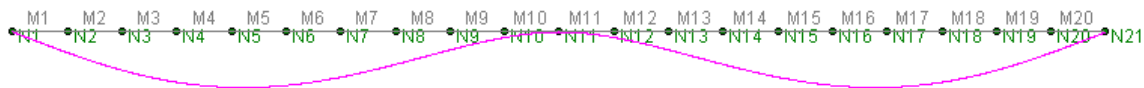


Figure 3.2.14: Deflection in Risa 3D Analysis

3. Point Load Present Deck Weight

The deck weight of the target bridge is 1672 k-ft. The moment caused by the cantilevered beam weight is 340.3 k-ft. Then point load should cause $1672 - 340.3 = 1331.7$ k-ft at the face of diaphragm. Therefore $P = 1331.7 / (25 - 1.5 - 1.5) = 60.5$ k.

Note: The actual preloading load is 32.2 k by using a 98 ft -98 ft long target bridge.

4. Anticipate Failure Load

The cylinder test shows that girder concrete strength is 12.834 ksi at the 28th day.

Table 3.2.3: Concrete Mix of Interface Block

Type 1 cement	648.33 l lb
Fly ash	103.33 lb
47-B Sand & gravel	1760.00 lb
0.5" BRS limestone	1180.00 lb
322-N (water reducer)	23.00 oz
Rebuild 1000 (water reducer)	12.06 oz/100 lb cement
Rebuild 1000 (water reducer added in the laboratory)	7.10 oz/100 lb cement
Air Entrainment Agent	2.33 oz
Water in 47-B Sand & gravel	4.43 gal.
Water in 0.5" BRS limestone	1.41 gal.
Water added in the plant	20.62 gal.
Total water	220.76 lb
W/C ratio	0.29
Slump	9 in

Table 3.2.4: Interface Block Concrete Strength (First Casting, Designed Strength is 6 ksi)

Time	f'_c (ksi)
3rd day	4.990
7th day	5.401
18th day (Preloading time)	7.476
35th day (One day before final test)	7.409

Table 3.2.5: Concrete Mix of Deck

Type 1 cement	657.00 lb
47-B Sand & gravel	2108.00 lb
0.5" BRS limestone	936.00 lb
322-N (water reducer)	19.60 oz
Rehobuild 1000 (water reducer)	11.69 oz/100 lb cement
Rehobuild 1000 (water reducer added in the laboratory)	3.90 oz/100 lb cement
Air Entrainment Agent	5.00 oz
Water in 47-B Sand & gravel	4.55 gal.
Water in 0.5" BRS limestone	0.22 gal.
Water added in the plant	14.15 gal.
Hot Water added in the plant	9.30 gal.
Water added in the laboratory	0.40 gal.
Total water	238.73 lb
W/C ratio	0.36
Slump	9.5 in.

Table 3.2.6: Deck Concrete Strength (Second Casting, Designed Strength is 4 ksi)

Time	f'_c (ksi)
3rd day	1.491
7th day	1.988
21st day (One day before final test)	6.316

The critical section for the flexural design of a negative section is at the face of the diaphragm. There are 16- 0.6" strands and a 0.5" thick G36 shoe plate in the bottom of the girder. 10- 1 3/8" diameter threaded rods are placed above the top flange. The interface block is 39 in. wide and 3.5 in. high. Deck reinforcement includes 8 #4 in the top layer and 8 #5 in the bottom layer. The total deck steel is 4.08 in² with a centroid 41.53 in. from the girder's bottom fiber.

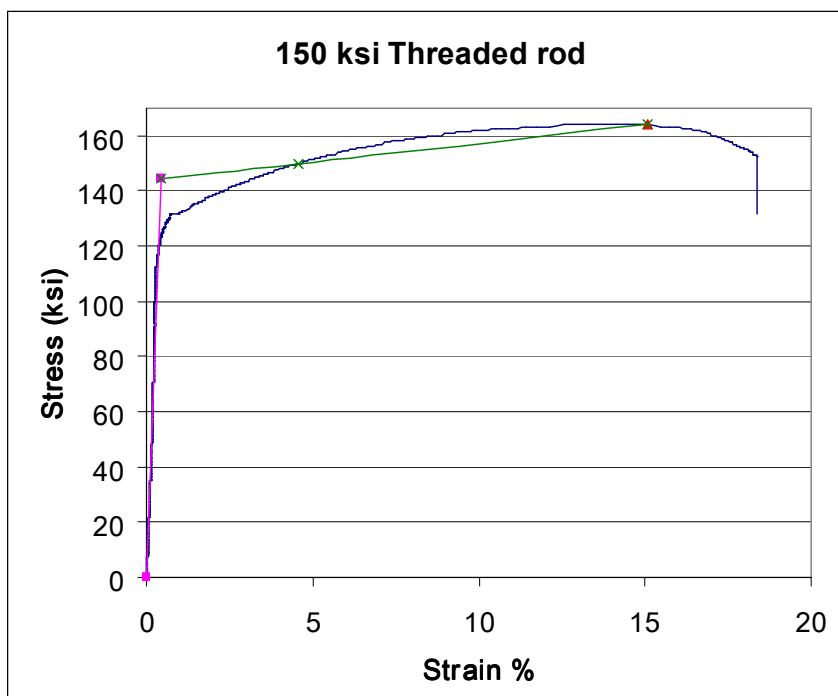


Figure 3.2.15: Stress-Strain Diaphragm of TR

The stress-strain diagram can be presented by Mattock¹ power formula,

$$f_{si} = \varepsilon_{si} E_s \left[Q + \frac{1-Q}{\left\{ 1 + \left(\frac{\varepsilon_{si} E_s}{k f_y} \right)^R \right\}^{1/R}} \right] \leq f_u$$

where E is the tangent slope of the first linear part. From the test data, E = 33995 ksi.

f_y is the stress when $\varepsilon = 0.01$. From the test data, $f_y = 131.654$ ksi

f_u and ε_u are strength and strain at tensile failure, here $f_u = 163.932$ ksi, $\varepsilon_u = 0.151$

K is the factor for the intersection point between the elastic linear part and the hardening part.

Draw a line to simulate the hardening part. Then the intersection point is $\varepsilon = 0.00425$,

$f_{inter.} = 144.472$ ksi. Hence $K = f_{inter.}/f_y = 144.472 / 131.654 = 1.097$

$$Q = \frac{f_{pu} - f_{inter.}}{\varepsilon_{pu} E - f_{inter.}} = \frac{163.932 - 144.472}{0.151(33995) - 144.472} = 1.327$$

R is determined by solving the power formula equal to f_y when $\varepsilon = 0.01$

$$0.01(33995) \left[1.327 + \frac{1-1.327}{\left\{ 1 + \left(\frac{0.01(33995)}{1.097(131.654)} \right)^R \right\}^{1/R}} \right] = 131.654$$

Therefore R = 3.75

In our Excel, E = 29000, Q = 0.016, $f_y = 127.5$, R = 3.75, K = 1.04

Table 3.2.7: Material Data

	Girder concrete	Concrete of diaphragm and interface block	Deck concrete	TR strength
Specified material data	8.500	6.000	4.000	150
Actual material data	12.834	7.409	6.316	164

Table 3.2.8: Specimen External Load Required to Match Strength I

Location	Face of diaphragm					Centerline of diaphragm					At end of shoe place away from pier				
	M_t	M_g	M_{deck}	M_t-M_g- M_{deck}	P	M_t	M_g	M_{deck}	M_t-M_g- M_{deck}	P	M_t	M_g	M_{deck}	M_t-M_g- M_{deck}	P
125 ft, 8' 8" spacing	6536	188	153	6196	282	6950	213	173	6565	279	4739	98	80	4561	294
98 ft - 98 ft with 10' 2" spacing	5091	188	153	4751	216	5491	213	173	5106	232	3358	98	80	3180	205

Unit: k and k-ft

Table 3.2.9: Anticipate Flexural Moment Capacity of the Specimen

Location	M_n at section		
	Centerline of diaphragm	Face of diaphragm	At end of shoe place away from pier
Theoretical result with specified material data	8390	7383	5230
Theoretical result with actual material data	8377	7647	6621
Testing result	9362	8744	6099

Table 3.2.10 Anticipate Failure Load

		First stage		Second stage		
Flexural capacity	1st grout strength f_c	7.409	ksi	Deck f_c	6.316	ksi
	Rod area at pier	15.8	in. ²	Deck area of specimen	530.2	in. ²
	first grout width b_v	39	in.	deck and haunch height	11	in.
	thick. of cast	3.5	in.	deck bar area	4.08	in. ²
	$W_{g-grout}$	0.14	k/ft	bar's centroid	41.53	in.
	girder and cast w_t	0.82	k/ft	deck selfweight including 1st grout	0.55	k/ft
	$P_{g-grout}$	3.34	k	P_{g-deck}	13.0	k
	$M_{g-grout}$	39.26	k.ft	M_{g-deck}	152.5	k.ft
	d_e	35.7	in.	d_e	36	in.
	M_n from flexural strength	6694	k.ft	M_n from flexural strength	7647	k.ft
	P_n	294.0	k	P_u	332.1	k
Vertical shear capacity (without considering shoe plate)	h	38.9	in.	h	46.4	in.
	Effective shear depth d_v from flextural cap	34.8	in.	d_v from flextural capacity	35.7	in.
	max. $d_v < \min(0.9d_e, 0.72h)$	28.0	in.	max. $d_v < \min(0.9d_e, 0.72h)$	32.8	in.
	d_v	28.0	in.	d_v	32.8	in.
	$V_n < V_{n1} = 0.25f_c b_w d_v$	530.2	k	$V_n < V_{n1} = 0.25f_c b_w d_v$	620.3	k
	$V_c = 2(0.0316) \sqrt{f_c} b_w d_v$	37.4	k	$V_c = 2(0.0316) \sqrt{f_c} b_w d_v$	43.77	k
	$V_r = \frac{A_v f_y d_v (\cot \theta + \cot \alpha) \sin \alpha}{s}$ (LRFD-5.8.3.3-4)	347.3	k	$V_r = \frac{A_v f_y d_v (\cot \theta + \cot \alpha) \sin \alpha}{s}$	406.3	k
	$V_n < V_{n2}$	384.7	k	$V_n < V_{n2}$	450.1	k
	shear capacity V_n	384.7	k	V_n	450.1	k
P_n	365.4	k	P_u	421.1	k	
Horizontal shear between 1st cast layer and girder top flange	TR area	1.58	in. ²			
	TR spacing	24.0	in.			
	TR yield strength	120.0	ksi			
	$V_{nh} = 12 c b_w \pi + \mu [A_{tr} f_y + P_c]$ $\leq \min(0.2f_c A_c, 0.8A_c)$	165.6	k/ft			
	V_{nh}	374.4	k/ft			
change to vertical shear capacity	386.5	k	(C8.5.4.1-1) change to vertical shear capacity	452.2	k	
P_n	367.2	k	P_u	423.2	k	
Horizontal shear between two layers				V_n	152.6	k/ft
				$\leq \min(0.2f_c A_c, 0.8A_c)$	452.7	k
change to vertical shear capacity				change to vertical shear capacity	416.8	k
Simulate the real bridge	deck weight of target bridge	1614.6	k.ft			
	selfweight	227.0	k.ft			
	Point load moment	1387.5	k.ft			
	P	63.1	k			
	Span	125	ft			
	Deflection at the midspan of target bridge	2.98	in.			
	Deflection at 25ft from pier of target bridge	1.19	in.			
	E_c at diaphragm face	7064	ksi			
	I_r at diaphragm face	77047	in. ⁴			
	deflection caused by selfweight	0.13	in.	Use the section properties of first stage		
$\Delta = \frac{wL^4}{8EI}$			max deflection caused by max P	4.9	in.	
$\Delta = \frac{PL^3}{3EI}$			deflection caused by selfweight	0.2	in.	
deflection caused by P	1.07	in.				
P causing the deflection	72.9	k	total max deflection	5.0	in.	

The expected load is the concentrated load applied with the jet at the end of girder.

Table 3.2.11: Result of Anticipated Failure Load (Kips)

	Location	1.5 ft from diaphragm face	at the end of shoe plate, 8 ft away from pier centerline
First stage test criteria	Flexural strength	294.0	38.9
	Vertical shear strength	365.4	514.4
	Horizontal shear between 1st cast layer and girder top flange	367.2	361.0
	P causing the deflection	72.7	----
	Point load present deck weight	63.1	----
Second stage test criteria	Flexural strength	332.1	415.1
	Vertical shear strength	421.1	361.2
	Horizontal shear between first cast layer and second cast layer	423.2	362.9
	Horizontal shear between first cast layer and girder top flange	416.8	528.2
	Expected failure load	332.1	361.2

5. End Zone Shear

Required shear reinforcement at the end zone is:

$$A_t = 0.021 \frac{P_i h}{f_s L_t} = 0.021 \frac{(202.5 * 16 * 0.217)(35.4)}{20(60 * 0.7)} = 0.62 \text{ in.}^2$$

The required shear reinforcement is 2#5@3". Within $h/4 = 8.85''$, the number of shear reinforcement is $8.85/3 = 2.95$. Shear reinforcement is $2.95 * 0.31 * 2 = 1.83 \text{ in.}^2 > 0.62 \text{ in.}^2$ OK!

6. Welding Length

The sole plate thickness is 1.25 inches and shoe plate thickness is 0.75". Both of them are G 36 ksi. The minimum thickness between the sole plate and shoe plate is 0.75". The fillet size should not be less than 0.25" and not larger than $(0.75'' - 1/16)$. (Manual of Steel Construction Table J2.4) Hence 5/8" size is used.

The welds transfer load from one shoe plate to the other shoe plate through the sole plate. The width of the sole plate is $38.4 - 0.75 * 2 = 36.9''$. The length is 30".

$$V_u = 0.5 * (36.9) * 36 = 664.2 \text{ k}$$

Use shielded metal arc welding (SMAW) for longitudinal loaded fillets,

$$D = (5/8) / (1/16) = 10$$

$$\phi R_n = 1.392DL = 1.392(10)L = 13.92L \text{ k/in.}$$

For base metal, $\phi R_n = 0.75t_s(0.6)F_u = 0.75(0.5)(0.6)(58) = 13.05 \text{ k/in.}$ Controls

Therefore $\phi R_n = 13.05L \text{ k/in.}$

For a transversely loaded fillet weld, the strength is 50% more than the longitudinal loaded fillet (Manual of Steel Construction, Page 8-8).

$$\phi R_n = 1.392DL(1.5)$$

Therefore the sum of strength for longitudinal and transverse fillet weld is:

$$13.05(30-4)(2) + 13.05(36.9)(1.5) = 1400.9 \text{ k} > V_u = 664.2 \text{ k. Ok!}$$

Member strength

Yielding of the sole plate is

$$\phi A_g F_y = 0.9(36.9)(1.25)(36) = 1494.5 \text{ k} > V_u = 664.2 \text{ k. Ok!}$$

7. Vertical TR Length Calculation

Sometimes it is efficient to cut the vertical TR earlier in the girder fabrication before strands are released instead of cutting them in the field. It is not easy to come up an equation to calculate the length of vertical TR (or girder camber). Calculations using a camber and deflection spreadsheet result in a parabolic curve which is a rough calculation of length.

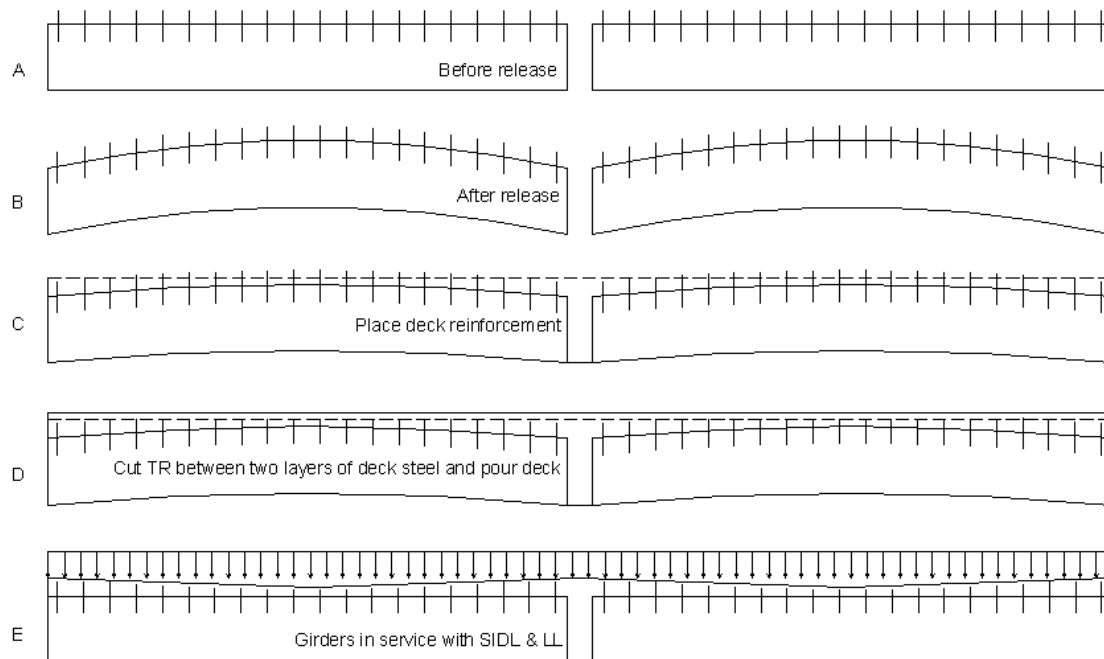


Figure 3.2.16: Vertical TR Construction Procedure

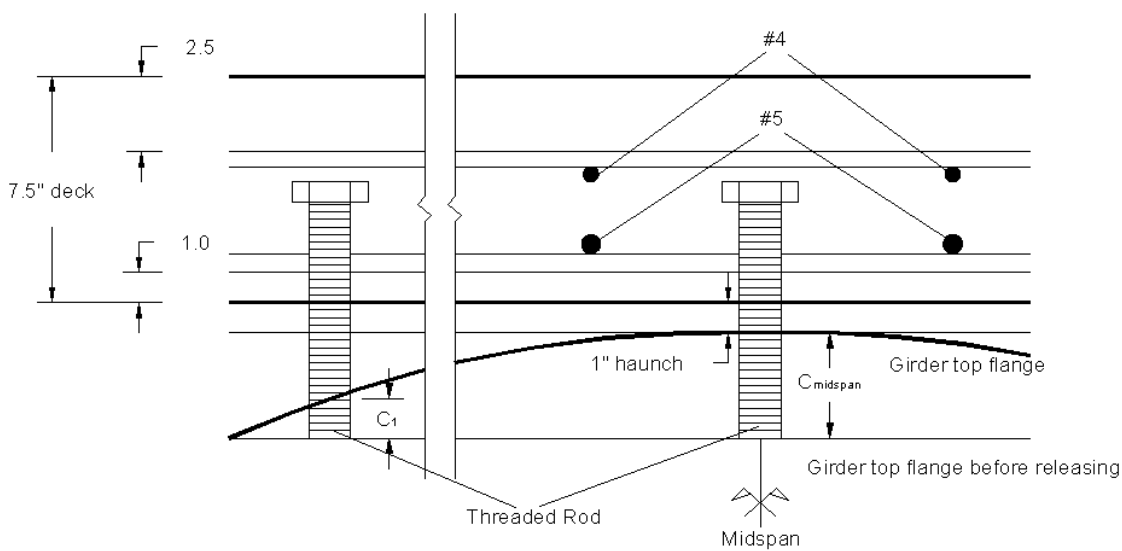


Figure 3.2.17: Steel Layout in the Deck around Vertical TR

Use 46.67 ft wide bridge, 8 ksi concrete, 9 ft girder spacing to get camber for each girder size.

Table 3.2.12: Camber

	Span	Location										
		0	0.1	0.2	0.3	0.4	0.5	0.6	0.7	0.8	0.9	1
NU 900	100	0	1.17	1.97	2.49	2.78	2.87	2.78	2.49	1.97	1.17	0
NU 1100	120	0	1.47	2.47	3.11	3.47	3.58	3.47	3.11	2.47	1.47	0
NU 1350	130	0	1.21	2.02	2.53	2.81	2.90	2.81	2.53	2.02	1.21	0
NU 1600	140	0	0.99	1.63	2.03	2.24	2.30	2.24	2.03	1.63	0.99	0
NU 1800	160	0	1.22	2.01	2.48	2.73	2.81	2.73	2.48	2.01	1.22	0
NU 2000	180	0	1.46	2.38	2.93	3.21	3.29	3.21	2.93	2.38	1.46	0
Average		0	1.25	2.08	2.60	2.87	2.96	2.87	2.60	2.08	1.25	0

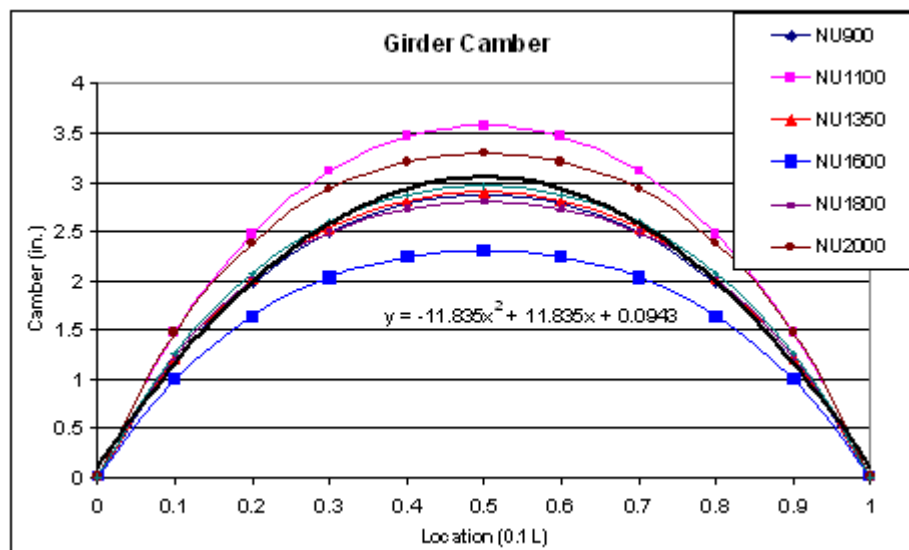


Figure 3.2.18: Girder Camber at Each 10th location

Assume haunch thickness at mid-span is 1". The head edge of threaded rod would be exactly below the top layer of flexural deck steel. Deck thickness below top steel is $7.5 - 2.5 - 0.5 - 0.5 = 4"$

Table 3.2.13: Length of Vertical TR above Girder Top Flange

	Span	Location										
		0	0.1	0.2	0.3	0.4	0.5	0.6	0.7	0.8	0.9	1
NU 900	100	7.87	6.70	5.90	5.38	5.09	5.00	5.09	5.38	5.90	6.70	7.87
NU 1100	120	8.58	7.11	6.11	5.47	5.11	5.00	5.11	5.47	6.11	7.11	8.58
NU 1350	130	7.90	6.69	5.88	5.37	5.09	5.00	5.09	5.37	5.88	6.69	7.90
NU 1600	140	7.30	6.32	5.67	5.28	5.07	5.00	5.07	5.28	5.67	6.32	7.30
NU 1800	160	7.81	6.58	5.80	5.33	5.08	5.00	5.08	5.33	5.80	6.58	7.81
NU 2000	180	8.29	6.83	5.91	5.37	5.09	5.00	5.09	5.37	5.91	6.83	8.29
Average		7.96	6.71	5.88	5.36	5.09	5.00	5.09	5.36	5.88	6.71	7.96

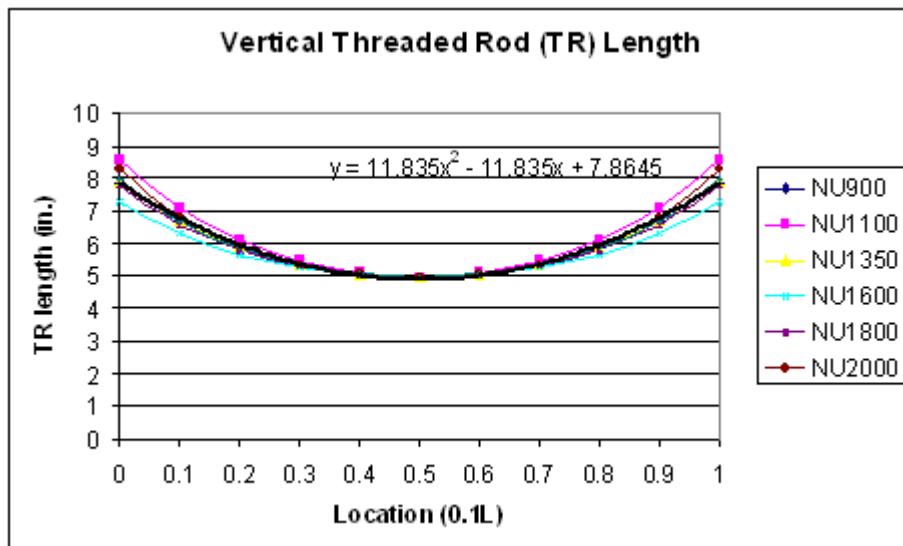


Figure 3.2.19: Vertical TR Length Calculation Diagram

The embedded length keeps a 12” constant value. In actual bridge girders, prestressing strands have to be draped underneath the vertical TR.

8. Confinement Analysis

Concrete is confined by #3 bars at non-uniform spacing in the transverse direction and close to the top of the girder bottom flange. The average spacing of 6.4” ($6.4 = 8 \cdot 12 / 15$) is used in the calculation. To be conservative, the shoe plate is considered as #4 @ 6.4” spacing. In the vertical direction, there are two plates and shear studs. By using Mander’s method, concrete strength can be increased from 8.5 ksi to 9.638 ksi with the confinement above.

Table 3.2.14: Confinement Analysis

E_s	ksi	29000						
longitudinal steel area	in ²	3.472						
A_g/A_c		2.0	ok				equations are based on some dat	
Unconfined Concrete Strength f_{c0}	ksi	8.5						
Confinement properties			x direction	y direction				
Section outline	in.	38.4	5.3					
length b_c -center to center	in.	37.90	2.75					
legs number		7	2					
lateral spacing S_L	in.	6.00	2.75					
Confinement Steel f_y	ksi	60	36					
Confinement longitudinal spacing S in.		6.4	2.75					
Confinement			Size	Area (in. ²)	Diameter, d_b (in.)			
			x direction	y direction	x direction	y direction	x direction	y direction
Wire		0	0	0	0	0	0	
Bar		5	3	0.31	0.11	0.625	0.375	
Plate /spacing				0	0			

$w = S_L - d_b$	in.	5.38	2.38	lateral Effective spacing assume the ineffective part is circular
$s = S - d_b$	in.	5.78	2.38	Longitudinal effective spacing
$\rho_{LS} = \frac{A_{LS}}{b_{\alpha} b_{\alpha y}}$		0.03		Longitudinal steel volumetric ratio
$k_e = \left(1 - \frac{\sum (w_i/6)^2}{b_{\alpha} b_{\alpha y}}\right) \left(1 - \frac{s_x}{2b_{\alpha}}\right) \left(1 - \frac{s_y}{2b_{\alpha y}}\right) / (1 - \rho_{LS})$		0.517		I change original equation into two directions
$f_L = \frac{\sum A_s f_y}{b_c S}$	ksi	0.54	0.45	
$f'_L = f_L k_e$	ksi	0.278	0.233	
$f'_{cc} = f'_{c0} + 4.1 f_L$	ksi	9.638	9.454	this equation is only for circular section.
$\epsilon_{c1} = \epsilon_{01} \left(5 \frac{f'_{cc}}{f'_{c0}} - 4\right)$	ksi	0.003		
$r = \frac{E_c}{E_c - f'_{cc} / \epsilon_{c1}}$		2.07		Curve Fitting Factor
ϵ_{ou}		0.0059		
$f_c = f'_{cc} \left(\frac{r(\epsilon_{cc} / \epsilon_{c1})}{r - 1 + (\epsilon_{cc} / \epsilon_{c1})^r} \right)$	ksi	8.193	at ϵ_{ou}	0.85f _c

The increased ratio of concrete strength is $9.638 / 8.5 = 1.13$.

For the concrete in the diaphragm, there are confinements in two directions. One direction of confinement comes from two girders and the other direction of confinement comes from the diaphragm. If $f'_c = 6$ ksi, and the strength is assumed to be increased 50% due to the confinement then $6 * 1.5 = 9$ ksi, which is larger than the 8.5 ksi designed concrete strength without considering confinement. If $f'_c = 4$ ksi, then $4 * 1.5 = 6$ ksi, which is not enough. Therefore in the diaphragm, 6 ksi concrete is necessary.

3.3 Construction and Testing

The two 25 ft long NU900 I girders were fabricated at Concrete Industries Inc.



Figure 3.3.1: Confinement at the End of the Girder and C shape Bar around TR



Figure 3.3.2: Vertical TR, C shape Bar, and Horizontal Shear Reinforcement



Figure 3.3.3: Common End Plate



Figure 3.3.4: Ten pieces 1 3/8" TR Placed on Top with 0.75" Gap



Figure 3.3.5: Welding the Sole Plate and the Shoe Plate Together



Figure 3.3.6: Forming for the Deck and Diaphragm

The strain gages would be put on the TR, shoe plate, sole plate and concrete at the girder bottom flange both inside of the diaphragm and outside of the diaphragm. The critical section at negative moment area is at the face of the diaphragm. The maximum gage number the computer can take is 24. All the strain gages, a total of 17, are on the north side of the girder near the load cell. The gage locations are shown in the following pictures:

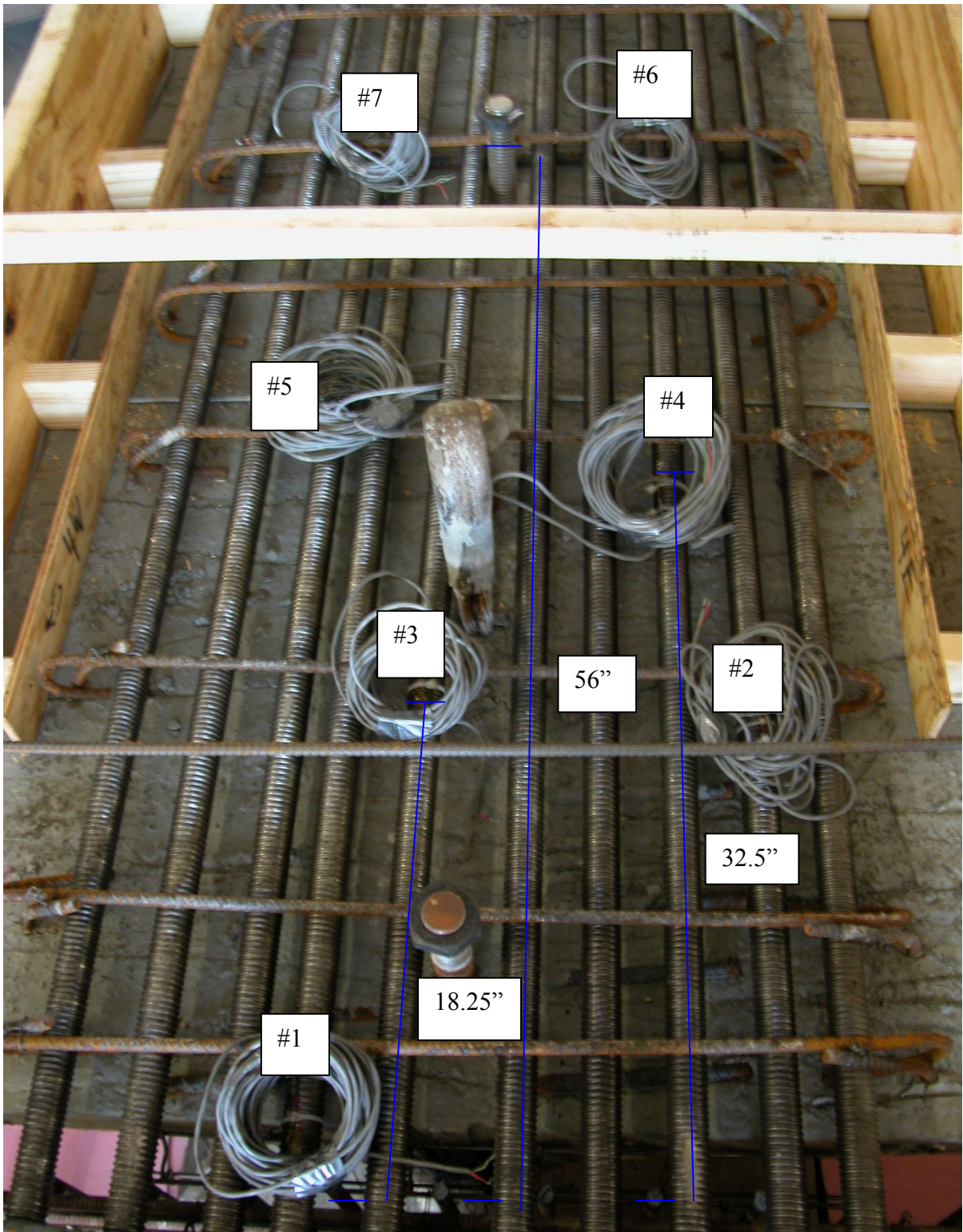


Figure 3.3.7: Strain Gages on TR

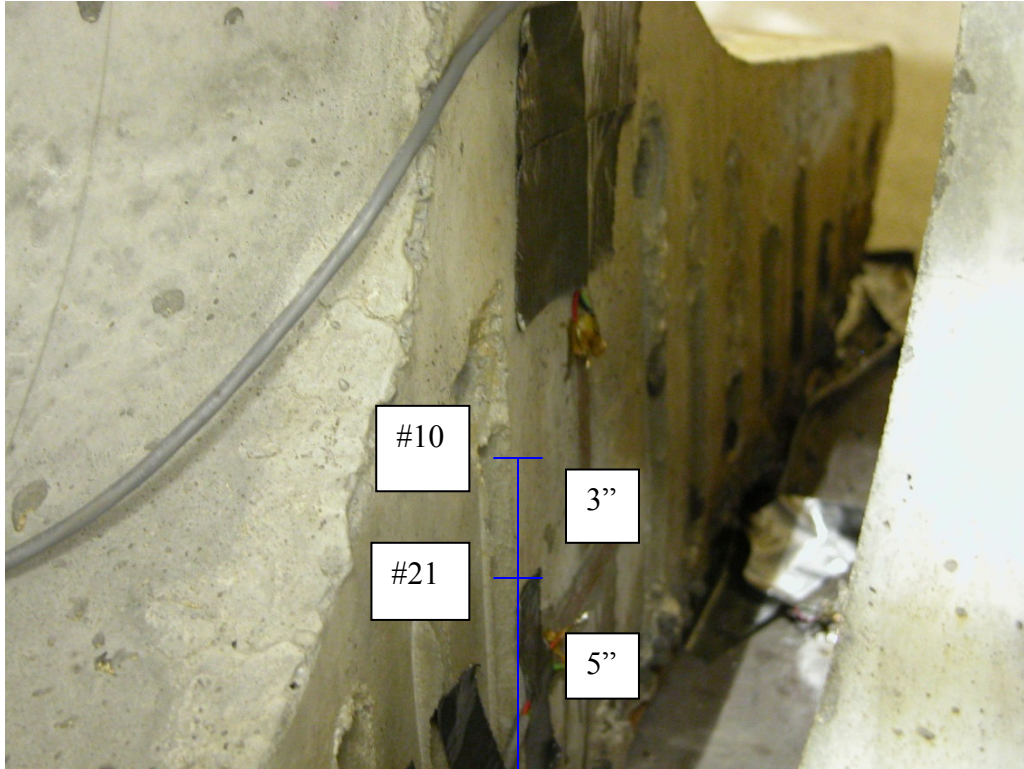


Figure 3.3.8: Strain Gages on the End of Girder

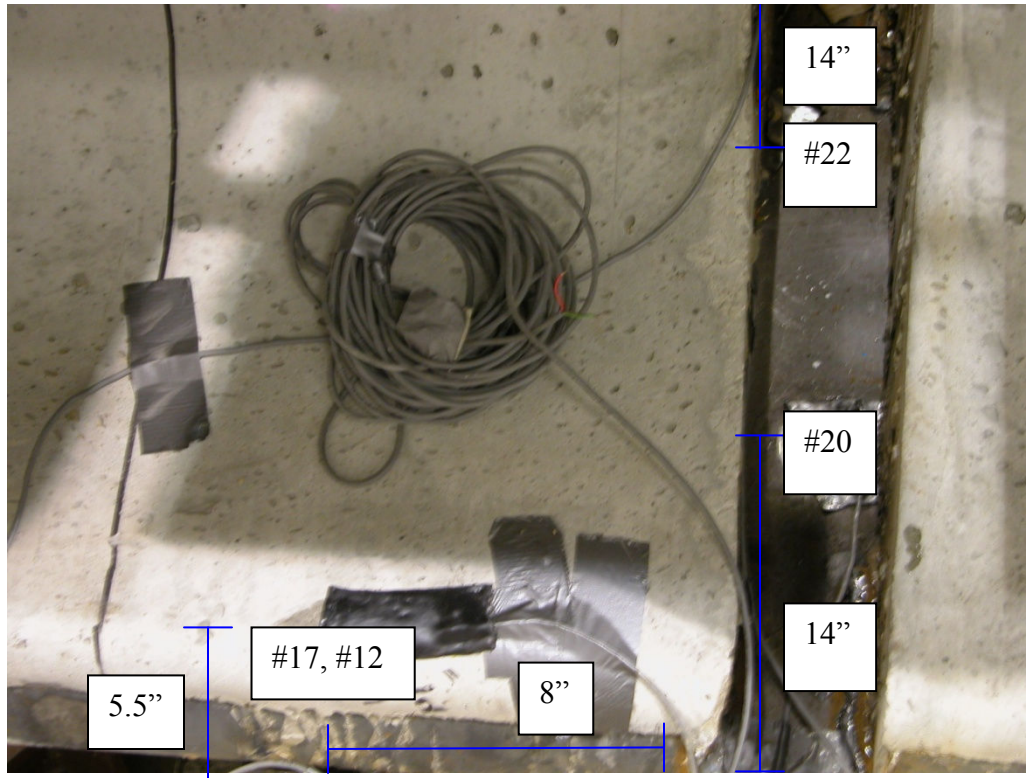


Figure 3.3.9: Gages in the Sole Plate and Girder Bottom Flange

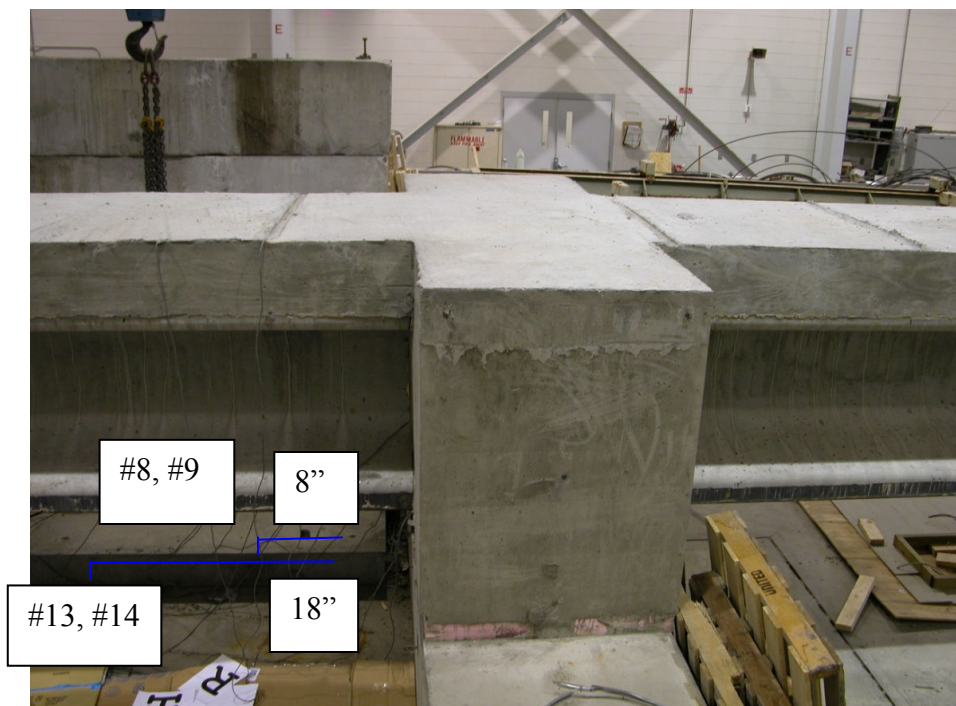


Figure 3.3.10: Strain Gages on the Girder Bottom Flange



Figure 3.3.11: Diaphragm Reinforcement

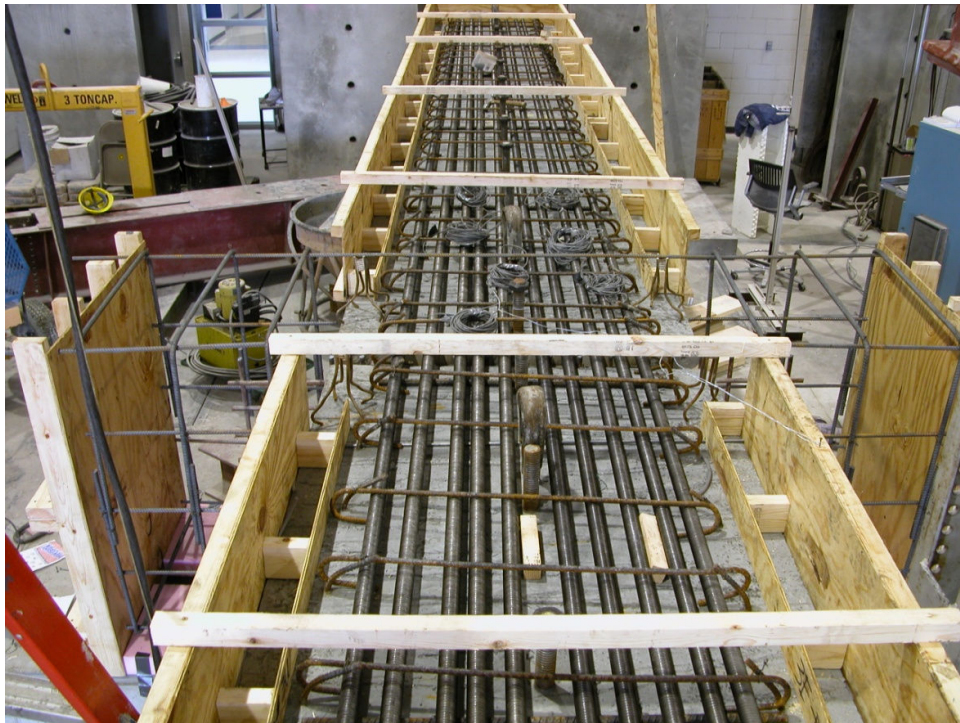


Figure 3.3.12: Horizontal and Vertical TR



Figure 3.3.13: Reinforcement at the End Where Load Works On



Figure 3.3.14: Pouring 6.0 ksi Concrete for the Diaphragm and the 3.5" high Interface Block



Figure 3.3.15: Place Deck Reinforcement



Figure 3.3.16: Pour Deck Concrete

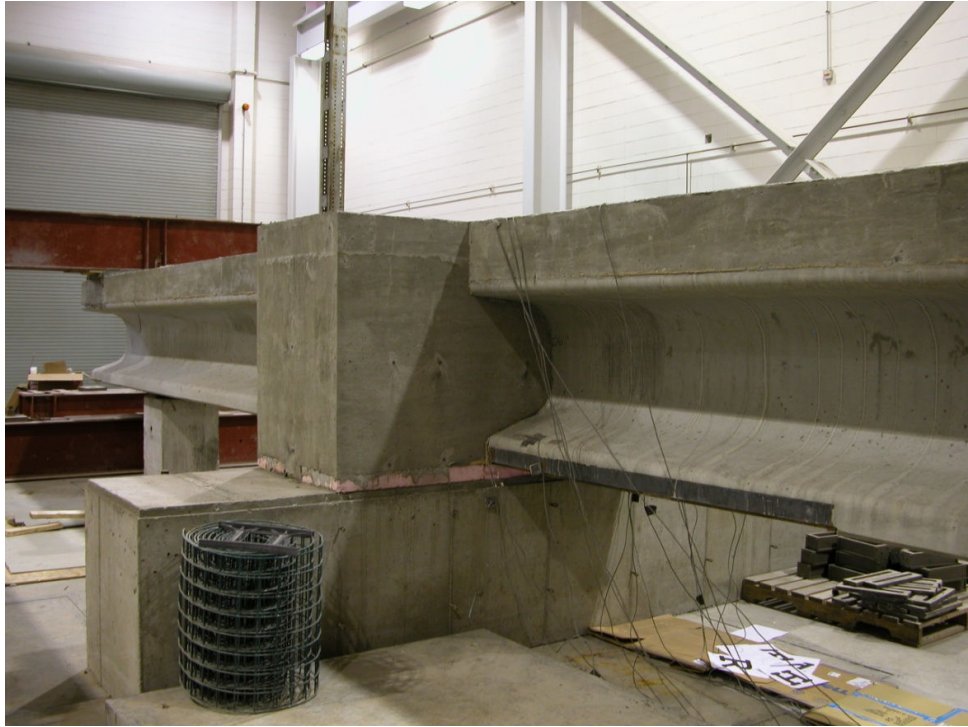


Figure 3.3.17: Deck, Girder and Diaphragm after Taking the Forms



Figure 3.3.18: Active End of Loading



Figure 3.3.19: Passive End of Loading



Figure 3.3.20: Final Flexural-shear Crack near the Pier, $P = 324$ kips

A large crack occurred at the lifting point because we did not cut the lifting out. In an actual bridge, it is cut.



Figure 3.3.21: Deflection at 324 k

STRAIN GAGE RESULTS

The maximum load is 324 kips. A large deflection was observed. The rotation at the loading end prevented further loading.

Table 3.3.1: Composite Section Properties

	A	y_b	E_c	n	A_{tr}	$A_{tr}(y_b)$	I	$A_{tr}(y_b-y)$
Girder	648.10	16	7,064	1.0	648	10434	110262	61638
deck	530.20	41	5,165	0.7	388	15857	3909	87790
Strands	3.47	2	28,500	4.0	11	21	0	5994
TR	15.80	37	29,000	4.1	49	1807	0	5921
Deck bar	4.08	42	29,000	4.1	13	526	0	3114
		26					278629	

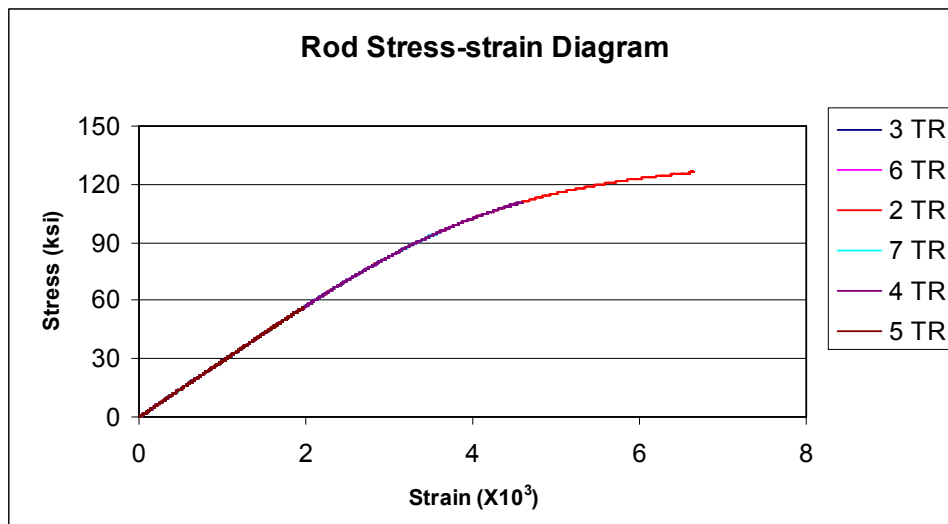


Figure 3.3.22: TR Stress

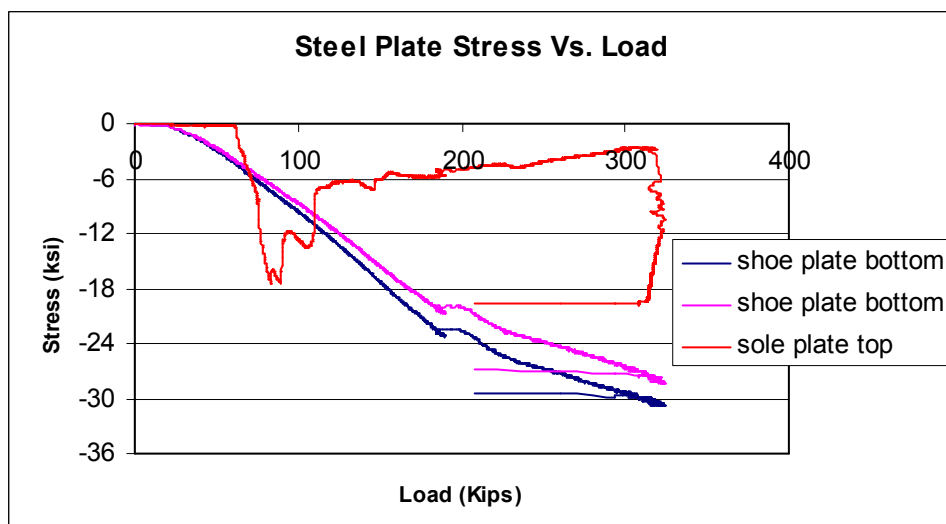


Figure 3.3.23: Steel Plate Stress

The concrete stress is calculated based on Popovics Equation, shown in the figure below.

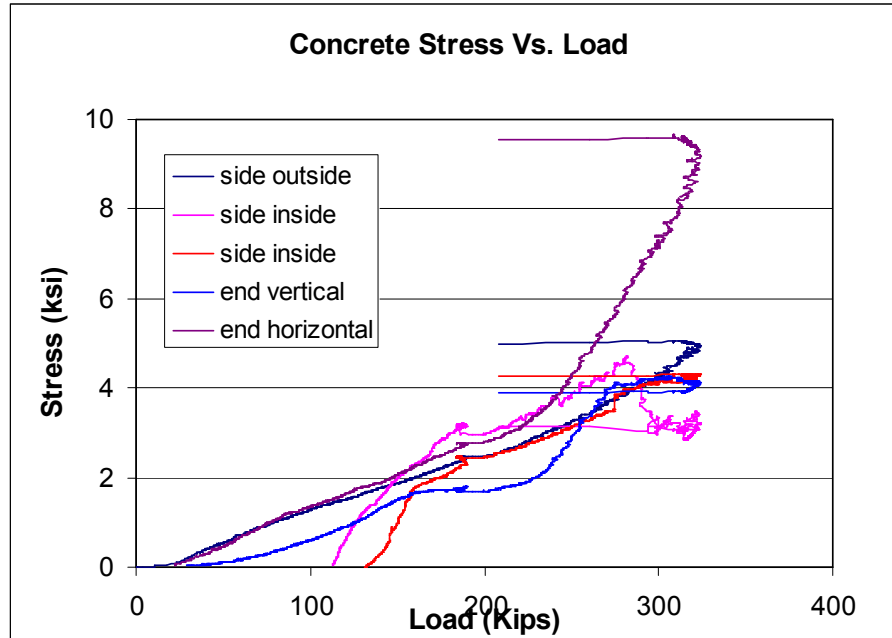


Figure 3.3.24: Stress of Concrete at Bottom Flange

RE-APPLY LOAD TO FAILURE

The authors added a roller underneath the steel beam to allow the end of the girder to freely rotate. Then the beam was reloaded again until the sole plate buckled at the face of the diaphragm when load was equal to 382 kips. Everything was fine in the deck.



Figure 3.3.25: Add a Roller to Achieve Larger Rotation

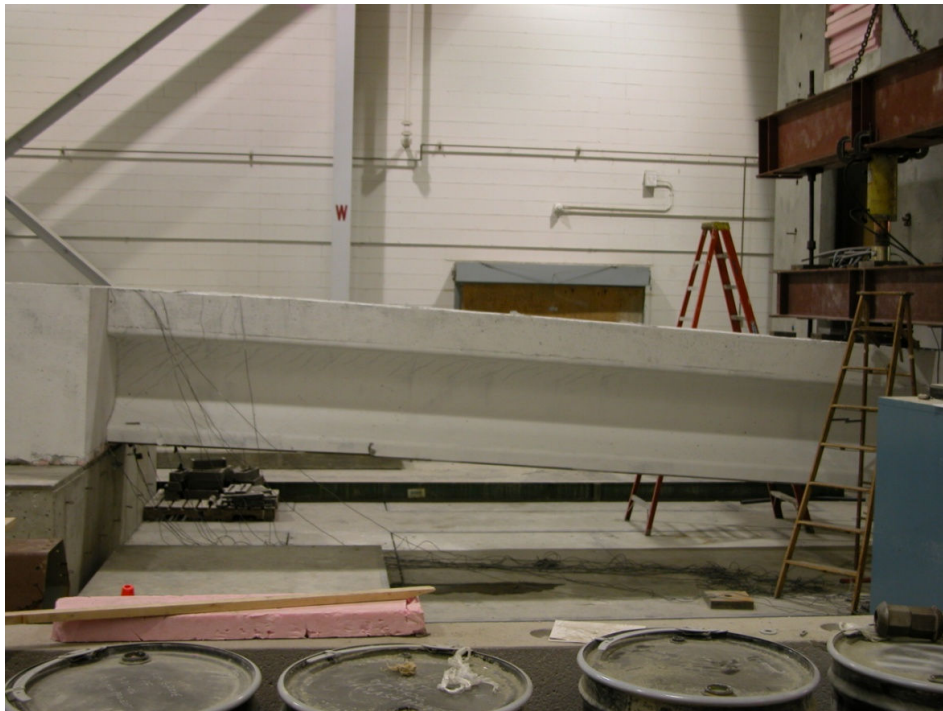


Figure 3.3.26: Large Deflection



Figure 3.3.27: Specimen Failure at 382 kips



Figure 3.3.28: Shoe Plate Buckled at the Face of Diaphragm



Figure 3.3.29: Crack on the Top at Failure

When the specimen was taken apart at the face of the diaphragm, there was no crushing of concrete around the TR or slippage between the concrete and the TR, as shown in Fig. 3-56.



Figure 3.3.30: No Slippage between TR and the Concrete around them

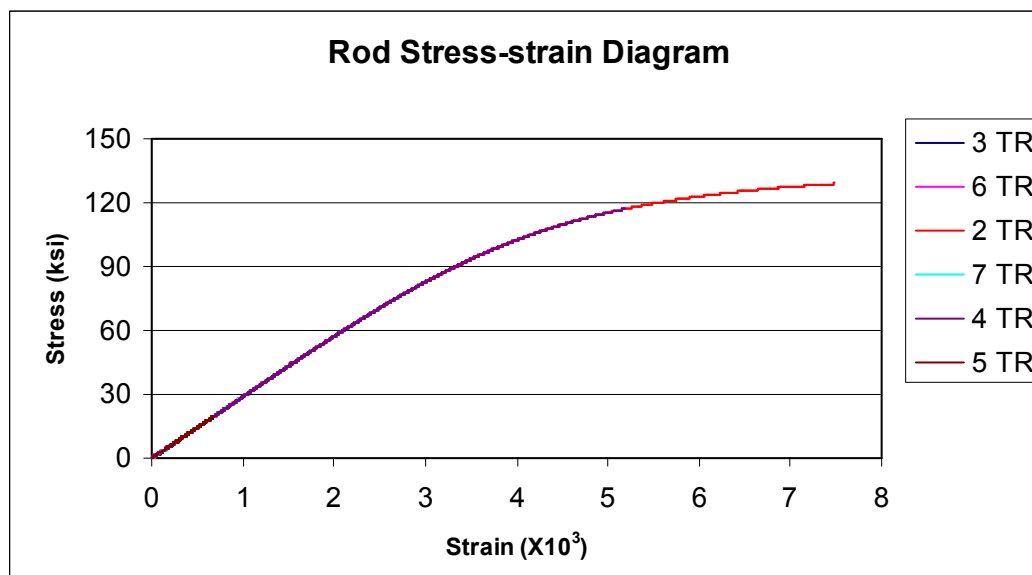


Figure 3.3.31: TR Stress

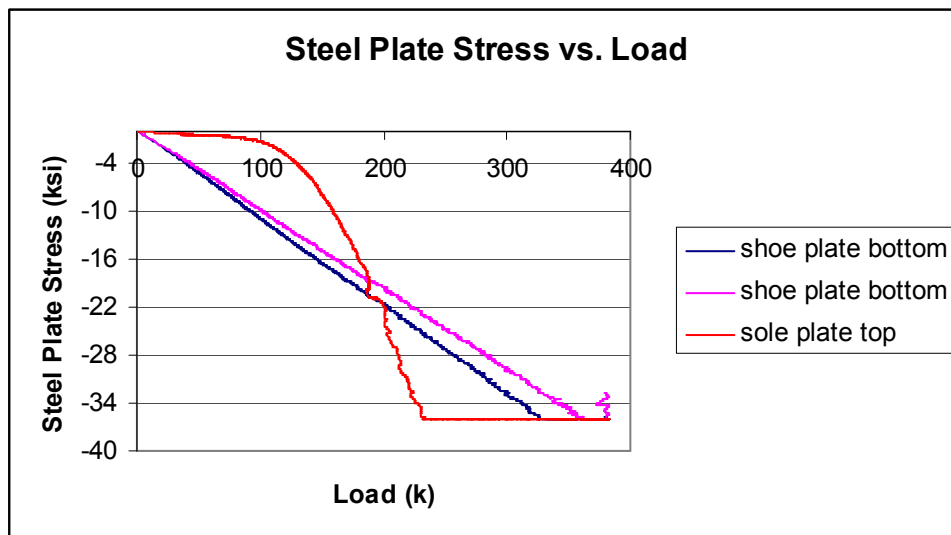


Figure 3.3.32: Steel Plate Stress

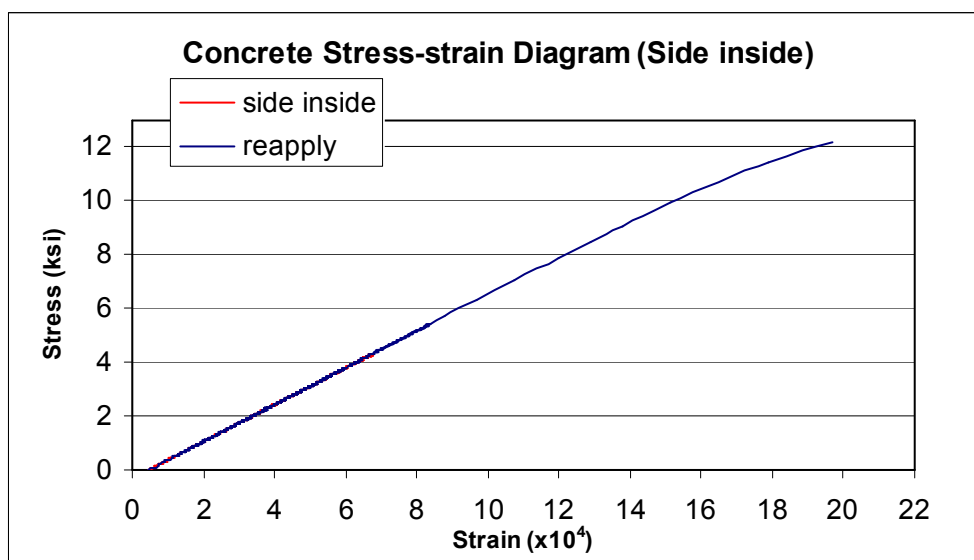


Figure 3.3.33: Concrete Stress at Bottom Flange

3.4 Conclusions and Recommendations

- The Threaded Rod Continuity System has been proven as efficient and cost-effective on recent projects in Nebraska.
- The most recent full-scale tests demonstrated excellent negative moment zone behavior.

- There was good bond between the TR and the concrete around them.
- The specimens showed good ductility.
- The confinement around TR was proven to be a good design.
- The specimens showed high horizontal shear resistance capacity.
- 10-1 3/8 G150 rods can be used at present.

RECOMMENDATIONS

1. Due to space limits at the web of I-beam near the vertical TR, draping strands should be draped just lower than the vertical TR.
2. The girder bottom flange is the most critical zone in TR continuity system. Based on the excellent performance of the details in the laboratory, the author recommends that shoe plate and shear studs be adopted as the standard detail for TR continuity system to strengthen the bottom zone near the pier. The concrete strength, deck reinforcement and TR number is designed specifically by the designer.

4. Threaded Rod Third Generation

4.1 Introduction

Several lessons were learned from previous threaded rod continuity systems. The third generation threaded rod continuity system was developed to address these concerns. Full Scale Testing of a third generation threaded rod continuity system was done at the Structures Lab at the University of Nebraska. The test consisted of two 25 ft girders with a 2 ft wide diaphragm. The objectives of the test are:

- Test the flexural capacity of the 3rd generation threaded rod continuity system.

- Verify the benefits of increasing the confinement in order to increase strength and ductility over the negative moment sections.
- Observe the behavior of the diaphragm and the relationship between girder concrete and diaphragm concrete compressive strength.

The third generation continuity system seeks to improve the second generation system. These improvements include removing the side confinement plates and increasing the confinement reinforcement around the diaphragm. The large bearing plate at the diaphragm was replaced with a smaller 18 inch plate. The trough was removed and the reinforcement was replaced with C-shaped bars. The system also proposes that the diaphragm concrete strength need only be one-half the girder concrete strength.

The girders were placed on bearing plates with a 4 inch gap in between. A 24" wide by 7-10" long diaphragm was placed in between the girders to provide support over the negative moment section. An end support was removed and a concentrated load was placed at the end of one girder to create cantilever-like loading. The following sections will further examine the lessons learned from previous threaded rod continuity systems. The entire fabrication, setup, and testing process of the third generation threaded rod continuity system will be described in detail.

4.2 Lessons learned from Second Generation

Through years of utilizing the Threaded Rod continuity system, there were a few suggestions emphasized by contractors and design engineers in order to improve the system. The three consistent challenges that were brought up while using this system are: the side confinement plate, bottom bearing plate, and the trough reinforcement located above the top flange of the girder.

4.2.1 Side Confinement Plate

The side confinement plate was used to confine the girder and its elements over the negative moment pier section. However, the threads that connect the side plates on both ends are difficult to manage and thread through the prestressing strands and reinforcement. An example of the side confinement plates are shown in Figure 4.2.1. Elimination of these plates would save cost and would require more confinement reinforcement within the bottom flange of the girder.

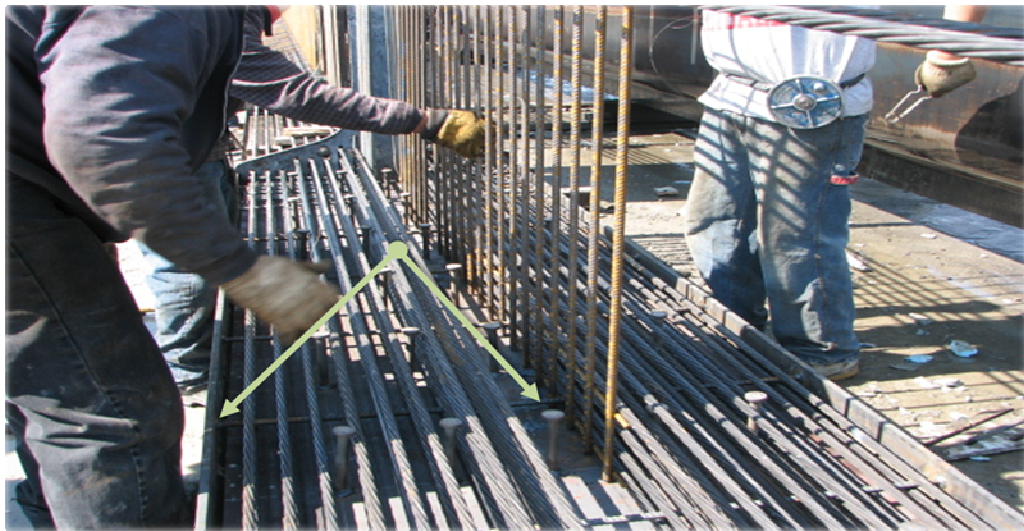


Figure 4.2.1: Side Confinement Plates

4.2.2 Bearing Plate

The second issue involves the bearing plate. The Grade 50W bearing plate sized at $\frac{3}{4}$ " x 8'-0" x 3'-0 $\frac{13}{16}$ " is embedded within the bottom flange of the girder over the pier section. The plate is connected with equally spaced shear studs to introduce composite action between the steel and concrete. However, a plate this size can be difficult to handle and was revealed to be a conservative approach. Furthermore, the cost of the plate can play a significant factor when performing a cost analysis. It is encouraged to reduce the plate size enough to still be able to

provide adequate compressive strength over the negative moment section. An example of this bearing plate is shown in Figure 4.2.2.



Figure 4.2.2: Bottom Bearing Plate

4.2.3 Trough Reinforcement

The third main issue with contractors on site is the trough reinforcement. After the concrete for the girder has been cast, the trough bars extrude from the top of the girder (Figure 4.2.3). After the threaded rods are placed over the interface block, the trough bars must be bent over the top of the threaded rods. This process creates an issue for contractors in their ability to bend the bars with limited space between the interface block and the trough bars. Furthermore, contractors must attempt to bring equipment on site to create a controlled bend that would enclose the threaded rods properly.

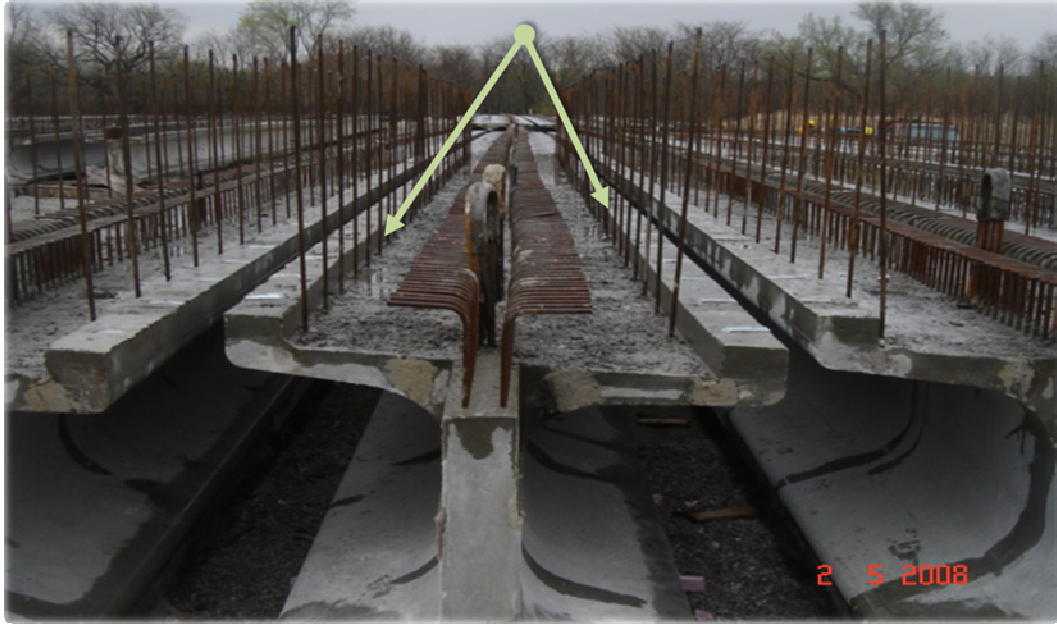


Figure 4.2.3: Trough Reinforcement

These three main issues along with others will now be addressed with an evolution into the 3rd Generation Threaded Rod Continuity System. This system will seek to maximize the total efficiency of the design and construction procedure. The following sections will now discuss the design, fabrication, and testing of the 3rd Generation TR Continuity System.

4.3 Design and Fabrication of NU 900 Girders

Two NU 900 girders were designed and fabricated at Concrete Industries in Lincoln, NE. The NU 900s were prestressed with 20 0.6 inch strand as shown in Figure 4.3.1.

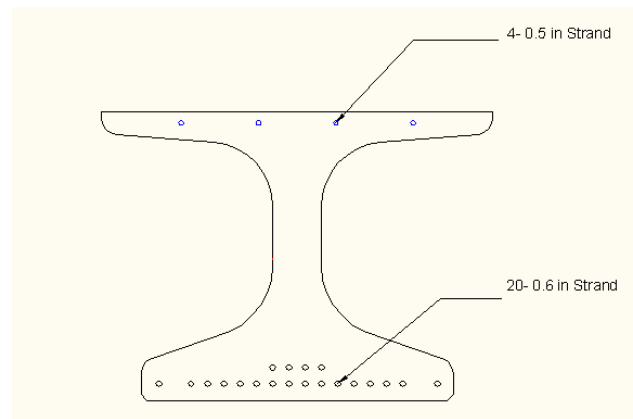


Figure 4.3.1: Strand Pattern for NU 900 test girder

The table below shows the section properties of an NU 900.

Table 4.3.1 NU 900

A		
=	648.1	in ²
y _t		
=	19.3	in
y _b		
=	16.1	in
I	110,26	
=	2	in ⁴
h		
=	35.4	in
w		k/f
=	0.697	t

The full reinforcement of the NU 900 is shown in Figure 4.3.2.

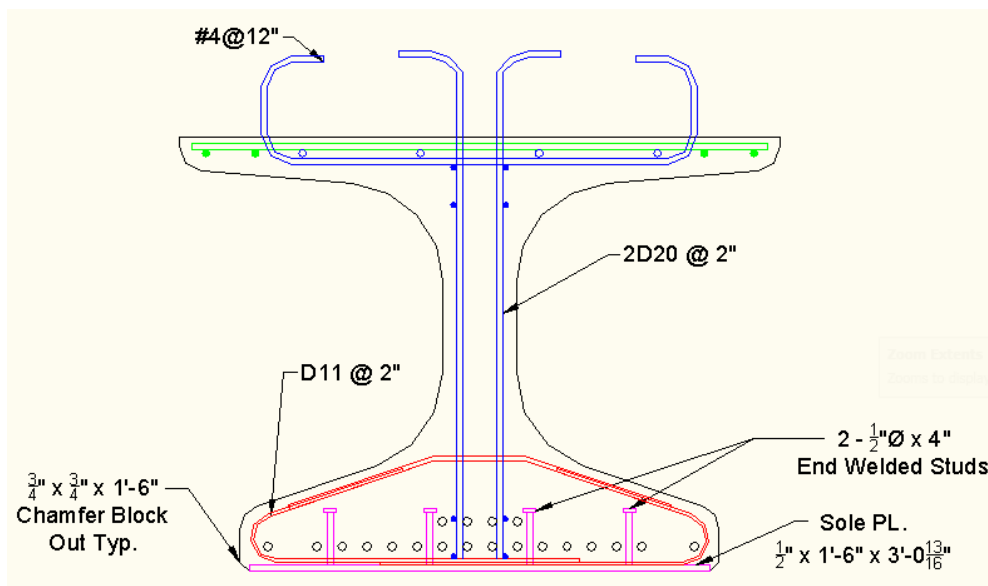


Figure 4.3.2: Test Girder Cross Section

The web shear reinforcement consisted of 2 D20 @ 2" welded wire meshes. #4 C-bars were placed in the top flange extended up into the deck to provide additional horizontal shear reinforcement. The confinement reinforcement consisted of D11 @ 2" near the diaphragm and D11 @ 6" over the rest of the girder as shown in Figure 4.3.3.

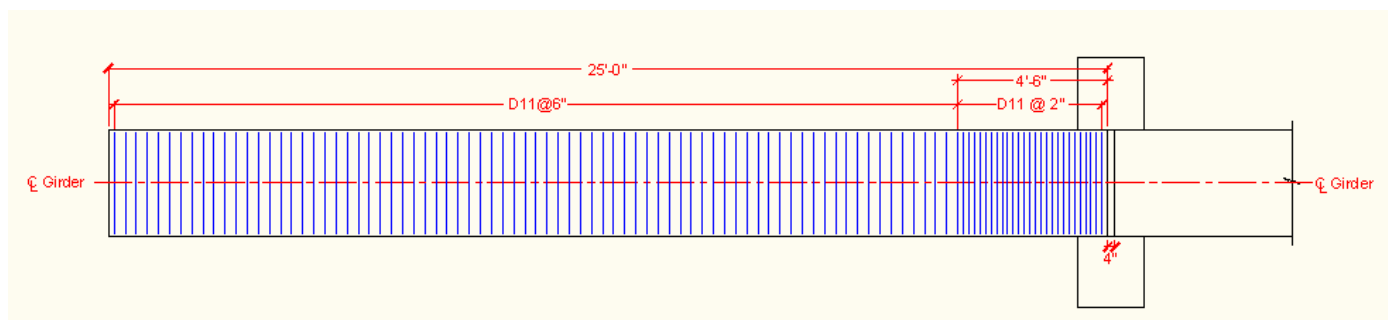


Figure 4.3.3: Bottom flange reinforcement plan view

The mix was an 8 ksi SCC mix used by Concrete Industries for bridge girders. Table 4.3.2 shows the compressive strength of the mix at important points.

Table 4.3.2: Mix Concrete Strengths

fci	f'c (28 days)	f'c (test date)
5981 psi	8236 psi	8603 psi

Figures 4.3.4 through 4.3.10 show the fabrication steps of the NU 900 test girders.



Figure 4.3.4: 18 inch end plate

The end plates had six ½ inch shear studs and four #6 bars welded for end zone reinforcement.

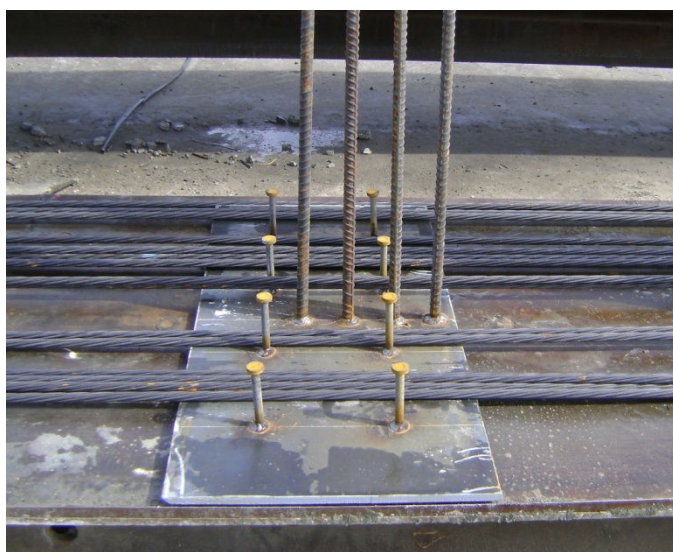


Figure 4.3.5: Placement of strands

After the 20- 0.6 inch strands and the 4- 0.5 inch top strands were all placed and tensioned, the bottom confinement, web reinforcement, and top flange reinforcement were placed.



Figure 4.3.6: Placement of confinement reinforcement



Figure 4.3.7: Placement of web and top flange reinforcement

The side forms were then placed and the concrete was poured.



Figure 4.3.8: Pouring of concrete

The girders were released at one day with an fci of 7 ksi.



Figure 4.3.9: Girders after release



Figure 4.3.10: Girder after release

Little to no cracking was noticed on the girders after release as shown above.

4.4 Threaded Rod Placement and Diaphragm/Interface Block Pour

The girders were delivered to the Structures Lab at the University of Nebraska Omaha. They were supported in the middle on 2 inch thick bearing plates supported by a large concrete block (See Figures 4.4.1 and 4.4.2). The other ends had removable supports. The girders were placed with a four inch gap at the location of the diaphragm as shown in Figure 4.4.3.



Figure 4.4.1: Placement of girder



Figure 4.4.2: 2 inch bearing plates



Figure 4.4.3: Placed girders with 4 inch gap

After the girders were in place, ten $1\frac{3}{8}$ " threaded rods were placed 0.625 inches above the top flange. The 50 ft long threaded rods rested on #5 bars. #4 C-bars at 1 ft spacing were tied on top of the threaded rod. See Figures 4.4.4 – 4.4.6.

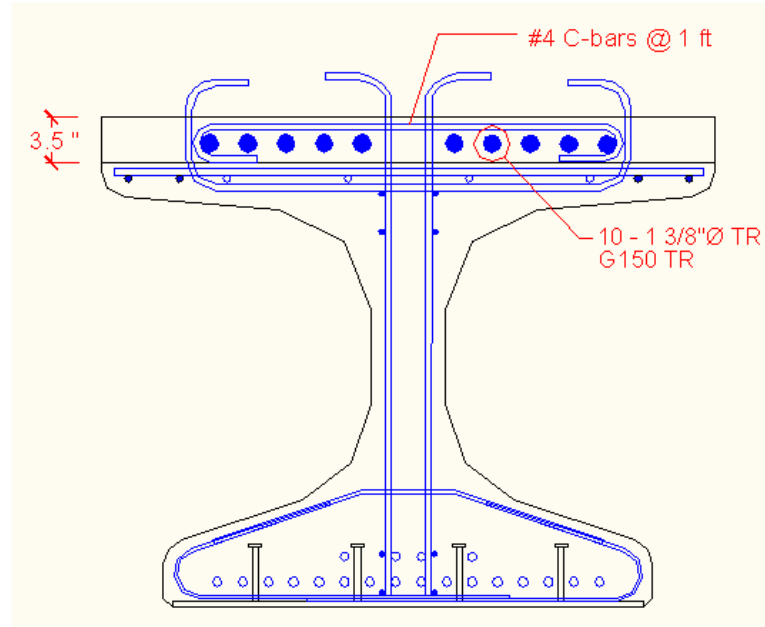


Figure 4.4.4: Cross section with interface block

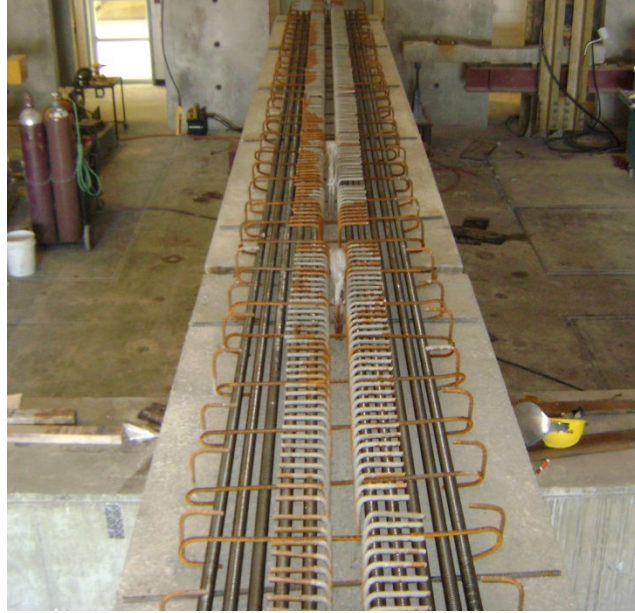


Figure 4.4.5: Placement of threaded rods

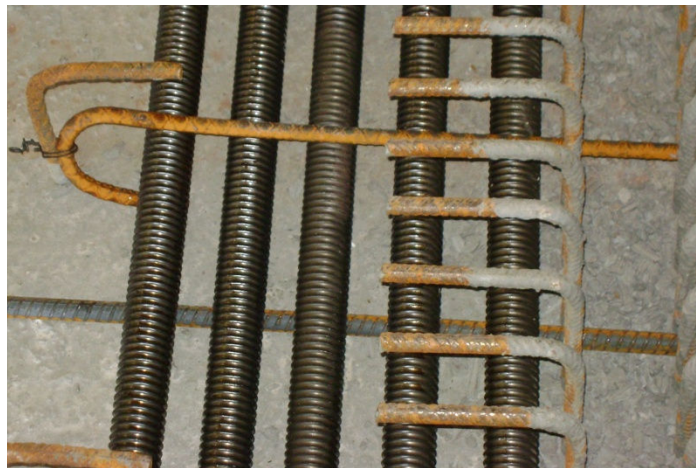


Figure 4.4.6: Placement of threaded rods

After the threaded rod and C-bars were tied, the diaphragm reinforcement was placed. The diaphragm was 2 ft wide by 7 ft -11 in. long (See Figures 4.4.7 - 4.4.8).

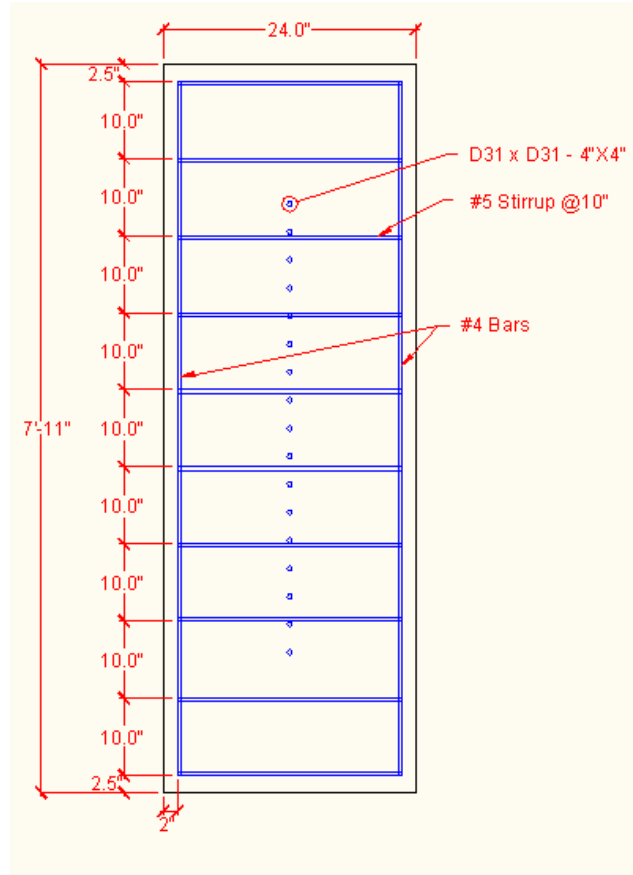


Figure 4.4.7: Plan view of diaphragm

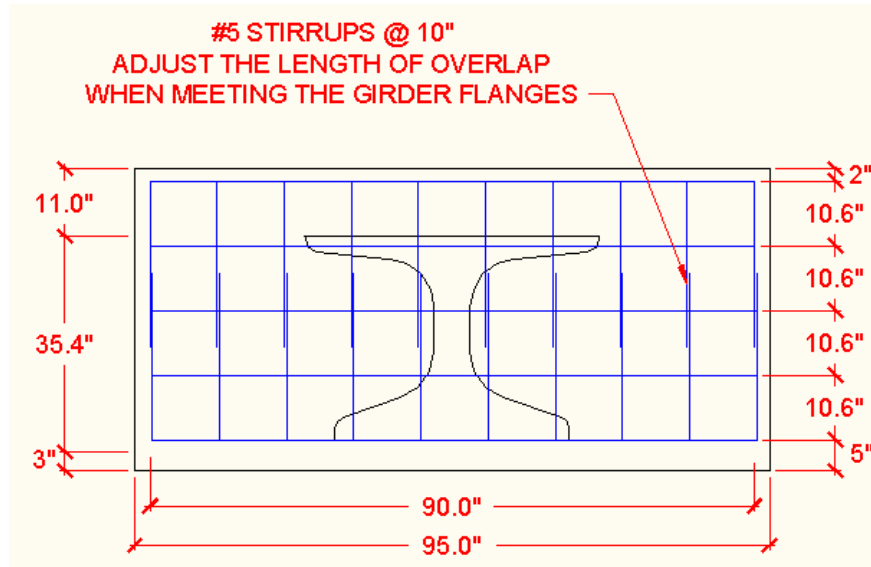


Figure 4.4.8: Side view of diaphragm

A 2 ft wide by 2 inch thick foam sheet was laid under the diaphragm. See Figures 4.4.9-4.4.10 for pictures of the diaphragm reinforcement before the pour.

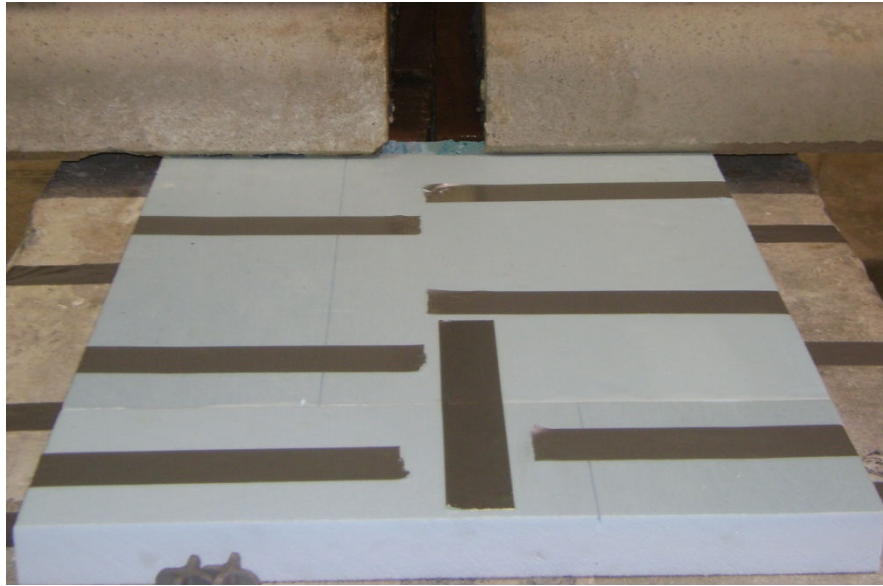


Figure 4.4.9: 2 inch foam sheet below diaphragm

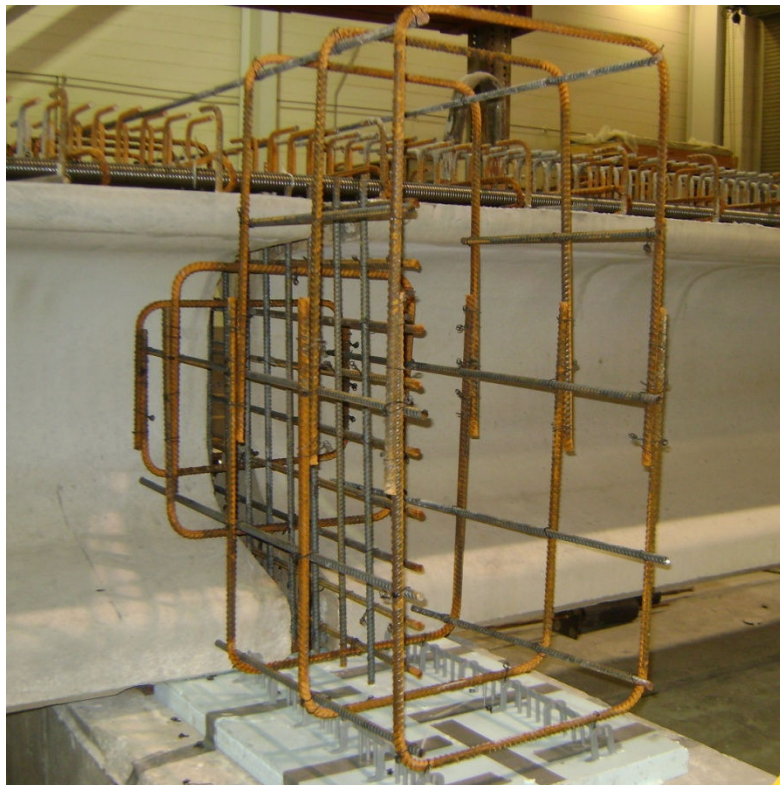


Figure 4.4.10: Diaphragm reinforcement

After all of the reinforcement for interface block and diaphragm was placed, the formwork was built and the concrete was poured.



Figure 4.4.11: Formwork around diaphragm

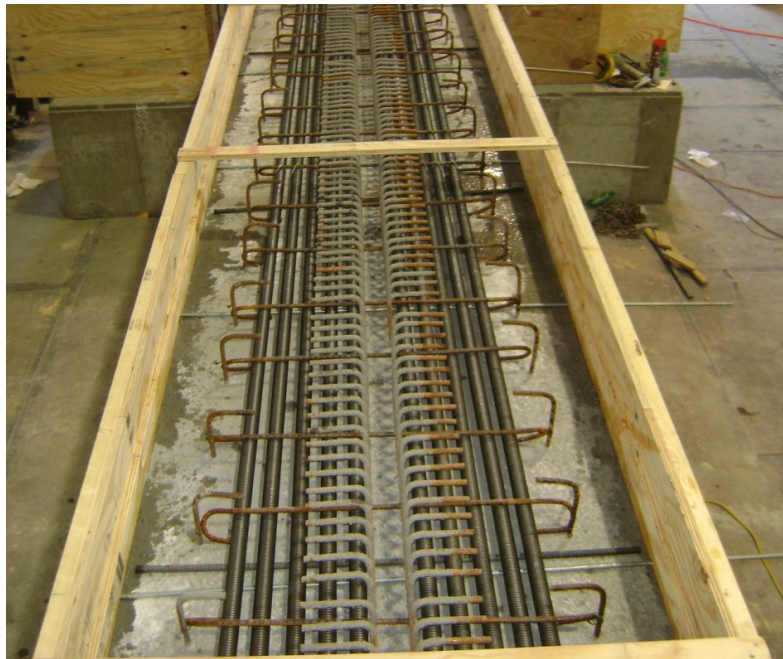


Figure 4.4.12: Formwork for interface block and deck

The concrete used for the interface block was a 4 ksi mix with 5 inch slump. The diaphragm was filled and vibrated, and a 3.5 inch layer of concrete was poured on the top flange (See Figures 4.4.13- 4.4.14).



Figure 4.4.13: Pouring of diaphragm



Figure 4.4.14: Pouring of 3.5 inch interface block

The concrete reached 4.3 ksi at the date of the test. Figure 4.4.15 shows the compressive strength of the interface block concrete versus time.

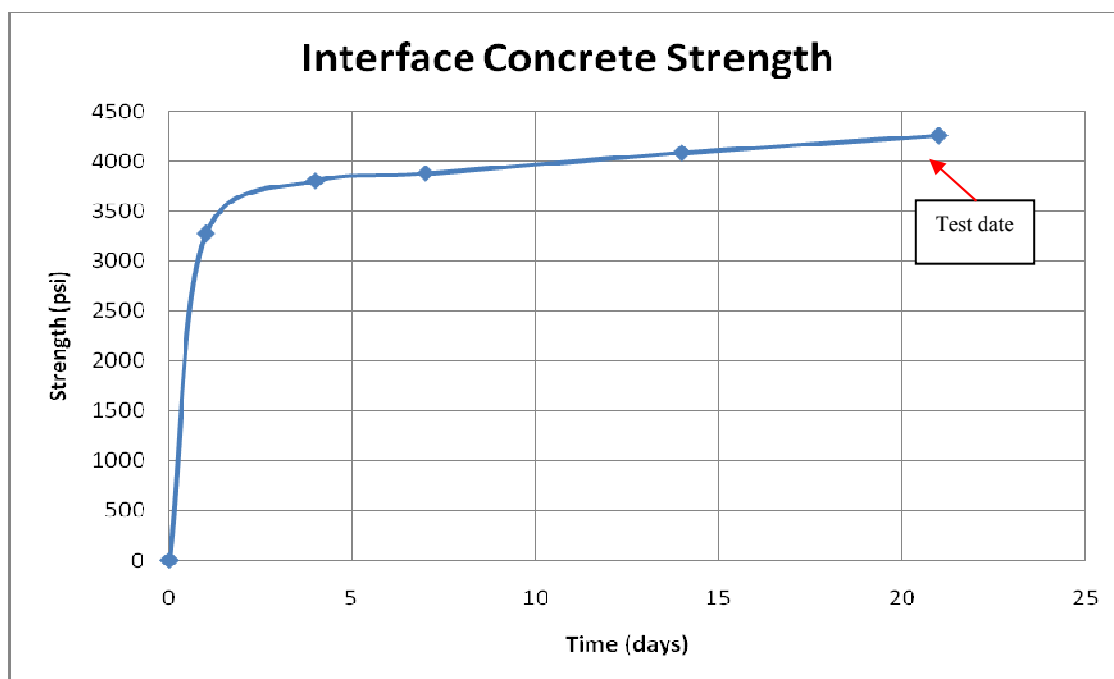


Figure 4.4.15: Concrete strength of interface block

4.5 Deck Reinforcement and Pour

After the diaphragm and interface block were poured. The 7.5 inch deck was reinforced and poured. The final cross section is shown in Figure 4.5.1.

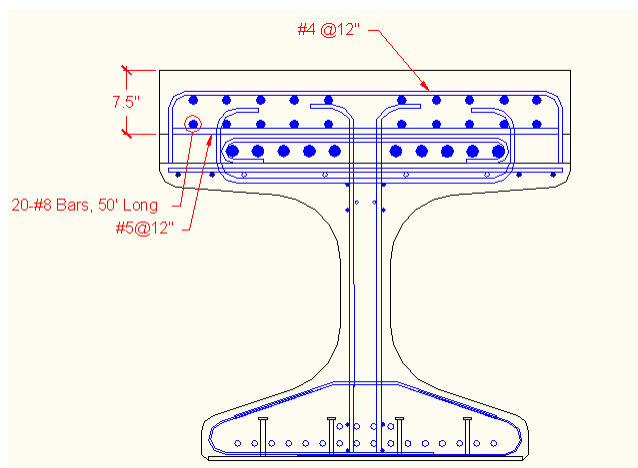


Figure 4.5.1: Final cross section with deck

The deck was reinforced with 20 #8 bars the full length of the specimen, 10 #8 for positive moment and 10 #8 for negative moment. #5 bars and bent #4 bars were used for secondary deck reinforcement. See Figure 4.5.2 for a picture of the deck reinforcement before pouring of the concrete.



Figure 4.5.2: Placement of deck reinforcement

The deck was poured using an SCC mix with 23 inch slump flow. The compressive strength of the mix over time is shown in Figure 4.5.3.

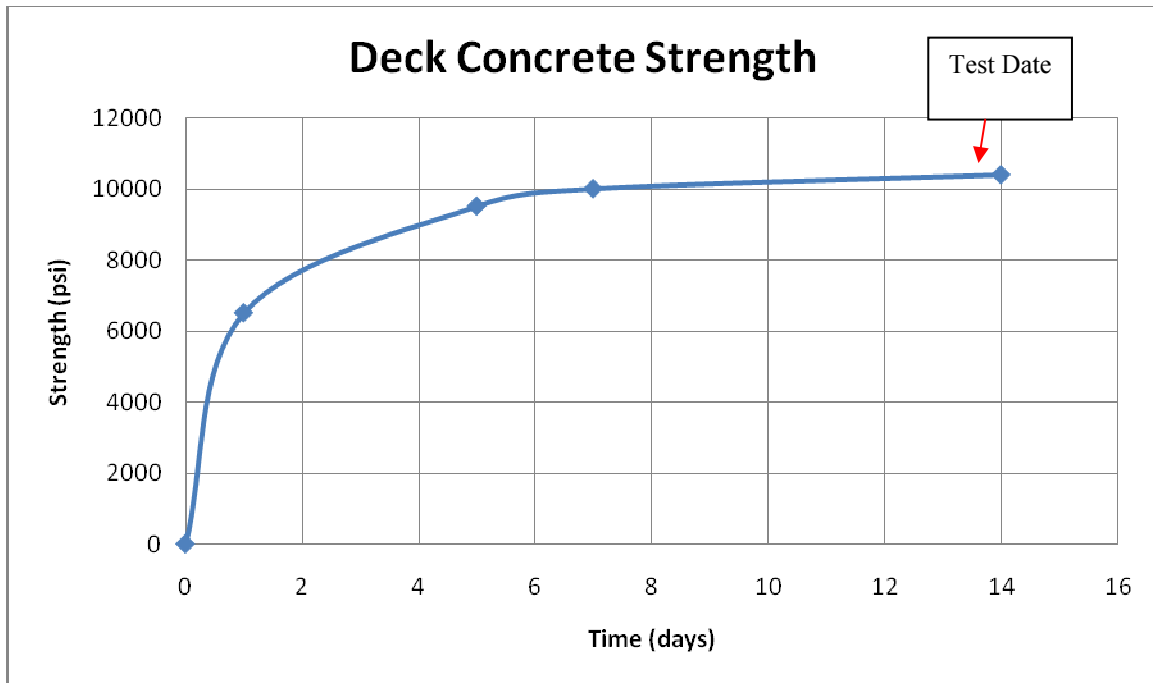


Figure 4.5.3: Compressive strength of deck concrete



Figure 4.5.4: Deck pour



Figure 4.5.5: Deck pour

4.6 Testing of Specimen

Test Setup

The third generation specimen was tested to determine the flexural capacity. The setup was a double cantilever supported at mid-span with two equal 25 ft spans on each side. Test frames were located 1 ft from each side. The north end was where the loading occurred. The south end had a frame supporting the top to prevent upward deflection from loading on the north end.



Figure 4.6.1.1: North end



Figure 4.6.1.2: South end

The load was applied 24 ft from the center of the diaphragm. Steel and concrete strain gauges were placed at various points on the specimen. 8 steel strain gauges were placed on the threaded rod. 6 concrete strain gauges were placed near the diaphragm.

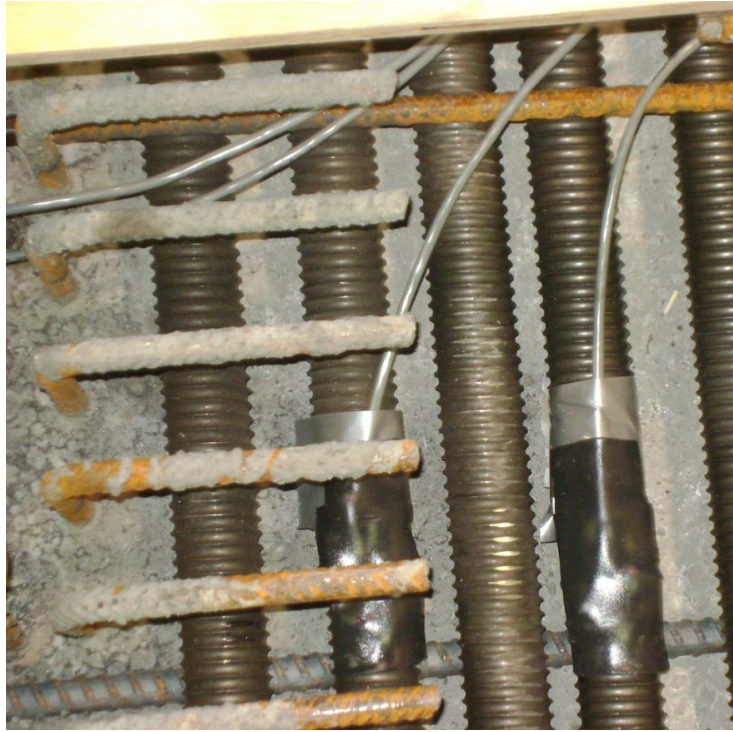


Figure 4.6.1.3: Steel strain gauges



Figure 4.6.1.4: Concrete strain gauges

The test measured load using a RocTest 330 kip load cell and measured deflection at the point of loading.

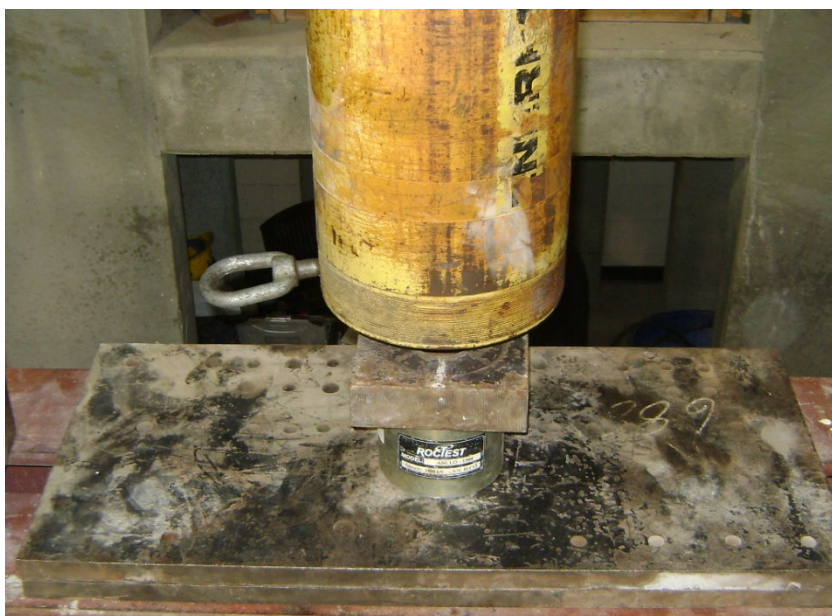


Figure 4.6.1.5: Jack and load cell

Summary of results

The third generation threaded rod continuity system was tested in flexure. The load was applied 24 ft from the center of the diaphragm. Failure occurred at 262 kips, which is close to the predicted failure load as shown in Table 4.6.2.1.

Table 4.6.2.1: Predicted load versus actual load

Predicted Failure Load	Tested Failure Load	Mode of Failure
260 kips	261,777 lb	Compression of bottom flange

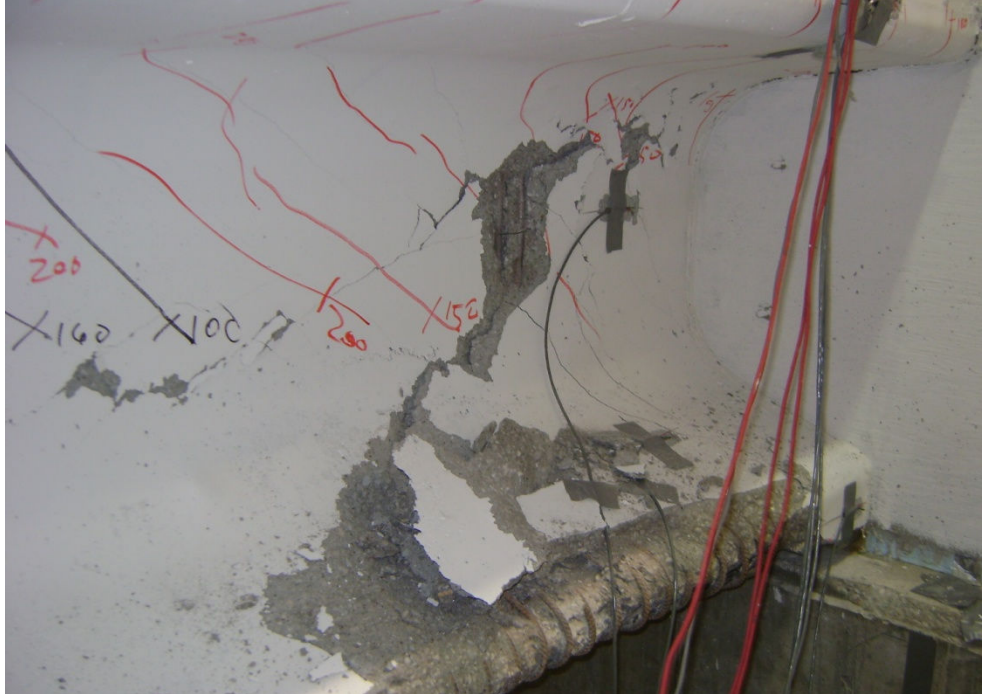


Figure 4.6.2.1: Failure near diaphragm



Figure 4.6.2.2: Failure near diaphragm

Figure 5.6.2.3 shows the load deflection curve for the test. The deflection reached nearly 8 inches.

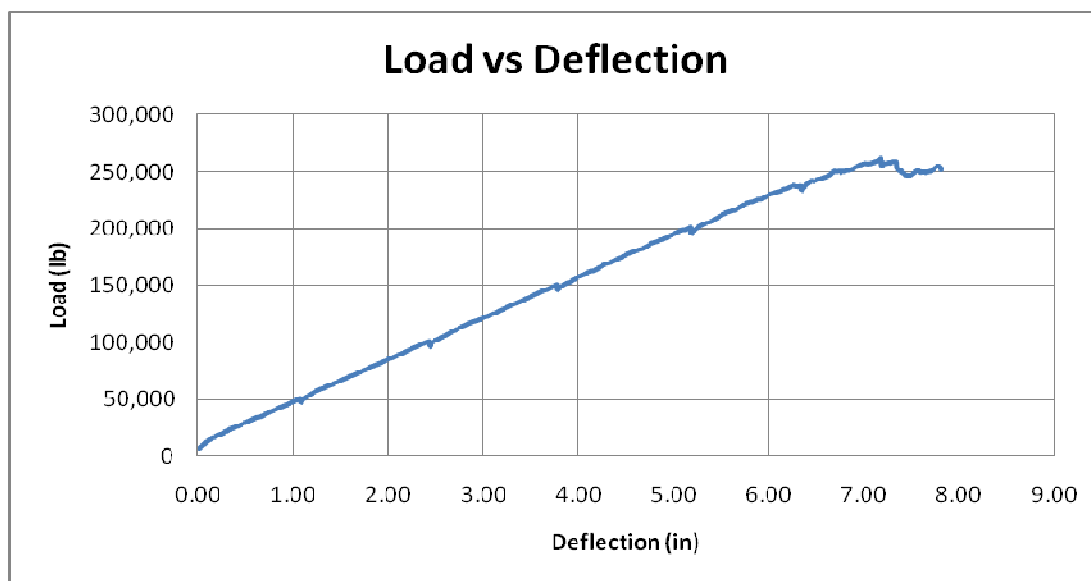


Figure 4.6.2.3: Load Deflection Curve

Of the 8 steel strain gauges attached near the diaphragm, 6 of them gave readings that were quite consistent as shown in Figure 4.6.2.4. Strain gauge 3 reached the highest stress of 82 ksi.

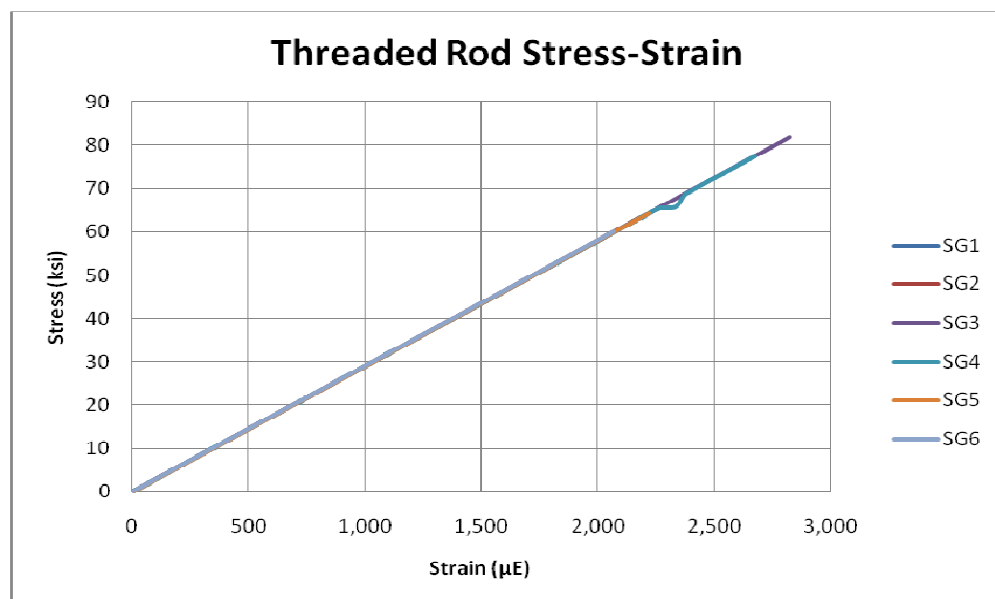


Figure 4.6.2.4: Thread Rod Stress-Strain Diagram

Six concrete strain gauges were attached to the girder near the diaphragm as shown in Figure 4.6.2.5. The web strain gauge did not give an accurate reading. The other five stress- strain diagrams are shown below.

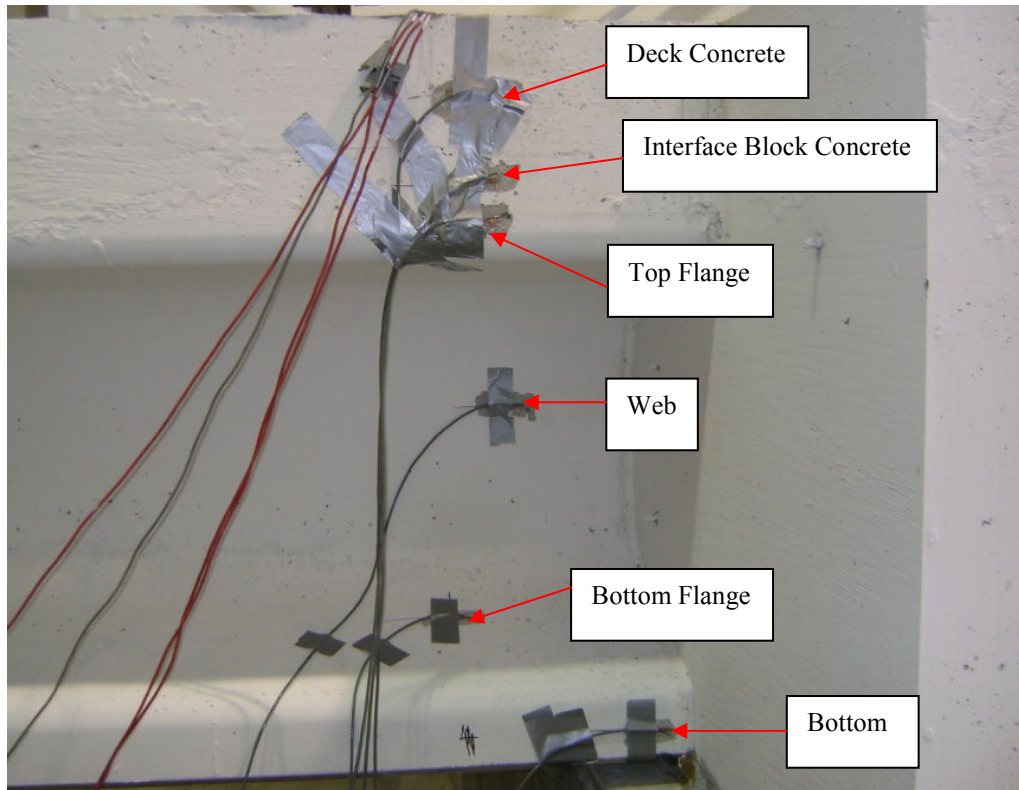


Figure 4.6.2.5: Arrangement of concrete strain gauges

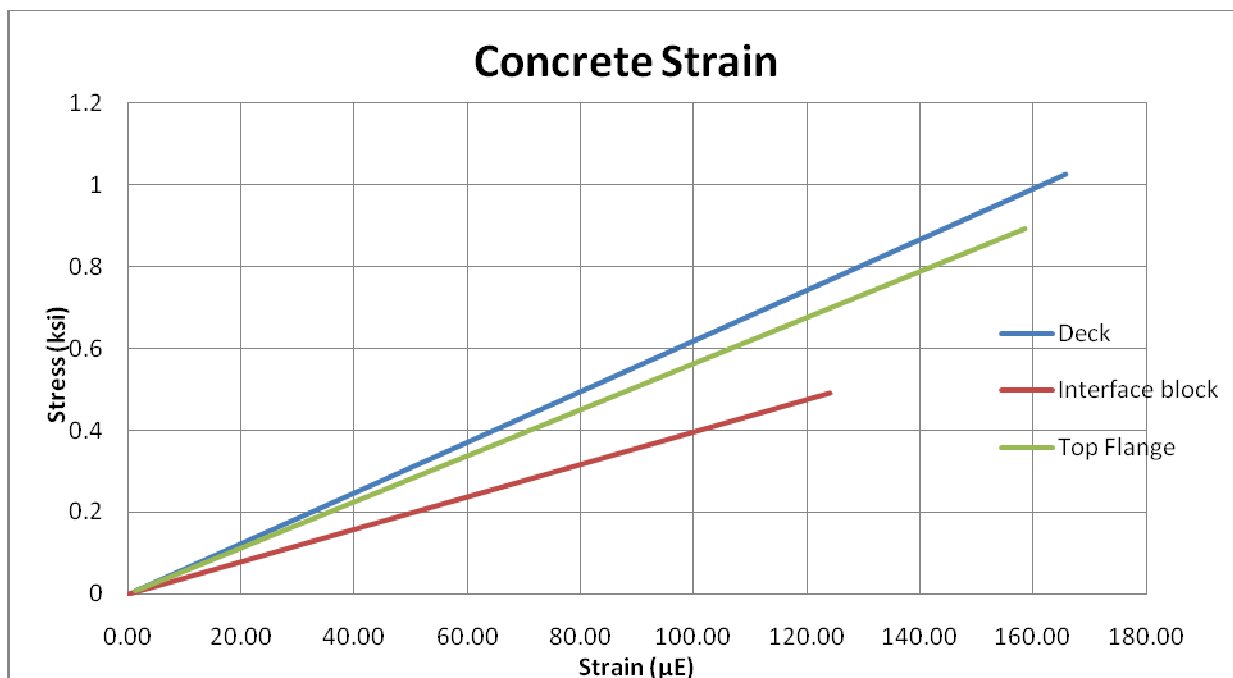


Figure 4.6.2.6: Stress-strain diagram of deck, interface, and top flange

The stress in the top two layers reached a maximum of around 1ksi. This is much less than the compressive strengths of the deck and interface block concrete on the test date, which were 10.4 ksi and 4.3 ksi, respectively. The strain in the top flange reached 0.5 ksi, which is significantly less than the girder compressive strength of 8.6 ksi on the date of the test.

As would be expected, the strain in the bottom flange and at the very bottom of the girder was significantly higher. The stress near the top of the bottom flange reached approximately 4 ksi (See Figure 4.6.2.7). The bottom of the girder, where failure occurred, reached a stress of over 9 ksi, which is close to the tested 8.6 ksi compressive strength of the girder concrete (See Figure 4.6.2.8).

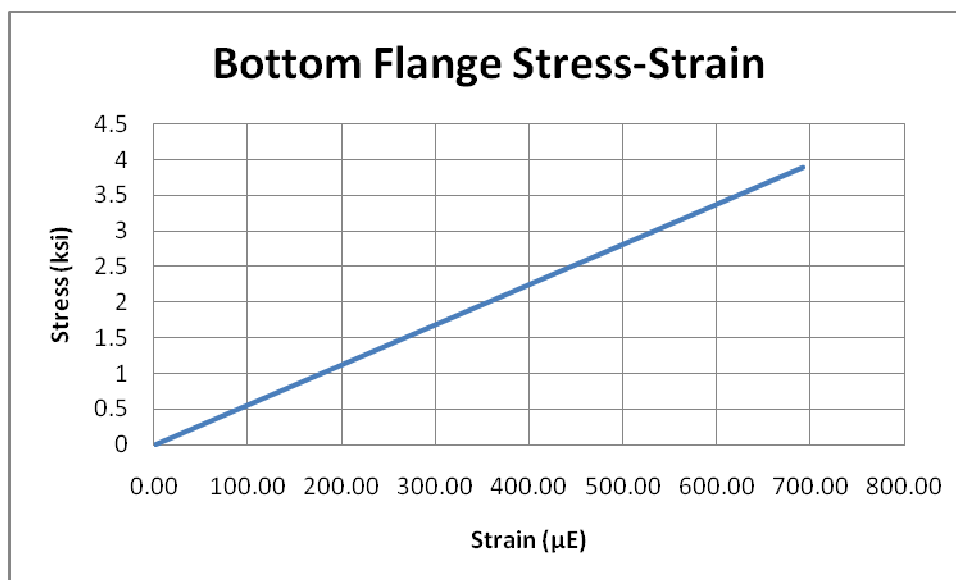


Figure 4.6.2.7: Stress-strain diagram of bottom flange

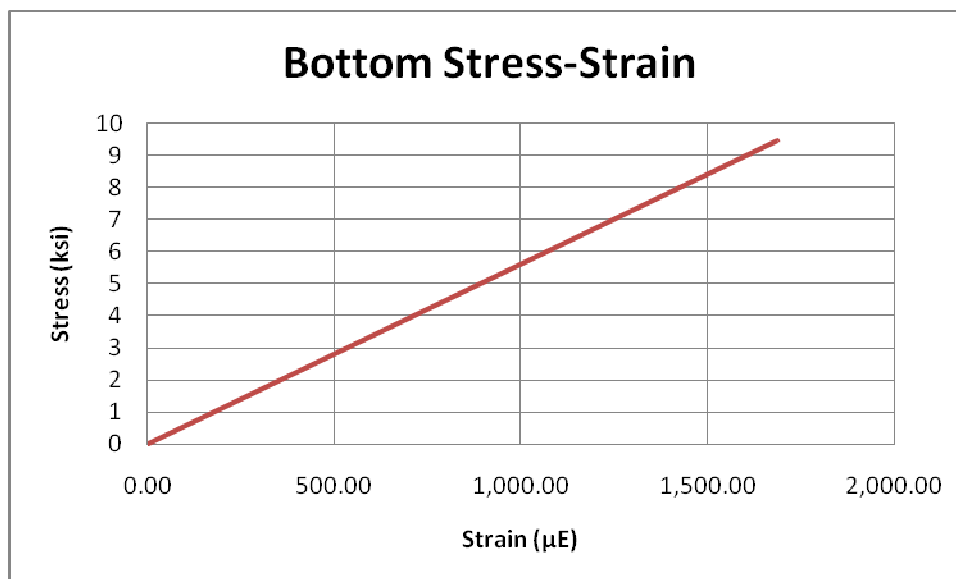


Figure 4.6.2.8: Stress-strain diagram of bottom

The test demonstrated the viability of the third generation threaded rod continuity system. The moment capacity was reached before failure. The diaphragm was strong enough even with a compressive strength of half the girder concrete strength.

5. Conclusions

5.1 Use of 0.7-Inch-Diameter Strands

This report presents the experimental investigation carried out to introduce the use of 0.7-in.-diameter, Grade 270, low-relaxation strand in pretensioned concrete bridge girders. A full-scale NU900 I-girder was designed using 0.7-in.-diameter strands. Transfer and development length of 0.7-in.-diameter strands were evaluated experimentally and compared with the values predicted using the AASHTO LRFD specifications' provisions for 0.5-in.-diameter and 0.6-in.-diameter strands. The main conclusions of this study can be summarized as follows:

- ❖ Production challenges of using large diameter strands are mainly those associated with handling a heavier and stiffer strand. Extra caution should be considered while pulling the strand out of the spool and feeding it along the bed. The availability of strands and chucks is not a problem. Minor modifications might be needed to enlarge the bulkheads openings and increase the prestressing capacity of the jacking equipment and/or prestressing bed.

- ❖ The transfer length of 0.7-in.-diameter (18 mm) strands is approximately 31 in. which is closer to the transfer length predicted using the ACI 318-08 equation of $50d_p$, than the prediction using the 2007 AASHTO LRFD specification equation of $60d_p$

5.2 Threaded Rod Continuity System

The third generation Threaded Rod (TR) continuity system does provide a reliable and efficient design technique for bridge continuity over the pier. The TR continuity system has evolved over the years to create the most effective design. The relationship between diaphragm and prestressed bridge girders can be used to predict the required concrete strength of the diaphragm. Test results showed that using diaphragm concrete strength of 50% of the girder

concrete strength is adequate. The Threaded Rod Continuity System has been proved to be efficient and cost-effective on recent projects in Nebraska for the following reasons:

- The most recent full-scale tests demonstrated excellent negative moment zone behavior.
- There was good bond between the TR and the concrete around them.
- The specimens showed good ductility.
- The confinement around TR was proved to be a good design.
- 10-1 3/8 G150 rods can be used at present.

Appendix A: Pacific Street Bridge Construction Photos

The Pacific Street Bridge over I-680 in Omaha, Nebraska was built in August 2008 as a replacement for an existing bridge due to its deteriorated condition and substandard width. The old bridge had a width of 74 ft and was composed of four spans that measured 44 ft 6 in., 73 ft, 73 ft 6 in., and 30 ft long. Each span consisted of 11 steel I-girders at 7 ft spacing. The new Pacific Street Bridge consists of two 98 ft long identical spans with a 17 degree skew angle. The bridge has six traffic lanes with a total width of 105 ft 8 in. The bridge superstructure consisted of twenty NU900 I-girders, ten for each span that are 35.4 in. deep and spaced at 10 ft 8 in. Each girder had a specified 28-day compressive strength of 10,000 psi and was pre-tensioned using 30-0.7 in. diameter strands. The 8 in. thick cast-in-place concrete deck had a specified 28-day compressive strength of 5,000 psi and was post-tensioned using 36-0.6 in. diameter mono strands in the longitudinal direction.



Figure A.1: Aerial View of Previous Bridge

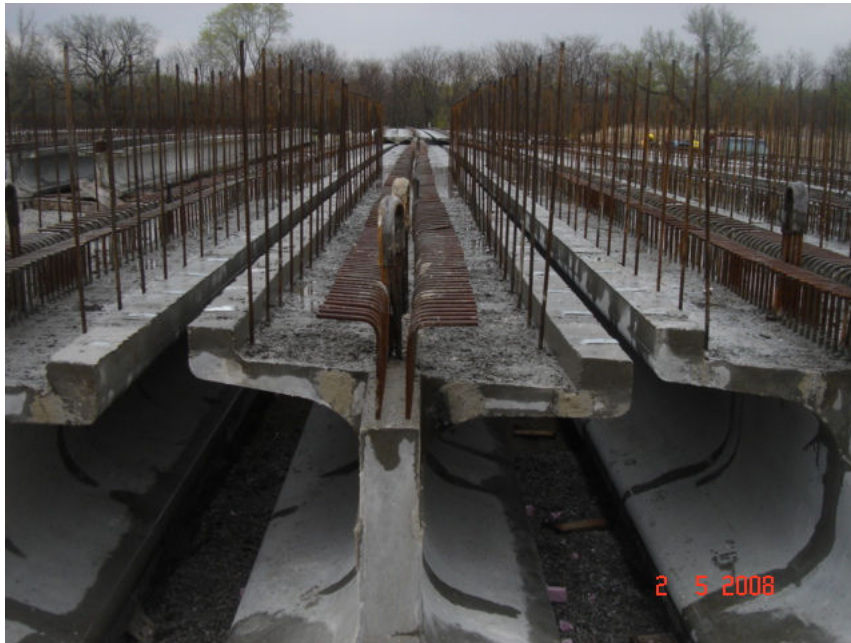


Figure A.2: NU 900 Girders



Figure A.3: Placement of Deck



Figure A.4: Girders at diaphragm section



Figure A.5: Bridge construction



Figure A.6: Post tensioning jack



Figure A.7: Excavation



Figure A.8: Bridge Construction



Figure A.9: Bridge Construction



Figure A.10: Bridge Construction



Figure A.11: Pouring of Concrete



Figure A.12: Pouring of Concrete



Figure A.13: Barriers



Figure A.14: Completed bridge

A.1 Cracking

It should be noted that the Pacific Street Bridge has experienced an unusual amount of cracking. The contractor reported difficulties with weather that caused a delay during placement and probably led to increased shrinkage in pavement. Another possibility is that slag was added for the first time to the 7BD-4000 mix used for bridge decks; however, this is not thought to be a reason for cracking.



Figure A.15: Shrinkage Cracking



Figure A.16: Shrinkage Cracking



Figure A.17: Shrinkage Cracking

REFERENCES

- AASHTO. 2007. AASHTO LRFD Bridge Design Specifications. 4th Edition with 2008 Interim Revisions.
- American Association of State Highway and Transportation Officials (AASHTO) M203. 2007. “Standard Specification for Steel Strand, Uncoated Seven-Wire for Concrete Reinforcement”, Washington, DC.
- American Association of State Highway and Transportation Officials (AASHTO) (2007) “AASHTO LRFD Bridge Design Specifications”, 4th Edition with 2008 interim revisions, Washington, DC.
- American Concrete Institute (ACI) Committee 318. 2008. Building Code Requirements for Structural Concrete (ACI 318-08) and Commentary (ACI 318R-08). Farmington Hills, MI: ACI.
- ASTM A416 (2006) “Standard Specification for Steel Strand, Uncoated Seven-Wire for Prestressed Concrete”, West Conshohocken, PA.
- Buckner, C. D., (1995) “A Review of Strand Development Length for Pretensioned Concrete Members,” State of the Art Report, *PCI Journal*, V. 40, No. 2, March-April, pp. 84-105.
- Burns, Ned H. “Development of Continuity Between Precast Prestressed Concrete Beams”, *PCI JOURNAL*, V. 11, No. 3, June 1966, pp. 23-36
- Hanson, N. W.; and Kaar, P. H., (1959) “Flexural Bond Tests of Pretensioned Prestressed Beams,” *ACI Journal*, V. 55, No. 7, pp. 783-803.
- Hennessey, S. A., Bexten, K., Sun, C., and Tadros, M. K., “Value Engineering of Clarks Viaduct in Nebraska,” Proceedings of the Second International Symposium on High Performance Concrete and PCI National Bridge Conference, Nashville, TN, October 2002.

- Hennessey, S. Butler, T., Lafferty, M., and Sun, C. "Value Engineering in Practice, a Look at the Clarks Viaduct in Nebraska" *PCI JOURNAL*, V. 50, No. 5, September-October 2005, pp. 40-49
- James, B. (2001) "Narrows Bridge, Perth, WA", The newsletter of Engineering Heritage Australia, The Institution of Engineers, Australia, No. 11, June.
- Lane, S., and Rekenthaler, D. (1998) "The Ties That Bind: The 10-Year Fight for 0.6-Inch Diameter Strands", FHWA, TFHRC, *Public Roads Magazine*, Vol. 61· No. 5.
- Ma, Zhongguo (John), Huo, Xiaoming, Tadros, Maher K., and Baishya, Mantu "Restrained Moments in Precast/Prestressed Concrete Continuous Bridges," *PCI JOURNAL*, V. 43, No. 6, November-December 1998, pp. 40-57
- Nebraska Department of Roads (NDOR) (2008), "Bridge Operations, Policies & Procedures (BOPP), Lincoln, NE
- Nebraska Department of Roads (NDOR) (2008) "NDOR Bridge Office Policies and Procedures".
- Precast/Prestressed Concrete Institute (PCI) (2003) "Precast Prestressed Concrete Bridge Design Manual", 2nd Edition, Chicago, IL.
- Reiser, N.P. (2007) "Innovative Reinforced/Prestressed Concrete Bridge Superstructure Systems" MS Thesis, University of Nebraska-Lincoln, NE.
- Russell, B. W., and Burns, N. H. 1996. Measured Transfer Lengths of 0.5 and 0.6 in. Strands in Pretensioned Concrete", *PCI Journal*, Sept.-Oct.
- Russell, H. G., Volz, J. S., and Bruce, R. N. (1997) "Optimized Sections for High-Strength Concrete Bridge Girders", Federal Highway Administration (FHWA), FHWA-RD-95-180, August.

- Sun, C., Badie, S. S., and Tadros, M. K., “New Details for Precast Concrete Girders Made Continuous for Deck Weight,” Proceedings of the TRB 81st Annual Meeting, Washington, DC, January 2002
- Tadros, Maher K., Ficeneq, Joseph A., Einea, Amin, and Holdsworth, Steve, “A New Technique to Create Continuity in Prestressed Concrete Members”, PCI JOURNAL, V. 38, No. 5, September-October 1993, pp. 30-37
- Tadros, Maher K., Sun, Chuanbing, “Implementation of the Superstructure/Substructure Joint Details”, NDOR Project SPR-PL-1(038) P514, December 2003
- Tadros, M. K. “Design Aids for Threaded Rod Precast Prestressed Girder Continuity System.” Nebraska Department of Roads. August 2007
- Vadivelu, J., and Ma, Z. (2008) “Potential Impact of 0.7-inch Strands on Precast/Prestressed Concrete Bridge I-Girders: Spacing of Large Diameter Strands”, Proceedings of the 2008 PCI National Bridge Conference, Orlando, FL, October.
- Wang, Ning. “Threaded Rod Continuity System For Precast Prestressed Girder Bridges.” Dissertation, University of Nebraska-Lincoln. November 2006